LOCALIZATION AND EXPRESSION OF ET-1 RECEPTORS IN THE NORMAL AND GLAUCOMATOUS DOG EYE

By

MARIA E. KÄLLBERG

A DISSERTATION PRESENTED TO THE GRADUATE SCHOOL
OF THE UNIVERSITY OF FLORIDA IN PARTIAL FULFILLMENT
OF THE REQUIREMENTS FOR THE DEGREE OF
DOCTOR OF PHILOSOPHY

UNIVERSITY OF FLORIDA

2003

Dedicated to my family and my friends who made this work come true.

ACKNOWLEDGMENTS

I would like to thank everyone who helped and supported my scientific work and my graduate education, especially those listed below.

Dr. Dennis E. Brooks invited me to Florida and made the dream of my life come true. Thanks to Dr Brooks I will be able to dedicate my professional life to ophthalmology as a researcher and clinician. I thank him for his support through the years. The precious friendship we have developed will always help me whatever challenges life has to offer in the future.

Dr. William W. Dawson guided me through the world of vision research and electrophysiology, which for me was unknown territory. He has inspired me not only by his knowledge but also by his way of questioning axioms and looking for new truths. I am thankful to Dr Dawson and his wife, Judyth, for their concern and warm generosity.

Dr. Adrian M. Timmers meant a great deal to me and my project. He opened his laboratory for me and patiently taught and helped me through every necessary step of the molecular biology part of my project. His positive and supportive attitude was extraordinary.

I would like to thank Dr. Kirk N. Gelatt for sharing with tireless enthusiasm his tremendous knowledge in research and clinical ophthalmology. I am also grateful for the many times he helped me in his own positive way whenever I needed good advice.

Dr. Don A. Samuelson broadened my view of comparative ophthalmology. He and his laboratory technicians, Mrs. Patricia Lewis and Ms. Mae Chisholm, were very helpful in accomplishing all the challenges in histologic methods that I encountered during my time as a graduate student.

I owe Dr. Adolfo G. Garcia many thanks for his contribution to my project. I am grateful to have gotten not only scientific help but also a friendship for life.

My dear friend, Dr. András M. Komáromy, has been by my side from the very first page of this new chapter of my life. András made the transition easy by always being there for me whenever I needed help or support.

Dr. Franck J. Ollivier, dear friend and colleague, deserves lots of thanks for the wild scientific discussions and many laughs.

With all my heart I thank my best friend, Kerstin Bergvall, who helped me through many tough times.

Ann Ellis gave me many hours of help teaching me electron microscopy.

I would like to thank Dr. Stacy E. Andrew, the ophthalmology residents at the University of Florida, and various ophthalmologists in Florida (especially Dr. Salisbury and Dr. Brogdon) for their contributions.

Mr. Harold L. Sapp gave valuable technical assistance.

Dr. Carol Detrisac was very helpful in reviewing my histology slides.

Dr. George Lambrou, CIBA Vision Ophtha, Novartis, provided very generous financial and technical support.

I would like to thank Ms. Marinela Capanu and the Interdisciplinary Center for Biotechnology Research at the University of Florida for their help with statistic analysis of the data.

Dr. Nancy Szabo at the Analytical Toxicology Core Laboratory at University of Florida has been extremely helpful with analyzing my samples and sharing her expertise.

Dr. Thomas Yorio, Dr. Ganesh Prasanna, Dr. Ragu Krishnamoorthy, Dr. Martha Stokely, Christina Hulet, and Santos Narayan at the Health Science Center, Fort Worth, Texas deserve a special thanks for their tremendous support.

I owe many thanks to the Office of Research and Graduate Studies at the College of Veterinary Medicine, University of Florida. Associate Dean Charles Courtney III and Mrs. Sally O'Connell made it possible for me to become a graduate student and to successfully finish my dissertation. Sally helped me through several storms.

Finally I would like to thank my parents for supporting me the whole way through my training and for helping me to realize my dreams. The sometimes overwhelming distance from home was overridden by the closeness of our relationship.

TABLE OF CONTENTS

page

LIST OF TABLES

LIST OF FIGURES

Abstract of Dissertation Presented to the Graduate School
of the University of Florida in Partial Fulfillment of the
Requirements for the Degree of Doctor of Philosophy

LOCALIZATION AND EXPRESSION OF ET-1 RECEPTORS IN THE NORMAL AND GLAUCOMATOUS DOG EYE

By

Maria E. Källberg

May 2003

Chair: Dennis E. Brooks
Major Department: Veterinary Medicine

The goal of this study was to document any differences in the levels of the endothelin-1 (ET-1) peptide and nitric oxide (NO) in aqueous humor and vitreous; and in the location and density of the ET-1 receptors, ET_A and ET_B, in the glaucomatous dog eye as compared to the normal dog eye. Comparisons were made between normal (n=30) and glaucomatous (n=14) samples for the following parameters:

- Levels of NO and ET-1 in aqueous humor and vitreous, as measured by enzyme immunoassay.
- Localization of ET receptors in the retina and choroid was done by immunocytochemistry.
- Expression of receptor protein in the retina and choroid, as measured by Western Blot technique.
- Retinal mRNA levels of ET-1, and the ET receptors, as measured by Real Time Polymerase Chain Reaction.
- Retinas were evaluated histologically.

The numerical data were analyzed using an ANOVA 2*2 factorial analysis. The two factors of interest were the disease, with two levels (glaucomatous and normal); and breed, with two levels (Cocker and non-Cocker).

The findings in the glaucomatous eyes were the following:

- Endothelin-1 increased in aqueous humor and vitreous, with a larger increase in the Cocker group.
- Nitric oxide increased in aqueous humor and vitreous, with a larger increase in the non-Cocker group.
- Degree of degeneration of the retina was correlated to ET-1 levels in aqueous humor and vitreous.
- Distribution of ET receptor labeling was similar in normal and glaucomatous sections for both ET receptors.
- Endothelin-1 mRNA in the retina increased nonsignificantly in the Cocker group and decreased nonsignificantly in the non-Cocker group.
- Endothelin receptor expression decreased in both groups with a significant decrease for the ET_B receptor in the non-Cocker group.
- Levels of ET receptor mRNA increased significantly in the Cocker group, while the increase in the non-Cocker group was not significant.

The distinct results for the two groups might imply a unique response of ET-1 and its receptors in narrow-angle glaucoma in Cocker Spaniels.

CHAPTER 1
INTRODUCTION

Glaucoma

Role of Endothelin in Glaucoma

Glaucoma is the final common pathway of a group of diseases with decreased retinal ganglion cell (RGC) sensitivity and function, RGC death and optic nerve head (ONH) cup enlargement, an incremental reduction in visual fields, and blindness. Glaucoma is a neurodegenerative disease as it results in neural cell death [1]. All of these diseases in dogs result in or are associated with increased intraocular pressure (IOP), although the etiology of primary glaucoma is likely to be multifactorial. Mechanical, vascular, and other factors may influence individual susceptibility to optic nerve damage.

At every level of IOP there is a risk of glaucomatous damage, although the risk increases with increasing IOP. Damage can occur with extreme rapidity as in angle closure glaucoma, or may progress slowly as in the chronic primary open angle glaucomas (POAGs). Intraocular pressure cannot be used by itself to determine the presence of glaucoma; or to determine whether optic nerve damage will occur or progress. This variation in ONH susceptibility has been suggested to result from varying capacity for circulatory autoregulation to prevent IOP-induced ONH ischemia [1].

Ischemia of the optic nerve and retina may be induced by high IOP, or by vascular dysfunction such as a deficit in autoregulation, hypoperfusion, or vasospasm [2]. Inadequate blood supply of the retina and optic nerve is known to lead to death of ganglion cell neurons partly through the release of glutamate, an excitatory amino acid

transmitter [3]. Neurons, which contain ionotropic glutamate receptors [e.g., N–methyl-D-aspartate (NMDA) receptors], are particularly susceptible to ischemia/reperfusion [4]. The neurons in the retina that express such receptors are the ganglion cells and a subset of amacrine cells. In ischemia/reperfusion, neurotransmitters (e.g., glutamate) are released that overactivate their appropriate receptors. Such overstimulation, particularly of ionotropic glutamate receptors, generally leads to neural cell death [4].

Various ocular blood flow deficits have been seen in patients with POAG or normal tension glaucoma (NTG). Pillunat et al. [5-7] found evidence to suggest defective autoregulation in the ONH in POAG and NTG. Robert et al. [8] showed that the ability of glaucomatous eyes to adjust the blood supply in the optic disc to raised IOP is significantly reduced as compared to that of healthy eyes. Grunwald et al. [9] found a lack of hyperemic response of macular retinal blood flow after increased IOP in humans with POAG suggesting abnormal autoregulation. Patients with POAG with deteriorating visual fields despite an IOP lowered below 21 mm Hg show alterations in ocular blood flow regulation as compared to POAG patients with stable visual fields [10]. Cheng et al. [11] showed that patients with chronic angle-closure glaucoma (ACG) have decreased retrobulbar blood flow velocities and increased vascular resistance in the central retinal artery and temporal posterior ciliary arteries despite well-controlled IOP. Thus, evidence exists that in POAG, ACG and NTG there is defective autoregulation of blood flow to the ONH and retina.

Endothelin -1 (ET-1), being a very potent endogenous vasoconstrictor, has been examined as part of the etiology of glaucoma. The presence of endothelin (ET) receptors in the retina and choroid, particularly in retinal blood vessels, suggests that ETs may be

involved in regulating retinal blood flow, and could contribute to retinal ischemia. Chronic ischemia of the anterior optic nerve was induced in animal models [12,13], either by perineural infusion or intravitreal injections of ET-1. These studies have resulted in glaucomatous-like damage to the optic nerve. Henry et al. [14] demonstrated an impairment of ET_B receptor-mediated, endothelial cell-dependent, vasodilation in the forearm of human patients with normal-tension glaucoma. This indicates that the eye may be just one manifestation of a more generalized vascular disorder characterized by presumed endothelial cell dysfunction. Such an imbalance in the ET receptors might contribute to ET-induced ischemic damage in glaucoma.

Elevations of aqueous ET-1 are found in humans with POAG, and in the plasma and aqueous humor of patients with NTG [15-17]. Endothelin has also been found to induce efflux of glutamate from cultured rat brain astrocytes [18]. This suggests that ET, which is known to be released in ischemia, may exacerbate neurodegeneration by stimulating efflux of glutamate.

Temporary retinal ischemia in the piglet leads to an increase in endothelin-mediated vasoconstriction and a loss of tonic nitric oxide-dependent vasodilation remaining several hours after the ischemic insult [19]. Hypoxia-ischemia serves as a stimulus to enhance endothelin production in both brain and heart. Endothelin gene transcription is upregulated and ET release from cultured human vein endothelial cells is increased in response to acute hypoxia. Tissue responsiveness to endothelin, which can be modulated by receptor up and down-regulation, may also increase in response to an ischemic stimulus, but this has not yet been demonstrated in ocular tissues.

Astrocytes are the major glial cell type in the central nervous system and the ONH and are vital for retinal ganglion cell survival [20]. Optic nerve head astrocytes normally maintain the extracellular medium by regulating potassium and glutamate levels and also provide neurotrophic support for nearby neurons [21]. Like brain astrocytes, ONH astrocytes also respond to changes in the physiological state of the neuronal system by becoming metabolically active from a quiescent state and rapidly proliferating to the site of injury (reactive astrogliosis), especially under conditions of injury (ischemia or pressure-related) as seen in glaucoma. Astrogliosis disrupts axonal transport and also inhibits axon regrowth in the glaucomatous ONH [20,22]. Endothelins are implicated in the promotion of astrogliosis in the ONHs of experimental animals [13]. Intravitreal injection of ET-1 resulted in axon loss accompanied by glial proliferation in ONH of rabbits [13]. Prasanna et al. [23] showed that ET-1 induces astroglial proliferation in cultured human ONH astrocytes through ET_A and ET_B receptor activation suggesting that ET-1 could cause proliferation of ONH astrocytes in glaucoma.

Endothelin-1 may also have direct effects on optic nerve function. Intravitreal injections of ET-1 cause alterations in axonal transport in the rat optic nerve [24]. Likewise, continuous administration of ET-1 to the perineural region of the eye in monkeys resulted in altered neuronal activity in the visual cortex [25]. These findings suggest that intravitreal ET-1 can have direct effects on neuronal activity and survival.

Canine Glaucoma

The dog has the highest frequency of primary glaucomas of all animals, with the narrow- or closed-angle type being the most common [26]. The glaucoma classification scheme in dogs based on possible cause includes the primary glaucomas, secondary glaucomas, and congenital glaucomas [27]. In the primary glaucomas, the IOP elevation

develops without concurrent ocular diseases, is inherited in some canine breeds, and has a bilateral potential for development. Primary glaucomas may result from abnormal biochemical metabolism of the trabecular cells of the outflow system [27]. In secondary glaucomas, the increase in IOP is associated with some known antecedent or concurrent ocular disease that physically obstructs the aqueous outflow pathways. In the congenital glaucomas, the increased IOP is associated with an anterior segment anomaly, and the elevation in IOP develops soon after birth.

In the dog, the primary glaucomas are divided into open-angle and narrow- or closed-angle glaucoma according to the presence of an open or narrow anterior chamber angle and ciliary cleft at gonioscopy. Inherited open- and narrow-angle glaucomas occur bilaterally in purebred dogs. The primary glaucomas have been reported in at least 45 breeds and occur most frequently in United States among the American Cocker Spaniel (ACS), English Cocker Spaniel, Smooth and Wire Fox Terriers, Basset Hound, Sealyham Terrier, Miniature and Toy Poodles, and Beagle [27]. Other breeds recently identified with primary glaucomas include the Samoyed, Norwegian Elkhound, Bouvier de Flandres, Siberian Husky, Flat-Coated Retriver, Golden Retriver, Great Dane, Welsh Springer Spaniel, Akita, Chow-Chow, and Shar-Pei [27]. Some breeds appear affected with both the open- and narrow closed-angle types, which may suggest these glaucomas are related.

Advanced glaucomas in dogs show similar features independent of pathogenesis with an iridocorneal angle (ICA) closure and sclerociliary cleft collapse. The retina is degenerated with attenuated arteries, and the optic disc round, depressed, and atrophied. Intravitreal levels of the neurotransmitter glutamate are increased in dogs with glaucoma,

providing evidence for an ischemic mechanism for RGC death and optic nerve head atrophy in canine glaucoma [28]. In a study by Kallberg et al. [29] aqueous humor ET-1 was 3.5 times normal level in dogs with primary chronic glaucoma. These findings indicate a possible role for ET-1 in the pathophysiology of some types of glaucoma in dogs.

Primary narrow-angle glaucoma in American Cocker Spaniels

The mechanism of development of narrow and closed ICA in the ACS is not completely clear, but one hypothesis is that tight apposition of the iris slightly increases the pressure within the posterior chamber, which in turn causes forward displacement of the basal iris [27]. Eventually, the basal iris narrows the ICA and opening of the ciliary cleft. Apposition of basal iris across the filtration angle causes a potentially reversible angle closure. With continued apposition, peripheral anterior synechiae (PAS) develop, thereby permanently closing the pathways of aqueous outflow.

This mechanism corresponds to the development of angle-closure glaucoma in humans. The most common cause of angle closure in humans is pupillary block, also termed primary angle-closure glaucoma [30]. It impedes the flow of aqueous humor from the posterior to the anterior chamber between the anterior surface of the lens and the posterior surface of the iris. Pupillary block may be absolute, as when the iris is completely bound down to the lens by posterior synechiae, but most often is a functional block, termed relative pupillary block.

Angle-closure glaucoma in humans can present with a spectrum of symptoms, from none at all to severe pain, blurred vision, and nausea [31]. Intermittent angle closure defines repeated, brief episodes of angle closure with mild symptoms and elevated IOP. They may continue uneventfully for months or years. Attacks may be accompanied by

progressive PAS formation, leading to chronic angle closure due to a permanent closure of a portion of the angle. The IOP in eyes with chronic angle closure may be normal or elevated.

The greatest danger lies in the possibility of sudden conversion to acute angle-closure glaucoma. If the pupillary block becomes absolute, the pressure in the posterior chamber increases and pushes the peripheral iris farther forward to cover the trabecular meshwork and closes the angle with an ensuing rise of IOP. Attacks of acute angle-closure glaucoma are mild at first, but rapidly increase in severity. The symptoms of an acute attack result from the sudden, marked elevation of IOP to as high as 80 mm Hg.

Absolute glaucoma refers to an eye with no light perception and a persistently elevated IOP. The time required for a neglected angle-closure attack to cause total blindness in humans is variable and depends on the severity of the acute attack, but appears to be an average of 1 to 2 years [31].

Most affected dogs with angle-closure glaucoma present with either classic clinical signs of unilateral, acute congestive glaucoma of a few days duration, or with chronic, advanced glaucoma with buphthalmia, lens dislocation and cataract, retinal and ONH degeneration, and blindness. Often, the condition becomes bilateral within several months. In a study by Magrane [32] the mean age of affected dogs was 6 years (range, 3-10 years), with the second eye usually affected within 12 months.

Both the history and clinical course suggest that this form of glaucoma may be a series of acute IOP attacks, with the subsequent magnitude of the IOP elevation gradually increasing. Tonographic measurements of aqueous humor outflow are usually within normal limits in dogs with narrow ICAs, but they are lower than normal (0.10-0.15

μL/min per mm Hg) in dogs with very narrow and closed (due to synechial formation) ICAs and clefts [27]. Tonometry of the acute congestive glaucomas often yields IOPs as great as 50 to 70 mm Hg, and the corneal edema that parallels the elevation in IOP after approximately 40 mm Hg usually prevents gonioscopy. Gonioscopy of the ACS with ocular hypertension usually reveals a narrow to closed ICA and reduced ciliary clefts; as the glaucoma progresses, angle closure and ciliary cleft collapse with peripheral anterior synechial formation commonly occurring. More recently, pectinate ligament dysplasia in the ACS has also been reported, but it does not appear to occur frequently [27].

In a study by Lovekin and Bellhorn [33] three Cocker Spaniels, bred for glaucoma, were followed with repeated clinical examinations, tonometry, aqueous outflow, and water drinking and betamethasone tests. The results were compared with similar test results on 82 controls. Eyes were removed from the three Cocker Spaniels being studied and compared with the eyes of four other Cocker Spaniels that had manifest glaucoma.

The studied Cocker Spaniels had reduced IOP regulatory mechanism as compared to the control dogs, and increased IOP was more easily provoked in them than in the control dogs. However, pathologic changes indicating glaucoma were not seen in histologic sections of the ICAs of their eyes. The authors concluded that an abnormal physiology concerned with the regulation of IOP preceded pathologic changes in the angle structures of their eyes.

Definite histopathologic changes were shown in the eyes of Cocker Spaniels with manifest glaucoma. The eyes resembled human angle-closure glaucoma or absolute glaucoma with loss of trabecular meshwork, anterior synechia, and attenuation of the intrascleral venous plexus. The histologic ICA structures of an eye of a Cocker Spaniel

with no history of glaucoma showed a lack of trabecular meshwork. This eye, having an IOP of 24 mm Hg, was under prophylactic treatment because of manifest glaucoma in the other eye.

Changes of the ocular fundus in the ACS may not correlate with the duration and magnitude of the elevated IOP [27]. It is not unusual for an ACS to present with a high IOP (70-80 mm Hg) and a history of signs of glaucoma being present for less than 1 week, yet after lowering the IOP to less than 20 mm Hg, the dog loses its vision. Ophthalmoscopically, the ocular fundus cannot be visualized until the IOP is lowered and the corneal edema reduced. The optic nerve and retina may initially appear to be normal, with some vascular attenuation detected. With the IOP maintained at 20 mm Hg or lower however, progressive retinal and ONH degeneration eventually become apparent within a few weeks. In some of these dogs, the retinal degeneration may affect only limited areas, appearing as radiating or fan-shaped zones from the ONH that represent areas of retinal and choroidal degeneration caused by ischemia from the occlusion of individual short posterior ciliary arteries.

The continued progression of ONH degeneration and deterioration of the animal's vision despite lowering of IOP is classic evidence for the role of non-IOP related factors in glaucomatous optic neuropathy. Among animals tested at the University of Florida, intravitreal glutamate levels are much higher in the ACS with glaucoma than in Samoyeds, Shar Peis, and Akitas [28]. In all probability, the initial primary optic nerve injury from the elevated IOP induces RGC degeneration and apoptosis caused by glutamate excitotoxicity, neurotropin deprivation, accumulation of intraneuronal calcium, and formation of nitric oxide (NO), proteases, and oxygen free radicals. The injured,

apoptotic RGC releases more glutamate, predisposing the eye to further, secondary degeneration of adjacent healthy RGC and their axons. This domino effect occurs independent of further IOP-induced primary injury.

Primary open-angle glaucoma in the Beagle

Primary open-angle glaucoma in the Beagle is the most extensively investigated canine glaucoma. Beagles with spontaneous, hereditary open-angle glaucoma start to develop symptoms between 8 and 16 months of age [26]. The iridocorneal angle and sclerociliary cleft are initially normal. The increase in IOP and decline in the facility of outflow develop slowly. The increased IOP produces slight enlargement of the axial length of the globe, which in turn results in lens subluxation and narrowing of ICA and sclerociliary cleft in dogs between 1 and 4 years of age. Animals 2-4 years of age have IOP's in the range of 25 mm Hg to 40 mm Hg. Eventual ICA and sclerociliary cleft closure result in IOPs of 40 mm Hg to 60 mm Hg in animals 4 to 6 years old.

Light microscopic examinations of the aqueous outflow structures indicates no abnormalities in the early affected animals [34,35]. The retinal blood vessels, especially the small peripapillary retinal arterioles and veins, gradually disappear. The optic disc becomes round, depressed and atrophied with the loss of myelin.

Optic nerve capillary endothelial cells are ultrastructurally abnormal prior to detectable increases in IOP [36]. Spherical, membrane-bound, electron-dense inclusions resembling Weibel-Palade bodies are found in pericytes and endothelial cells in both preglaucomatous and glaucomatous eyes. These changes are usually associated with microcirculatory abnormalities in humans and diabetic dogs.

Abnormal blood flow has been detected in the exterior and internal ophthalmic arteries, the anterior ciliary arteries, and short posterior ciliary arteries, but not the

primary retinal arteries in the glaucomatous Beagle as measured by color Doppler imaging [37]. Furthermore, while treatment with Ca-channel blockers increases blood flow in orbital vessels of normal Beagle dogs, the blood flow of glaucomatous Beagles remains unchanged. This indicates an inability of the vessels to respond to stimuli, which may be due to an altered vascular structure with hypertrophy or dysfunctional regulation by endothelial receptors.

Ophthalmic Vascular Morphology and Physiology

The eye is one of the most highly perfused organs in the body [38]. In dogs and humans, the eye has two separate systems of blood vessels that differ anatomically and physiologically: the retinal vessels, which supply the inner layers of the retina, and the uveal or ciliary vessels, which supply the rest of the eye.

The main supply of blood to the eye and orbit of the dog is via the internal maxillary artery (as a branch of the external carotid artery) that after passing through the alar canal branches to give rise to the external ophthalmic artery (EOA) [39]. The internal ophthalmic artery (IOA) in dogs is a small artery that arises from the anterior cerebral artery at the level of the optic chiasm [40]. It passes through the optic canal on the dorsal surface of the optic nerve in dogs, and runs rostral by the nerve to anastomose with a branch of EOA about midway between the optic canal and the posterior pole of the globe. By comparison, in primates the entire global microcirculation and most of the orbital circulation are supplied via the internal carotid artery, which gives rise to the IOA [39].

Two long posterior ciliary arteries (LPCA), one medial and one lateral, arise from the anastomoses of the external and internal ophthalmic arteries in dogs. Six to ten short posterior ciliary arteries (SPCA) arise, surround the scleral canal of the canine optic nerve and supply the lamina cribrosa, choroid, retina, and ONH circulations in dogs. The SPCA

thus give rise to two very biologically distinct circulations. The peripapillary choroid also derives its blood supply from the SPCA at the ONH margin, although the choroidal and ONH circulations are not continuous. Peripapillary choroidal blood flow is directed anteriorly away from the optic disc as the venous drainage of the peripapillary choroid is anterior to the vortex veins. Choroidal arteries branch into smaller vessels before supplying the choriocapillaris, the innermost layer of choroidal vessels.

The retina in dogs and primates has a large vascular network in the major part of the sensory retina. The blood vessels extend from the optic disc to the region of the ora serrata. While the location of the blood vessels within the retina may differ somewhat between species, the general pattern of the major retinal arterioles and venules is generally similar in that they lie superficially in the nerve fiber layer and RGC layer, radiating from the optic disc. The smaller arterioles, venules and capillaries are organized into two dense capillary networks: an inner plexus, being situated at the level of the nerve fiber layer and/or ganglion cell layer; and an outer plexus, which in the dog is situated at the border between the inner nuclear layer and the outer plexiform layer.

Primates possess a cone-rich region completely free of rods called fovea. No retina of the domesticated animals has a fovea, but an area of high cone density frequently occurs and is often referred to as the “area centralis”. This area lies 3- to 4-mm dorsolateral to the optic disc in the dog. At the level of the “area centralis” there are no major retinal vessels, but capillary networks lie in different layers of the retina. The thickness of the innermost vascular plexus varies with the thickness of the nerve fiber layer. In the temporal retina near the raphe where the nerve fiber layer is very thin,

capillaries are almost absent. In the peripapillary retina where the nerve fiber layer is thick, the capillaries form a dense, multilayered plexus.

The arrangement (number and location of capillaries) of the superficial capillary network is directly related to the thickness of the nerve fiber layer and the ganglion cell layer, which are thought to be metabolically demanding [41]. The multilayer arrangement leads to a plexus of numerous capillaries fed by a single, relatively large arteriole. Consequently, the retinal microvasculature is subjected to a large pressure head, and changes in its resistance are likely to play a significant role in blood flow regulation.

Blood vessels can be identified on the basis of distinct characteristics. Arteries are large, with multiple layers of smooth muscle cells, the muscularis, surrounded by the adventitial layer consisting of circumferentially oriented collagen fibers. An inner elastic lamina separates the muscularis from the endothelium. A basement membrane surrounds the endothelial cells and blends with the internal lamina elastica. Arterioles have smaller caliber, a single layer of smooth muscle cells, and no, or only minimal, internal elastic lamina. The endothelium is continuous and the cells are covered by a basement membrane. Capillaries have a minimal wall thickness consisting of endothelial cells and their basement membrane [42]. The endothelial lining of capillaries is supported by circumferentially oriented pericytes with contractile features [43].

The endothelial cell monolayer lining blood vessels was long thought to simply function as a diffusion barrier. It is now recognized that the endothelium has a crucial role in regulating vascular homeostasis [44]. The location of endothelial cells between the circulating blood and the vascular smooth muscle cells gives them a strategic position to regulate vascular permeability and influence vascular hemostatic metabolic functions

[45]. The vascular endothelium plays an active role in vasomotor function of both macro- and microvasculatures, including maintenance of vascular tone and regulation of blood flow [46]. Vascular tone depends on a balance between the endothelial vasodilators (e.g., (NO) and vasoconstrictors (e.g., ET) such that reduced formation of vasodilators would result in vasoconstriction and a decrease in vasoconstrictors would result in vasodilation. Therefore, endothelial cells play an important role in modulating the microvascular tone and autoregulation. Endothelial cells also strongly affect coagulation, platelet function, and fibrinolysis [45].

Regulation of Blood Flow

Autoregulation plays a very important role in the control of blood flow in a tissue. The goal of autoregulation in a tissue is to maintain a relatively constant blood flow, capillary pressure, and nutrient supply in spite of changes in perfusion pressure [46]. This is accomplished through the ability of the cardiovascular system to adjust the resistance of particular vessels by controlling the diameter of their lumen.

The blood flow in the ONH and intraocular vessels (when pressure in the central retinal vein is normal) is calculated by using the following formula:

Flow = Perfusion pressure / Resistance to flow
Perfusion pressure = Mean blood pressure (BP) - intraocular pressure (IOP)
Mean blood pressure = Diastolic BP + 1/3 (systolic - diastolic BP)

From this formula, it emerges that the blood flow depends on 1) resistance to blood flow, 2) blood pressure, and 3) IOP.

Factors that normally govern microcirculatory vascular smooth muscle tone involve vasoactive nerves, and circulating hormones, as well as endothelial cell derived factors, and myogenic and metabolic factors [47]. According to the metabolic hypothesis, local arterial smooth muscle tone is regulated by metabolic change in the tissue [46]. Local

concentration of metabolic products, O_2 and CO_2, plays a role in maintaining autoregulation. Accumulation of CO_2 and a reduction in O_2 is due to hypoxia or lack of ability to wash out metabolites, causing vasodilation. The myogenic hypothesis states that a rise of intravascular pressure causes vasoconstriction because stretching of the vessel wall is counteracted by vasoconstriction in the arterioles. Responses to changes in transmural pressure, i.e. stretching are not dependent on endothelium-derived vaso-active substances [48]. The endothelial cytoskeleton together with its extracellular matrix is thought to provide a mechanical linkage between the site of the shear stress and the smooth muscle cells. The change in pressure causes activation of protein kinase C, an intracellular modulator of Ca^{2+} -dependent contractile processes. The role of the endothelium in flow-induced contraction, caused by stretching of the vessel wall, may thus be that of a conduit for the mechanical disturbance. This autoregulation of blood flow may also have neurogenic control. However, there is not much proof of this occurring in the ocular vessels because vessels in the retina and ONH have no autonomic nerve supply [38]. The choroid, by contrast, is richly supplied by the autonomic nerves and yet has no appreciable autoregulation [49].

Alterations in blood flow through the microcirculation were long thought to be solely achieved by changes in tone of precapillary sphincters. It is now well accepted that retinal pericytes also have the capacity to act as important regulators of local blood flow. Pericytes are perivascular cells with multifunctional activities. They are contractile cells adjacent to the endothelial lining of capillaries supporting the microvasculature. The regulatory mechanisms and vessel-wall cross-talk between these cells and the microvascular endothelium have been shown to be identical to the those of smooth

muscle cells [43]. These interactions are very important in the retinal microcirculation where autoregulation is vital for the maintenance of smooth and uninterrupted blood flow.

Pericytes are more numerous in the retina than in any other microcirculation in the body [43]. Within the retinal microvasculature there is a rapid transition from vascular smooth muscle cells to pericytes at the interface of the precapillary and terminal arterioles. Modulation of blood flow by pericytes in very small ophthalmic arteries and capillaries has been shown in several studies [50-52]. The capacity of pericytes to regulate the blood flow through capillaries indicates an important role of the pericytes in the control of microcirculation of the retina and the ONH.

Blood flow in the retina and prelaminar ONH circulations have been shown to possess autoregulatory capacity in several species by remaining stable during IOP-induced changes in perfusion pressure, whereas blood flow in the choroid is sensitive to changes in IOP [53-55]. However, the latter concept remains debatable. In particular, the choroidal tissue just nasal to the optic nerve may be capable of blood flow autoregulation in instances of increased IOP, as has been shown in the cat [56]. Furthermore, investigations have shown that the choroid is capable of autoregulation in the rabbit [57]. The autoregulatory capacity of the human choroid is unknown [56].

Endothelin and Nitric Oxide

Synthesis, Secretion and Clearance of Endothelin

In 1988, Yanagisawa et al. [58,59] identified endothelin (ET), a very potent endothelium-derived vasoconstrictive factor. The substance, a 21-amino acid peptide, was isolated from the endothelial cells of pig aorta and is known today as ET-1. Endothelin-1 has also been found to be expressed in non-vascular tissues, such as the

brain, kidney, lung and others [60]. Subsequent studies have shown that the ET isolated from endothelial cells is one of a family of isopeptides.

Three isoforms of the peptide exist: ET-1, ET-2, and ET-3, but only ET-1 can be detected in endothelial cells of vascular tissue. Endothelin-2 and ET-3 can be found in the intestine, adrenal gland and brain. Endothelin-3 is relatively abundant in neuronal tissues [60]. Each ET isoform is a product of separate genes that code for a precursor protein mRNA that share high sequence homology [44]. The endothelins are synthesized from precursors known as preproendothelins (preproET) comprised of 160 and 238 amino acid residues. Before they are finally processed into 21 amino acid peptides, these large precursors undergo an intermediate cleavage by endopeptidases to form the 37-41 amino acid precursors proendothelins (proET), also named “Big ET”. “Big ET” is further processed by a specific endothelin converting enzyme (ECE) to form the 21 amino acid active peptide.

Smooth muscle cells are target cells and so express a nonselective ECE (ECE-1) on their cell surface associated with the plasma membrane to convert exogenous “Big ET”. The pro-ET-1 released from endothelial cells can therefore be converted into ET-1 in the vascular smooth muscle surface [60]. However, the major part of conversion of “Big ET-1" into ET-1 takes place in the endothelial cells, and it is assumed that the ET-1 is concentrated primarily in these cells, although it is not stored there. The enzyme present in endothelial cells is an ECE (ECE-2) selective for “Big ET-1" more than “Big ET-2" or “Big ET-3". The ECE located in vascular smooth muscle acts equally on the different progenitor peptides [60]. In the retinal microcirculation pericytes have been shown to respond to ET-1 secreted by the retinal capillary endothelial cells [43,61].

The secretion of ET-1 by endothelial cells is regulated at the level of peptide synthesis, because the endothelial cell contains no dense secretory granules in which ET-1 can be stored and then later released. The expression of preproET-1 mRNA and release of the peptide are stimulated by several factors including adrenaline, thrombin, vasopressin, angiotensin II, insulin, cytokines, transforming growth factor β (TGF β), arginine, and physical stimuli such as shear stress of the endothelium. Ischemia and hypoxia also result in synthesis and release of ET-1 [60]. Endothelin-1 synthesis is inhibited via a cGMP-dependent mechanism by NO, prostacyclin, natriuretic peptides and heparin [60].

Hisaki et al. [62] showed that removal of the endothelium does not completely prevent the action of “Big ET-1" in the perfused rat mesenteric bed, suggesting that smooth muscle cells also can synthesize ET-1. Smooth muscle cells in culture express ET-1 mRNA and release ET-1. According to Warner [63] within a diseased blood vessel with damaged endothelial cells, the vascular smooth muscle may produce ET-1 that is not regulated by endothelial cell agonists.

Most of the ET-1 released by the endothelial cells (approximately 80% of the synthesized amount) is secreted abluminally acting as a local hormone in a paracrine manner on the surface of the vascular smooth muscle [60]. The plasma half-life of ET-1 in humans is less than 1.5 min because of its efficient extraction by the splanchnic and renal vascular beds [44]. Endothelin-1 is also reported to be taken up by the lungs but the clearance differs between species [64].

Extraction of ET-1 follows binding to cell surface receptors, which are then internalized, allowing degradation to be carried out within the cell. Endothelin-1 is found

to be internalized by both ET_A receptors and ET_B receptors [65,66]. Both receptors seem to be agonist-occupied after internalization for one to four hours. Endothelin-1 is then dissociated from the receptor and possibly degraded. It has been shown that internalized ET-1 continues to evoke signaling events in the cells, which has been suggested to be one of the reasons that ET-1-stimulated effects are long-lasting [65]. A possible candidate for an intracellular degrading enzyme is a soluble protease found in human platelets, vascular smooth muscle and endothelial cells [64]. The fate of the internalized receptors will be discussed in the chapter about endothelin receptors.

Nitric Oxide

Nitric oxide plays an important role in combination with ET-1 to produce a balanced effect on blood vessel activity. Nitric oxide is an inorganic free radical, produced from L-arginine by the enzyme nitric oxide synthase (NOS) [63]. Nitric oxide synthase exists in at least three isoforms, but it is only the calcium-regulated isoform, endothelial NOS (eNOS), that appears responsible for NO formation within the healthy endothelium. The stimulation of a endothelial cell membrane receptor by an agonist such as acetycholine, histamine, thrombin, ET-1 or bradykinin leads to an increase in intracellular calcium, which in turn activates NOS [49]. Mechanical forces, such as stretch and shear, can also stimulate the production of NO.

When NO reaches its target smooth-muscle cell it activates the enzyme guanylate cyclase, responsible for the production of the 3'5'-cyclic guanosine monophosphate (cGMP), a second messenger. The increase in cGMP ultimately leads to smooth-muscle relaxation by reducing the intracellular calcium content [49]. A basal release of NO maintains ocular vessels in a constant state of mid-dilation [67].

Retinal capillary endothelial cells have been shown to constitutively express the enzyme NOS [68]. The enzyme guanylate cyclase has been shown to be expressed in retinal pericytes making it possible for the cells to synthesize cGMP on exposure to NO. Cultured pericytes relax to sodium nitroprusside (a NO donor), which stimulates guanylate cyclase and increases cGMP [69]. In addition the pericytes have been shown to respond to prostacyclin [67].

In normal vessels there is a balance between the endothelial production of NO and ET-1. The ability of NO to down-regulate ET-1 production and of ET-1 to stimulate NO production by endothelial cells acts to maintain a matched degree of constrictor-dilator tone.

In a number of disease states there is suspected to be a breakdown in the balance between ET-1 and NO [63]. Endothelial cell reduction in NO production may be compensated for by the induction of inducable nitric oxide synthase (iNOS) within the vascular smooth muscle. However, iNOS produces NO in an uncontrolled manner. In such disease states, ET-1 production is often increased. This increase in ET-1 production may well underlie deleterious increases in blood vessel reactivity and reductions in tissue perfusion [63].

Endothelin Receptors

Endothelin receptors exist both in vascular smooth muscle, pericytes, and the endothelium. In 1990, two ET receptors (ET_A and ET_B) were isolated [44]. Both receptors belong to a family of heptahelical G-protein coupled receptors. Although these two receptors have approximately 60% similarity in amino acid sequence, several domains are less homologous to each other and contribute to the functional differences between the ET_A and ET_B receptors.

The two ET receptor subtypes vary in their affinities to endogenous ligands. Endothelin receptor-A has a high affinity to ET-1 and ET-2, and a low affinity to ET-3. Endothelin receptor-B has an equally potent affinity to all three ligands [70].

Endothelin receptor-A exists on smooth muscle cells and mediates vasoconstriction, while the ET_B receptor is located on endothelial cells and mediates release of relaxing factors, such as prostacyclin and nitric oxide. Recent research indicates that ET_B also exists on vascular smooth muscles and mediates vasoconstriction. The relative contributions of ET_A and ET_B receptors to vasoconstriction is variable, and depends on the species and the vessel type studied [44].

Endothelin causes vasodilation at very low concentrations, and a marked and sustained contraction at high concentrations. The dilator response to endothelin involves activation of the ET_B endothelial receptors, linked to NO and/or prostacyclin release by endothelial cells [45]. At higher concentrations, such that all the endothelial ET_B receptors are occupied, ET diffuses through the intima toward the vascular smooth muscle. The constrictive response involves the activation by endothelin of ET_A and ET_B receptors on smooth muscle cells [45]. This vasoconstriction is correlated with a sustained increase of intracellular Ca^{2+} produced via a two-phase mechanism. The binding of ET-1 to the receptor activates phospholipase C (PLC) which hydrolyses phosphatidilinositol-4,5-biphosphate (PIP_2) into two products, inositol triphosphate (IP_3) and diacylglycerol (DAG). The initial increase in intracellular Ca^{2+} concentration is caused by a rapid mobilization of intracellular calcium stores by IP_3. This ET-1 mediated signaling upstream of IP_3 interaction with the Ca^{2+} stores is regulated by tyrosine kinases which also participate in the contractile response of α-adrenoceptor agonists, histamine

and angiotensin II. The maintained increase in intracellular Ca^{2+} levels is brought about by exterior Ca^{2+} entry via a calcium channel of the plasma membrane.

At least two types of non-selective cation channels as well as voltage-operated calcium channels are activated by ET-1 [71]. One is activated by low and the other by high concentrations of ET-1. The channel activated by low concentrations of ET-1 is inhibited by NO and therefore ET and NO seem to affect the same channel. The increased production of DAG also stimulates the translocation of protein kinase C (PKC) from cytoplasm to membrane and its subsequent activation [72]. Activation of PKC leads to phosphorylation of many proteins. Phosphorylation of myosin light chains induces smooth muscle contraction.

The binding of ET-1 to the ET_A receptor gives rise to a long-lasting response while the response of the ET_B receptor upon ligand binding is of more transient nature. Moreover, it has been shown that the ET_B receptor mediated vasodilation response to repeated injections of ET-1 shows tachyphylaxis, whereas the vasoconstrictor response in the same study did not [66]. This implies different pathways for the two receptors following internalization.

Bremnes et al. [73] investigated the regulation and intracellular trafficking pathways of the endothelin receptors. Their study demonstrated that both receptor subtypes are rapidly internalized upon agonist stimulation. Internalized ET_A and ET_B receptors both enter early endosomes (sorting endosomes). However, from this location, the two receptor subtypes are targeted to different intracellular fates. Whereas the ET_A receptor is directed to the pericentriolar recycling compartment and subsequently reappears at the plasma membrane, the ligand bound ET_B receptor is directed to

lysosomes for degradation. Thus, further clearance of plasma ET-1 by the ET_B receptors will be limited by the supply of de novo synthesized receptor molecules to the cell surface. This mechanism also explains the transient nature of the ET_B mediated response and the tendency for development of tachyphylaxis upon repeated stimulation of the ET_B receptor. The conclusion from this group was that the rapid recycling of ET_A may provide a basis for the prolonged contractile response mediated through this receptor, whereas lysosomal targeting of ET_B suggests a role for this receptor in clearance of ET from the circulation.

Chun et al. [74] showed that ET-1 remains intact and bound to the ET_A receptor for up to two hours after endocytosis. Their hypothesis for the prolonged signal response of the ET_A receptor was that ligand-occupied ET_A receptors may continue to activate the G-protein after endocytosis.

Retinal pericytes express both isoforms of the endothelin receptor, ET_A and ET_B [75]. The pericyte ET_A receptor mediates contraction through the same pathway as the ET_A receptor on smooth muscle cells, i.e. through the phospholipase C/inositol phosphate signaling pathway [43]. The exact nature of the second messenger signaling downstream to ET_B receptor activation in the retinal pericyte remains uncharacterized. However, a study has linked endothelin - 3 stimulation of renal mesangial cells (also classified as pericytes) to the production of NO [43]. This mechanism was postulated to buffer the contractile effects of ET-1 especially when local levels are inappropriately high. This is in opposition to the constrictor response evoked by activation of the ET_B receptor on smooth muscle cells. Mc Donald et al. [76] showed by binding studies of various fragments of ET-1, -2, and -3 using an in vitro model of microvascular pericytes that it is

highly likely that the ET_B receptor on retinal pericytes are different from those on the endothelium.

There is considerable heterogeneity in pericyte surface endothelin receptor expression with some cell types expressing only the ET_A and others ET_B [77]. The cell membranes of vascular effector cells may show both receptor types and one may be preferentially expressed. This is certainly the case in retinal pericytes where receptor binding studies have revealed the presence of several hundred thousand high-affinity ET_A receptors but only twenty to thirty thousand ET_B receptors on a single cell. It is also noteworthy that retinal pericytes express many more ET_A receptors than vascular smooth muscle [75].

At concentrations where ET-1 exerts no direct contractile effect, it potentiates the response to other vasoconstrictor hormones such as norepinephrine and serotonin [45]. The potentiating effects are due to an increased Ca^{2+} sensitivity of smooth muscle cells and can be prevented by pretreatment with calcium antagonists of the dihydropyridine type.

Endothelin and the Ophthalmic Circulation

The endothelial-dependent regulatory mechanisms are present in the entire cardiovascular system but there is a great heterogeneity of responses from one organ to the other, in arteries and veins, and in vessels of different diameter. This heterogeneity may be explained by a different smooth muscle content in different vessels, and/or different expression of receptors.

Haefliger et al. [78] showed that the effect of both NO and ET-1 increased with decreasing vascular diameter, when comparing the response to chemical or hormonal agonists of the porcine ophthalmic artery with the response of the ciliary artery.

Endothelin-1 has also been shown to contribute to hyperoxia-induced retinal vasoconstriction through its ET_A receptor in the human retina [79]. Systemic ET-1 administration in healthy subjects reduces pulsatile blood flow in the choroid and optic disc at doses which do not affect systemic hemodynamics or flow velocity in the ophthalmic artery [80]. This indicates that ocular circulation is particularly sensitive to changes in local ET-1 concentration and confirms the hypothesis that ET-1 may play a role in ocular vascular diseases.

Granstam et al. [81] showed a reduction of retinal blood flow, but no effect on the choroidal blood flow, by intravitreal ET-1 injections in cats. In contrast, Kiel et al. [82]has shown that the choroidal circulation in rabbits is regulated by ET_A and ET_B receptors mediating opposing effects on choroidal vascular resistance. Their results also suggested that endogenous ET preferentially elicits ET_B vasodilation, most likely by stimulating endothelial nitric oxide release.

Endothelin-1 is well distributed in ocular tissue and is localized in aqueous humor, iris, ciliary body, retina, and choroids [83,84]. The ET-1 of retinal origin is mostly vessel oriented but is also found in the retinal ganglion cell layer, the photoreceptor inner segments, and the outer plexiform layer. Narayan et al. [85] has shown that cultured RPE cells (ARPE-19cells) produce and release ET-1 by stimulation of muscarinic receptors. In the same study mRNA expression for preproET-1, ET_A and ET_B receptors was detected in the RPE cells.

Both ET_A and ET_B -type receptor binding sites have been detected in the vascular smooth muscle of choroidal and retinal vessels of humans and rats [83]. In the same study extravascular binding sites of the ET_B -type were found in the ganglion cell layer. In a

study in humans and rabbits the ET_A -like receptor binding sites were localized to the retinal and choroidal blood vessels, whereas the ET_B -like receptor binding sites were localized to the neural and glial cells of the retina [86].

Endothelin and Aqueous Humor Production and Outflow

In the anterior part of the eye, ET_A receptors have been found in human ciliary smooth muscle (HCSM), ciliary non-pigmented epithelial (NPE) cells, and trabecular meshwork (TM) cells [87,88]. Endothelin receptor-B receptor expression has been observed in cell cultures in HCSM cells [89]. Sugiyama et al. [90] showed a role for both ET_B and ET_B receptors in regulating IOP.

Endothelin-1 affects the contractility of ciliary smooth muscles (CSM) and TM cells consequently regulating aqueous humor [91]. Studies have shown that ET-1 decreases aqueous humor formation and increases outflow facility in rabbits and monkeys [92-94]. Endothelin-1 has also been shown to decrease the activity of sodium potassium ATPase, a key enzyme involved in ion transport and aqueous humor production [95].

Since it has been shown that ET-1 decreases IOP and increases overall outflow facility, the direct effect of ET-1 of the trabecular meshwork cells is functionally antagonistic to the direct effect on ciliary muscle [96]. Thus intertrabecular spaces could be narrowed by contracting trabecular fibres and widened by ciliary muscle contraction. According to Wiederholt [96] an alternative possibility might exist: in the presence of both tissues, contraction of the trabecular meshwork may increase the rigidity of this tissue allowing the ciliary muscle contraction to be more effective in altering the geometry of the trabecular meshwork. Although contraction of the ciliary muscle dominates the overall effect on outflow facility in the human (and most likely in the dog)

eye, the concept of antagonism between ciliary muscle and trabecular meshwork should be considered in the interpretation of mechanism of action of ET-1 on aqueous outflow and IOP.

Purpose of Study

The goal of this study was to document any differences in the location and density of endothelin-1 receptors in the glaucomatous dog eye as compared to the normal dog eye. In addition, the levels of the endothelin-1 peptide and nitric oxide in aqueous humor and vitreous were compared in the normal and glaucomatous dog eye.

The hypotheses were the following:

- The localization of endothelin-1 receptors differs in the retinal and choroidal vessels in the normal canine eye and the glaucomatous canine eye.
- The density of endothelin-1 receptors differs in the retina of the normal canine eye and the glaucomatous canine eye.
- The concentration of endothelin-1 and nitric oxide in aqueous humor and vitreous differs between the normal canine eye and the glaucomatous canine eye.

The objectives were:

- To identify the localization of endothelin-1 receptors in the retinal and choroidal vessels of normal and glaucomatous canine eyes as measured by immunogold labeling.
- To identify the density of endothelin-1 receptors in the retina of normal and glaucomatous canine eyes as measured by Western Blot and Real Time PCR.
- To determine the levels of endothelin-1 and nitric oxide in the aqueous humor and vitreous of normal and glaucomatous canine eyes as measured by immonoasssay.

CHAPTER 2
MATERIAL AND METHODS

Study Design

The normal and glaucomatous canine eyes in this study were from canine clinical cases at the University of Florida and Universidad Nacional Autonoma de Mexico in Mexico City. All dogs went through an ophthalmic examination prior to inclusion in the study (Tables 2-1 and 2-2).

Enucleated normal eyes (n=30) of 19 dogs and glaucomatous eyes (n=14) of 14 dogs were collected during one year. Normal and glaucomatous samples were obtained aseptically within 10 minutes after enucleation. The same technique was practiced for all dogs irrespective of the procedure and hospital performing the procedure. Samples of aqueous humor, vitreous, retina, and choroid were stored for future analysis of protein and mRNA content. In addition, samples of the posterior segment of the globe, with retina and choroid attached, and the anterior segment including the iridocorneal angle, were gathered for histological and immunocytochemical studies.

The levels of nitric oxide (NO) and endothelin (ET) -1 in aqueous humor and vitreous were measured by enzyme immunoassay. The location of the ET_A and ET_B receptors were determined in the retina and choroid with immunocytochemistry and the expression of ET receptor protein with Western Blot technique. The mRNA levels of ET-1, and the ET_A and ET_B receptors, in the retina were assessed with Real Time polymerase chain reaction (PCR). The retinas and iridocorneal angles were evaluated

histologically. Comparisons were made between normal and glaucomatous samples for these parameters. A summary of samples and analyses is shown in Tables 2-3 and 2-4.

Clinical Examination of Dogs

Ophthalmic examinations of the glaucoma dogs in this study included tonometry (Tonopen, Mentor Ophthalmics, MA**)**, slitlamp biomicroscopy (Kowa SL 14,Kowa Optimed, CA), and indirect ophthalmoscopy (Heine Omega 150, Dover, NH). The mean (± SD) intraocular pressure (IOP) of normal dogs, as measured by Tonopen applanation tonometry, is 16.8 ± 4.0 mmHg. The glaucoma dogs in this study were clinically diagnosed with hypertensive glaucoma, i.e. with an IOP exceeding 25 mm Hg. Clinical signs also included episcleral congestion, mydriatic pupils, optic nerve cup enlargement, neuroretinal rim narrowing, optic cup deepening, and retinal degeneration. Slitlamp biomicroscopy, and indirect and direct ophthalmoscopy of each dog were performed by veterinary ophthalmologists with extensive experience.

Breeds, ages, and clinical parameters of the normal and glaucomatous dogs are shown in Tables 2-1 and 2-2.

Endothelin-1 and Nitric Oxide Levels in Aqueous Humor and Vitreous

Endothelin-1 Analysis

Samples of aqueous humor and vitreous were gathered from enucleated normal eyes (n=28) of 18 dogs and glaucomatous eyes (n=11) of 11 dogs (Tables 2-3 and 2-4). The samples were stored at -80º C until analysis. Measurements of ET-1 were made by enzyme immunoassay (BBE5 Human Endothelin-1 Parameter ELISA Kit, R&D Systems, MN) by the Analytical Toxicology Core Laboratory at University of Florida. Cross reactivities entail big endothelin, <1%; sarafotoxin, <2%; ET-2, 45%; ET-3, 14%. The fact that canine and human ET-1 have corresponding amino acid sequences validated this

kit for testing canine ET-1. The kit was first evaluated on dog plasma. The extraction method for ET-1 in plasma was then modified and validated for the much smaller sample size and different constituency of the aqueous humor samples. Unlike plasma, which requires an extraction prior to assay, aqueous humor samples can be assayed directly. When sufficient volume was available (>200 μL) each sample was run in duplicate.

Nitric Oxide Analysis

Measurements of total NO were made by enzyme immunoassay (Nitrate/Nitrite Colorimetric Assay Kit; Cayman Chemical Company, Ann Arbor, MI). In this method the two ultimate products of NO activity (nitrite and nitrate) are evaluated together rather than separately to enhance reliability. To achieve this, nitrate in the samples was first converted to nitrite by incubation with nitrate reductase. Griess reagents were then added to react with nitrite and form a purple azo end-product that absorbs strongly at 540 nm. Although common interfering species include antioxidants (such as ascorbic acid, 0.1 mM) and phosphate (>50 mM), the interferant of greatest concern for this assay is NADPH, an essential cofactor for Nitric Oxide Synthase (NOS) enzyme function. Because this species can inhibit formation of the azo product, a catalyst is added with the nitrate reductase to promote the conversion of $NADP^+$ to NADPH.

Aqueous and vitreous humor samples were prepared for the assay by centrifuge filtration through 30 kDa cut-off filters (Millipore Corporation, Bedford, MA) that had been pre-rinsed with HPLC-grade water. When sufficient volume was available (~100 uL) the samples were analyzed in duplicate.

Localization of Endothelin Receptors in the Retina and Choroid

To our knowledge, ET receptor antibodies have not been used previously on canine tissue. Therefore it was necessary to determine if the antibodies had an affinity for the ET

receptors in our samples. This was done by immunostaining of scleral vessels of a normal Beagle eye. The staining was evaluated by light microscopy. Following confirmation of the affinity of the antibodies, immunocytochemistry for evaluation of receptor location by transmission electron microscope (TEM) was done on normal and glaucomatous retinas and choroids in the study.

Light Microscopy

The tissue was immersion fixed in 4% paraformaldehyde 0.1M phosphate buffer solution (PBS), pH 7.4, for 10-12 hours. Following fixation the tissue was washed in 0.1M PBS, pH 7.4, dehydrated in an ascending series of ethanol, and embedded in paraffin. Paraffin sections were cut 6 μm thick and mounted on glass slides. After deparaffinization with graded concentrations of xylene and ethanol, slides were immersed in 3% hydrogen peroxide in methanol for 20 minutes at room temperature to block endogenous peroxide activity. The slides were then incubated with 2% non-fat dry milk and 2% cold water fish gelatin in 0.1 M PBS for 30 minutes to reduce non-specific background staining. Primary antibodies, rabbit anti-rat ET receptor type A (1:100) or rabbit anti-rat ET receptor type B (1:100) (Alomone Labs, Jerusalem), were incubated in damp chamber at 4ºC overnight. The treated slides were then incubated with biotinylated link antibody for 30 minutes at room temperature, then incubated with peroxidase-labeled streptavidin for 30 minutes at room temperature. Peroxidase activity was visualized by the 3-amino-9-ethylcarbazole (AEC) substrate-chromogen system.

Transmission Electron Microscopy

Normal dog eyes (n=5) from 5 dogs and glaucomatous dog eyes (n=5) from 5 dogs were collected (Tables 2-3 and 2-4).

The tissue was immersion fixed in 4% paraformaldehyde 0.1M PBS, pH 7.4, for 10-12 hours. Following fixation the tissue was washed in 0.1M sodium cacodylate, pH 7.4, with 3.5% sucrose, 0.5% DMSO, and 0.5mM calcium chloride followed by incubation for 1 hour in 1% tannic acid in 0.1M sodium-maleate buffer, pH 6.0. It was then dehydrated in an ascending series of ethanol. At 70% ethanol, 1% p-phenylenediamine (PPD) was added. This was followed by infiltration and embedding in LR White acrylic resin. Blocks were polymerized at 55º C for 12-20 hours. Ultrathin (80-90 nm) sections were collected on formvar carbon filmed, 150 mesh, nickel grids (Electron Microscopy Sciences, Fort Washington, PA). Sections were labeled by placing them on drops of primary antibody, rabbit anti-rat ET receptor type A (1:50) or rabbit anti-rat ET receptor type B (1:200) (Alomone Labs, Jerusalem), in damp chamber at 4ºC overnight. Goat anti-rabbit IgG labeled with 12 nm collodial gold (Jackson Immuno Research Laboratories, Inc., West Grove, PA) diluted 1:50 in 2% normal goat serum in Tris buffered saline (TBS), pH 7.6, were used as secondary antibodies. All rinses contained 0.05% Tween 20 and 0.2% Triton-X-100. For the negative controls the primary antibodies were excluded and the grids were incubated on PBS followed by incubation on colloidal gold labeled secondary antibody.

To assess aspecific binding, the primary antibodies were preabsorbed with the ET antigen. Detection of antibody binding to specimen after pre absorption is considered aspecific and not taken into account in the analysis.

Labeling of endothelial cells and smooth muscle cells was used as positive control since label of ET_A and ET_B receptors in these cell types have been reported extensively in

the literature. Grids were examined and photographed at 75 kV in a Hitachi H-7000 TEM (NSA Hitachi, Palo Alto, CA).

Morphology of Retina and Iridocorneal Angle

Retinas from 9 glaucomatous eyes and iridocorneal angles (ICAs) from 11 glaucomatous eyes were examined morphologically. Sections for evaluation of morphology were processed in the same manner as described above. Paraffin sections of the anterior segment were stained with Periodic Acid-Schiff (PAS) solution. Staining with toluidine blue was used for sections of both the anterior and posterior segment embedded in LR White resin. The degree of degeneration in the retina of the glaucoma dogs was graded in 3 groups according to severity: 1) No abnormalities in the nuclear layers, minor atrophy in the nerve fiber and ganglion cell layers; 2) Moderate atrophy and /or melding of the inner and outer nuclear layers; 3) Marked atrophy of all retinal layers. The degree of degeneration of the retina was correlated to the ET-1 levels in aqueous humor and vitreous (see Results; Endothelin-1 levels in aqueous humor and vitreous).

Endothelin Receptor Protein Expression in the Retina and Choroid

Normal dog eyes (n=11) from 11 dogs and glaucomatous dog eyes (n=13) from 13 dogs were used for protein analysis of the retina and choroid (Tables 2-3 and 2-4). The samples were stored in three different ways; 1) snap-freezing of the retina and choroid in liquid nitrogen with no preservative, 2) separation of the retina and choroid prior to freezing with no preservative, 3) separation of the retina and choroid and put in RNaLater solution (Ambion, Austin, TX) prior to freezing**.** The samples were stored at -80º C until analysis.

Protein Extraction

The protein was either extracted form tissue that was frozen without preservative or from tissue where retina and choroid were separated prior to freezing and stored with or without preservative.

Protein extraction from snap-frozen retina and choroid with no preservative. Retina and choroid from each eye were separated prior to homogenization. The samples were sonicated (60 Sonic Dismembrator, Fischer, Atlanta, GA) in 400-500 µL of Laemmli sample buffer (Bio-Rad Laboratories, Hercules, CA) containing 50 µL β-mercaptoethanol, 150 µL protease inhibitor cocktail [1 tablet Complete Mini EDTA-free (Roche, Chicago IL) dissolved in 1 mL distilled water], 10 µL aprotinin (10mg/mL), 10 µL leupeptin (10mg/mL), and 10 µL phenylmethylsulfonyl fluoride (PMSF) (40mg/mL) per mL of sample buffer. The samples were centrifuged and the supernatant was transferred into fresh tubes for Bradford colorimetric protein assay (Bio-Rad Laboratories, Hercules, CA).

Protein isolation from retina and choroid that was separated prior to freezing and stored with or without preservative. The tissue was homogenized in 1 mL of TRIZOL ™ Reagent (Total RNA Isolation Reagent, Life Technologies, Gaithersburg, MD) per 50-100 mg of tissue using a power homogenizer (Ultrasonic celldisrupter, Heat Systems, Ultrasonics Inc., Pharmingdale, NY) following the protocol supplied by the manufacturer. Tissue treated with TRIZOL ™ Reagent and chloroform for RNA extraction (see Endothelin Receptor mRNA Expression in the Retina) separated into an aqueous phase and an organic phase. After removal of the aqueous phase, containing RNA, the proteins in the organic phase were recovered by precipitation with isopropanol. Protein

content was determined by Bradford colorimetric protein assay (Bio-Rad Laboratories, Hercules, CA).

Western Blot

The protein samples were loaded on a 4% stacking, 10% resolving Tris-HCl ready gel (Bio-Rad Laboratories, Hercules, CA). Each gel was loaded with the same amount of protein for each sample. Kaleidoscope Prestained Standards (Bio-Rad Laboratories, Hercules, CA) were used as markers, and rat brain extract (SIGMA, Saint Louis, MI) as control on each gel. The electrophoresis was run at 100 V for 1 hour in a running buffer. The proteins in the gel were then electrotransferred on to a nitrocellulose membrane in a transfer buffer at 60 mA overnight.

Western-blotting was done using rabbit anti-rat ET receptor type A (1:100) and rabbit anti-rat ET receptor type B (1:200) (Alomone Labs, Jerusalem) as primary antibodies. The receptors were visualized using ECL Western Blotting System by following the manufacturer's protocol (Amersham Pharmacia, Piscataway, NJ). Donkey anti-rabbit horse radish peroxidase-linked antibody in Tris buffered saline/Triton X (TBS/T) (1:10,000) was used as secondary antibody. Detection reagents, supplied with the blotting kit, were incubated with the membrane for 1 minute. The membranes were then exposed to an x-ray film (BMX, Light 1; Fisher, Atlanta, GA) for 10, 30, and 120 minutes.

The films were scanned with GS-710 Calibrated Imaging Densitometer (Bio-Rad Laboratories, Hercules, CA) and the density of the ET receptor protein bands on each gel was determined using Scion Image for Windows (Scion Corporation, Frederick, MD). This program visualizes the density profile as a curve with optical density on the Y-axis and millimeter (mm) on the X-axis. The density of the bands was expressed as area under

the curve of each peak. The density measurements of the samples were normalized by dividing the value of each band with the value for the control (rat brain extract) of each gel. This resulted in a value expressed in arbitrary units (AU) for each sample. The AU for the ET receptors were compared between normal and glaucomatous retinal and choroidal samples.

Endothelin Receptor and Endothelin-1 mRNA Levels in the Retina

Isolation of Total RNA

Normal dog eyes (n=9) from 9 dogs and glaucomatous dog eyes (n=10) from 10 dogs were used for mRNA analysis (Tables 2-3 and 2-4). Total RNA was isolated from retinas that had been separated prior to freezing and stored dry or in RNALater (Ambion, Austin, TX) using TRIzol Reagent (Life Technologies, Gaithersburg, MD) following the protocol supplied by the manufacturer. The same retinal samples were used for mRNA determination as for Western Blot analysis (Tables 2-3 and 2-4).

The samples were homogenized in 1 ml of TRIZOL ™ Reagent per 50-100 mg of tissue using a power homogenizer (Ultrasonic celldisrupter, Heat Systems, Ultrasonics Inc., Pharmingdale, NY). The addition of chloroform followed by centrifugation separated the solution into an aqueous and an organic phase. RNA remained in the aqueous phase. After transfer of the aqueous phase, the RNA was recovered by precipitation with isopropyl alcohol. The organic phase was saved for protein isolation (see Endothelin Receptor Protein Expression in the Retina and Choroid). Potential contaminating DNA in the RNA samples was removed using the DNA-free kit from Ambion (Austin, TX). Optical density (OD) measurements were done on the RNA samples at 260nm.

Reverse Transcriptase Polymerase Chain Reaction

Primers for the reverse transcriptase polymerase chain reaction (RT-PCR) were designed using the software Vector NTI (Bethesda, MD) (Table 2-5). The primers used for the ET_A receptor were designed from the dog ET_A nucleotide sequence published by Louden et al. [97]. The ET_B primers were designed from a reported canine endothelin receptor B mRNA sequence (Gen Bank Accession number AF034530). The ET-1 primers were designed from canine ET-1 precursor, mRNA (Gen Bank Accession number AF333433). The amplicon sequences produced by the various primers were later used in the design of the primers for the Real Time PCR assay. All primers for the RT-PCR were purchased from Invitrogen Life Technologies (Frederick, MD).

Synthesis of cDNA from total RNA was done using the First strand cDNA synthesis kit from Amersham Pharmacia Biotech (Piscataway, NJ); the designed antisense primers were used to prime the cDNA synthesis.

PCR was performed in a total volume of 50 µL consisting of 6 µL cDNA, 5 µL 10X Buffer A [(500 mM KCl, 200 mM Tris-HCl,pH 8.4) Invitrogen, Carlsbad, CA], 1 µL 50 mM $MgCl_2$, 1 µL dNTP, 1 µL 5' primer (30 pmole/ µL), 1 µL 3' primer (30 pmole/ µL), and 0.5 µL Taq DNA polymerase (5,000 units/mL) (Invitrogen, Carlsbad, CA). All reactions were run in a DNA thermal cycler, Robocycler (Stratagene, La Jolla, CA), using 30 cycles of denaturation at 95º for 0.5 minute, annealing at 53º for 0.5 minute, and extension at 72º for 1.5 minutes. The last cycle contained 10 minutes at 72º. The PCR products were run on a 1 % agarose gel alongside a 1000 bp and a 100 bp DNA marker.

PCR products were recovered from the gel using the QIAEX II agarose gel extraction kit (Quigen Inc., Valencia, CA). Purified PCR products were ligated into a TA cloning vector, pCR®2.1, and transformed into TOP10 cells (Invitrogen, San Diego, CA).

Plasmids from clones containing inserts were isolated using the QIAprep Miniprep (Quigen Inc., Valencia, CA). The inserts were identified by restriction enzyme digestion with EcoR1 (Promega, Madison, WI) and subsequent agarose gel analysis. Plasmid DNA was then used to evaluate the primers for Real Time PCR.

Real Time Polymerase Chain Reaction

Primers and probes for the Real Time PCR were designed for the amplicons described above using Primer Express for Mac (Perkin-Elmer Applied Biosystems Inc, Foster City, CA) (Table 2-5). The primers and fluorogenic probes for the Real Time PCR were purchased from Perkin-Elmer Applied Biosystems Inc. (Foster City, CA). Random hexadeonucleotides ($pd(N)_6$ primers provided with the Amersham kit were used to prime the cDNA synthesis.

The Real Time probes had a reporter dye (6-FAM) conjugated to the 5' end and a quencher dye (TAMRA) conjugated to the 3' end. The principle of the Taqman system is that the fluorescence from the reporter dye is quenched by the quencher dye as long as the dyes are nearby to each other. The specific probe binds to the cDNA being amplified. When the Taqman polymerase replicates the target cDNA it cleaves the probe that is bound to the cDNA. This results in separation of the reporter and quencher dyes allowing the fluorescence of the reporter dye to be measured. The fluorescence increases in each cycle in proportion to the rate of probe cleavage.

The Real Time PCR was performed in a total volume of 25 µL consisting of 2X Taqman Universal PCR Master Mix, 300nM each of forward and reverse primers, 80 pM of fluorogenic probe, and 3 ng of template. Ribosomal RNA (rRNA) 18S was used as an endogenous control and active reference to normalize quantities of cDNA. In the reaction for the 18S rRNA the primers and probes were replaced with 20X Eukaryotic 18S rRNA

Endogenous Control (Applied Biosystems, Foster City, CA). The Thermal Profile for the Real Time PCR was 1 cycle for 2 min at 50º, 1 cycle for 10 min at 95º, followed by 40 cycles involving 15 sec at 95º and 1 min at 60º for each cycle. Fluorescence for each cycle was quantitatively analyzed on a Gene Amp 5700 sequence detection system (Perkin-Elmer Applied Biosystems Inc, Foster City, CA). The relative amount of cDNA in the samples was determined by the threshold cycle (C_T). The C_T is defined as the fractional cycle number at which the level of fluorescence released from the Real Time Probe surpasses the background threshold (Figure 2-1). The higher the starting copy number of the nucleic acid target, the sooner a significant increase in fluorescence is observed. In other words, the higher amount of cDNA in the sample, the lower the C_T value.

Each sample was run in triplicate to determine reproducibility of the PCR reaction. As a negative control the Real Time PCR was run without any cDNA as template. In addition, the Real Time PCR was run with total RNA, instead of cDNA, to rule out that genomic DNA was present and amplified in the samples. Cloned DNA sequences of both the ET_A and the ET_B receptor were amplified with primers and fluorogenic probes for the Real Time PCR to evaluate the selectivity and specificity of the primers and the fluorogenic probes. Amplification of both ET receptor DNAs were analyzed with various combinations of primers and probes, as shown in Table 2-6.

Additional controls analyzed aspecific amplification. One set of Real Time PCR reaction was carried out using DNAse treated total RNA, and a PCR reaction was also run with omission of cDNA , as a negative control. All reactions were run in triplicates**.**

Data Analysis

Morphology

The iridocorneal angles were qualitatively interpreted and a comparison was done between ICAs from normal and glaucomatous eyes. The degree of degeneration in the retina of the glaucoma dogs was graded in 3 groups according to severity: 1) No abnormalities in the nuclear layers, minor atrophy in the nerve fiber and ganglion cell layers; 2) Moderate atrophy and /or melding of the inner and outer nuclear layers; 3) Marked atrophy of all retinal layers. Spearman's correlation coefficient was used to determine any correlation between the degree of degeneration and the ET-1 levels in aqueous humor and vitreous.

The distribution of labeling of the ET_A and ET_B receptors in the retina and choroid was qualitatively interpreted in the normal and glaucomatous sections.

Endothelin-1 and Nitric Oxide Levels in Aqueous Humor and Vitreous

The data were analyzed using an ANOVA 2*2 factorial analysis in which the two factors of interest were the disease, with two levels (glaucomatous and normal), and breed, with two levels (Cocker and non-Cocker). In the presence of interaction the simple effects of each of the two factors were examined separately. The analyses were done on the means of right and left eye from each dog. All the statistical analyses were performed using SAS (version 8).

Endothelin Receptor Protein Expression in the Retina and Choroid

The expression of the ET receptors in arbitrary units (AU) versus controls were compared between normal and glaucomatous retinal and choroidal samples using the ANOVA 2*2 factorial design described above. Due to lack of tissue no analysis could be done including normal Cocker choroid. All analyses were done ignoring whether the

measurement was taken from left or right eye. In the case of interaction a separate analysis of the simple effects of each of the two factors, disease and breed, was done.

Endothelin-1 and ET Receptor mRNA Levels in the Retina

The ratios of the mRNA levels versus controls in AU were compared between normal and glaucomatous retinal samples using the ANOVA 2*2 factorial design described above. The variables were first log-transformed to improve the model-fit. All analyses were done ignoring whether the measurement was taken from left or right eye. In the case of interaction a separate analysis of the simple effects of each of the two factors, disease and breed, was done.

Table 2-1: Normal dogs in study.

Dog	Breed	Age	Sex	University	IOP in mm/Hg at enucleation
1	German Shepherd Mix	Adult	M	UF	OD: 15.7 OS: 17.7
2	Hound Dog	Adult	M	UF	OD: 11.3 OS: 15.7
3	Beagle	Adult	M	UF	OD: 21 OS: 10.3
4	Beagle	Adult	M	UF	OD: 17 OS: 20.7
5	Beagle	Adult	F	UF	OD: 9 OS: 10
6	Beagle	Adult	F	UF	OD: 14.7 OS: 15.3
7	Beagle	Adult	M	UF	OD: 19 OS: 18
8	Beagle	Adult	F	UF	OD: 16 OS: 16
10	Walker Hound	1 y	F	UF	OD: 14 OS: 17.5
11	Greyhound	10 y	F	UF	OS: 9
12	Greyhound	10 y	F	UF	OD: 8 OS: 7
13	Greyhound	1.5 y	F	UF	.
15	Walker Hound	1.5 y	F	UF	.
18	Hound Dog	2 y	F	UF	.
M1	Cocker Spaniel	4 y	M	MX	OD: 13 OS: 12
M2	Cocker Spaniel	6 y	M	MX	OD: 9 OS: 11
M3	Cocker Spaniel	4 y	M	MX	OD: 15 OS: 9
M4	Cocker Spaniel	3 y	M	MX	OD: 26 OS: 25
M5	Cocker Spaniel	6 y	F	MX	OD: 18 OS: 21

y, year; M, Male; F, Female; UF, Small Animal Clinical Sciences, University of Florida; MX, Universidad de Mexico, Mexico City; IOP, Intraocular pressure; OD, Right eye; OS, Left eye; ., Missing data point.

Table 2-2: Glaucoma dogs in study

Dog	Breed	Age	Sex	University	IOP at enucleation	ICA	Duration of disease	Fundus appearance
14	Cocker Spaniel	10 years	SF	UF	OD: 40	- [c]	1 y	- [c]
16	Bouvier de Flandres	3 years	CM	UF	OD: 29 (49) [a]	- [c]	3 mo	- [c]
17	Beagle	12 years	M	UF	OD: 30 (42) [a]	- [c]	10 y	- [c]
19	Cocker Spaniel	13 years	CM	UF	OS: 8 [b]	- [c]	> 4 y	- [c]
20	Cocker Spaniel	8 years	CM	UF	OS: 30 (48) [a]	- [c]	Chronic	- [c]
M6	Poodle	4 years	F	MX	OD: 34	Narrow	1 mo	Atrophy ONH Vascular attenuation.
21	Samoyed	6 years	SF	UF	OD: 41	- [c]	Chronic	- [c]
22	Cocker Spaniel	13 years	SF	UF	OD: 44	- [c]	Chronic	- [c]
23	Cocker Spaniel	12 years	SF	UF	OS: 28 (59) [a]	- [c]	3 mo	- [c]
24	Cocker Spaniel	8 years	SF	UF	OD: 50	-	2 mo	Retinal degeneration
25	Cocker Spaniel	15 years	SF	UF	OS: 45 (55) [a]	- [c]	3 mo	- [c]
26	Mix Terrier	8 years	SF	UF	OS: 30	- [c]	6 mo	Cupping ONH
27	Cocker Spaniel	6 years	SF	UF	OS: 37	-	6 mo	Cupping ONH
28	Basset	2 years	SF	UF	OS: 38	- [c]	6 mo	- [c]

y, year; M, Male; F, Female; UF, Small Animal Clinical Sciences, University of Florida; MX, Universidad de Mexico, Mexico City; IOP, Intraocular pressure; ICA, Iridocorneal angle; OD, Right eye; OS, Left eye; mo, month; ONH, Optic nerve head. [a] IOP prior to treatment; [b] No IOP prior to treatment; [c] Not visible due to corneal edema.

Table 2-3: Analyses on normal dogs.

Dog	ELISA ET-1 peptide and NO Aqueous humor/vitreous	Immunocytochemistry ET receptors Retina and choroid	Western Blot ET receptors Retina and choroid	Real Time PCR ET-1 mRNA Retina	Real Time PCR ET receptor mRNA Retina
1	OU	-	-	-	-
2	OU	-	-	-	-
3	OU	-	-	-	-
4	OU	-	-	-	-
5	OU	-	OS	-	-
6	OU	-	OD	-	-
7	OU	-	OD	OD	OD
8	OU	-	OD	OD	OD
10	OU	-	OS	OS	OS
11	OS	-	OD	OD	OS
12	OD	-	-	-	-
13	OS	-	-	-	-
15	OU	-	-	-	-
18	-	-	-	OD	-
M1	OS	OS	OS	OS	OS
M2	OD	OD	OD	OD	OD
M3	OD	OD	OD	OD	OD
M4	OS	OS	OS	OS	OS
M5	OS	OS	OS	OS	OS

OD, Right eye; OS, Left eye; OU, Both eyes; ET, Endothelin-1; NO, Nitric oxide; -, No analysis.

Table 2-4: Analyses on glaucomatous dogs.

Dog	ELISA ET-1 peptide and NO Aqueous humor/vitreous	Immunocytochemistry ET receptors Retina and choroid	Western Blot ET receptors Retina and choroid	Real Time PCR ET-1 mRNA Retina	Real Time PCR ET receptor mRNA Retina
14	OD	OD	OD	OD	OD
16	OD	-	OD	-	-
17	OD	-	OD	-	-
19	OS	OS	OS	OS	OS
20	-	OS	-	-	-
M6	OD	-	OD	OD	OD
21	-	-	OD	-	-
22	OD	OD	OD	OD	OD
23	OS	OS	OS	OS	OS
24	OD	-	OD	OD	OD
25	OS	-	OS	OS	OS
26	-	-	OS	OS	OS
27	OS	-	OS	OS	OS
28	OS	-	OS	OS	OS

OD, Right eye; OS, Left eye; ET, Endothelin-1; NO, Nitric oxide; -, No analysis.

Table 2-5: Primers and fluorogenic probes.

Reagent	Primer Sequence	Amplicon size
	Reverse Transcription PCR	
ET_A receptor		380 bp
Sense	5'-GTG GCT CTT CGG GTT CTA TT-3'	
Anti-sense	5'-GGC ATG ACT GGA AAC AAT TT-3'	
ET_B receptor		566 bp
Sense	5'-GAA TTA AAG GAA TTG GGG TTC C-3'	
Anti-sense	5' - GCA GTT TTT GAA TCT TTT GCT C- 3'	
	Real Time PCR	
ET_A receptor		81 bp
Sense	5'-CTT GAG AAT TGC CCT CAG TGA A-3'	
Anti-sense	5'-GCA AAA ATT ACA ACC AAG CAG AAA-3'	
Fluorogenic Probe	5'-TTT GCC ACT TCT CGA CGC TGC TTA AGA T-3'	
ET_B receptor		76 bp
Sense	5'-GGC CGT GGG TTT TGA TAT GA-3'	
Anti-sense	5'-CTG GGT AGG ATG AAG CAA GCA-3'	
Fluorogenic Probe	5'-AAC CAT TGA CTA CAA AGG ACG TTA CCT GCG A-3'	
Endothelin-1		86 bp
Sense	5'-TCC TGC TCT TCC CTG ATG GA-3'	
Anti-sense	5'-GGA ACA ATG TGC TCA GGA GTG TT-3'	
Fluorogenic Probe	5'-TGT CTA CTT CTG CCA CCT TGA CAT CAT CTG-3'	

Table 2-6: The controls for the Real Time PCR were run with the templates listed in the table. The templates were run with various mixes of primers and probes as listed in the table. ET_A, Endothelin A; ET_B, Endothelin B; 18S, 20X Eukaryotic 18S rRNA Endogenous Control.

Template	Primer/probe mix				
ET_A receptor sequence	A Primer A Probe	A Primer B Probe	B Primer B Probe	B Primer A Probe	18S
ET_B receptor sequence	A Primer A Probe	A Primer B Probe	B Primer B Probe	B Primer A Probe	18S
No Template	A Primer A Probe	B Primer B Probe	18S		
Total RNA	A Primer A Probe	B Primer B Probe	18S		

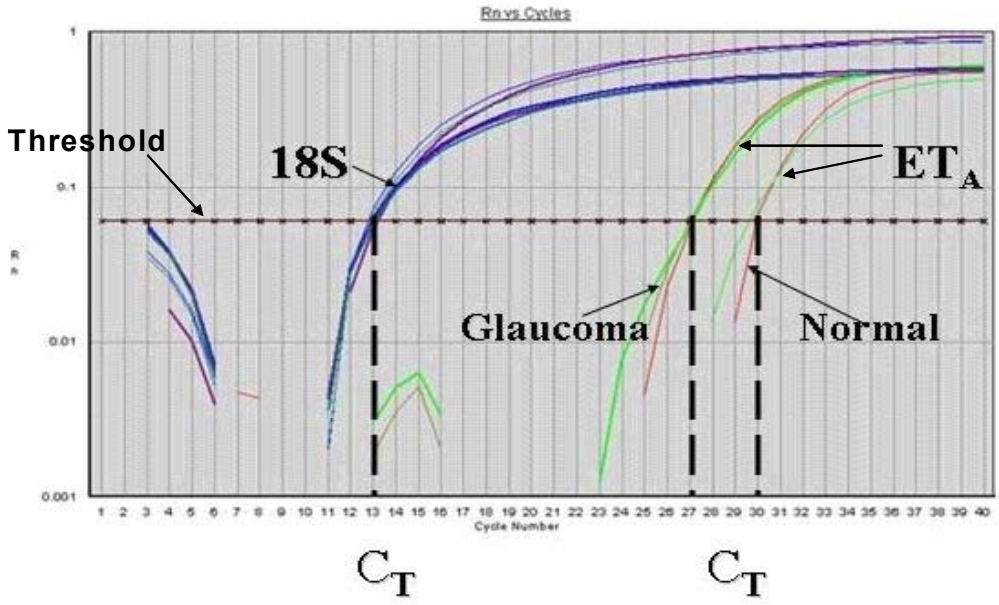

Figure 2-1: Real Time PCR amplification curves of a normal and a glaucomatous retina for the ET_A receptor and 18S rRNA. ET_A, Endothelin receptor A; 18S, 20X Eukaryotic 18S rRNA Endogenous Control; C_T, threshold cycle.

CHAPTER 3
RESULTS

Morphology

Iridocorneal Angle

The iridocorneal angles (ICAs) of the clinically normal dogs revealed no abnormalities (Figure 3-1). The outflow apparatus, including trabecular meshwork and scleral venous plexus was distorted in all glaucomatous eyes (Figure 3-2). The anterior corneoscleral trabecular meshwork was completely collapsed in all eyes. The uveoscleral meshwork was completely collapsed in some eyes, while in others it still had openings of varying sizes (Figure 3-3). In most dogs the remaining trabecular cells had a normal, slender appearance, while they were more rounded in other eyes. Melanin-containing cells were clustered in the angle (Figure 3-4). Anterior synechia were present in several globes (Figures 3-4, 3-5 and 3-6).

The termination of Descemet's membrane was enlarged in four of the six glaucoma Cocker eyes, but had normal thickness in all eyes of the non-Cocker glaucoma group (Figures 3-4 and 3-5). It was retracted in several eyes (Figures 3-4 and 3-6). The ciliary cleft in all eyes, except for the Beagle (dog 17) was covered by light to heavy amount of connective tissue (Figure 3-4).

Retina.

The clinically normal dogs showed no abnormalities of the retina (Figure 3-7). Retinal changes in the glaucomatous dogs varied from minor thinning of the ganglion cell layer and disorganization of the inner nuclear layer, to atrophy of all retinal layers

(Figures 3-8 and 3-9). The peripheral retina was most affected in all eyes with complete atrophy in 5 cases. A thinning of the inner plexiform layer resulting in closer apposition of the nuclear layers, melding, was noticed as an early sign of atrophy, while the nuclear layers still were intact. The photoreceptor nuclei were normal, with some chromatin clumping, in all glaucomatous eyes. The outer segments of the photoreceptors were swollen in several eyes.

The degree of degeneration in the central retina of the glaucoma dogs was graded in 3 groups according to severity: 1) No abnormalities in the nuclear layers, minor atrophy in the nerve fiber and ganglion cell layers; 2) Moderate atrophy and /or melding of the inner and outer nuclear layers; 3) Marked atrophy of all retinal layers (Table 3-1). There was a significant correlation at the 0.1 significance level between the total degree of central retinal degeneration, and total aqueous humor and vitreal ET-1 levels of glaucomatous dogs (Spearman correlation coefficient 0.6, $p = 0.0901$).

Endothelin Receptors in the Retina and Choroid

Evaluation of Endothelin Antibodies using Light Microscopy

Light microscopy showed a weak but distinct label for ET receptors of small scleral vessels of a normal Beagle. No labeling was detected when the primary antibody was omitted. (Figure 3-10).

Evaluation of Endothelin Antibodies using Transmission Electron Microscopy

There was no labeling when PBS was used instead of the primary antibody. The mixture of ET_A antibody with its antigen resulted in very minor labeling. In contrast, the mixture of ET_B antibody with its antigen showed only a small decrease in labeling as compared to the primary antibody. Intensity of the specific labeling corresponded to the concentration of the antibody dilution. The most distinct and specific labeling was

achieved with the ET_B antibody at a dilution of 1:200. The use of detergents was necessary to minimize extensive nonspecific labeling by the ET_B antibody. The difficulties in achieving an optimal protocol with reliable specific label by the ET_B antibody excluded any quantitative analysis of the immunocytochemistry.

Localization of Endothelin Receptors using Transmission Electron Microscopy

The distribution of ET receptor labeling was similar in the normal and glaucomatous sections for both receptors.

ET_A receptor

The ET_A receptor was observed in smooth muscle cells and pericytes of vessels in both the retina and the choroid.

ET_B receptor

Localization of the ET_B receptor occurred within vascular endothelium, smooth muscle, and pericytes of vessels in both the retina and the choroid (Figure 3-11).

Endothelin-1 Levels in Aqueous Humor, Vitreous and Retina

The ranges for aqueous humor and vitreal ET-1 levels all normal samples were 0.87 - 6.3 and 0.23 - 6.83 pg/mL respectively. The ET-1 aqueous humor and vitreal ranges for all glaucomatous samples were 1.91 - 14.56 and 1.13 - 5.96 pg/mL respectively. The ET-1 levels for normal and glaucomatous dogs are shown in Tables 3-2 and 3-3 and the least-squares means from the ANOVA 2*2 factorial analysis are plotted in Figures 3-12 and 3-13.

Analysis of Aqueous Humor

The mean (± STD) normal and glaucomatous canine ET-1 aqueous levels for all breeds were 2.8 (± 1.52) and 6.86 (± 3.46) pg/mL respectively. There was a significant increase in ET-1 for the glaucomatous eyes (versus the normal eye) ($p = 0.0004$). The

differences between least-squares means were also analyzed for each level of the two factors due to the presence of interaction. In the Cocker group, there was a significant increase in ET-1 for the glaucomatous eyes ($p = 0.0003$), while for the non-Cocker group the difference between the normal and glaucomatous eyes was not significant (Figure 3-12). There was no significant difference between the Cocker group and the non-Cocker group nor for the normal or for the glaucomatous eyes.

Analysis of Vitreous

The mean (± STD) normal and glaucomatous canine ET-1 vitreous levels for all breeds were 1.56 (± 1.86) and 3.47 (± 1.57) pg/mL respectively. The increase in the glaucomatous eyes was considered statistically significant ($p = 0.0023$). Due to the presence of interaction between the two factors, breed and disease, the differences between least-squares means were analyzed for each level of the two factors. In the Cocker group, there was a significant increase in ET-1 for the glaucomatous eyes ($p = 0.0005$), while for the non-Cocker group the difference between the normal and glaucomatous eyes was not significant (Figure 3-13). There was a significant difference between the Cocker group and the non-Cocker group ($p = 0.0099$) for the normal eyes but not for the glaucomatous eyes

Endothelin-1 mRNA Levels in the Retina

There was insufficient statistical evidence to indicate any significant breed or disease effect on the retinal mRNA levels of ET-1; breed by disease interaction was not found significant either (Table 3-4).

Correlation of Retinal Degeneration and ET-1 Levels in Aqueous Humor and Vitreous

The degree of degeneration of the central dorsal retina and central ventral retina was correlated to the ET-1 levels in aqueous humor and vitreous. The grading of the retinal degeneration is described in the Morphology section and the ranking of the glaucomatous central retinas is shown in Table 3-1. The gradual decrease in thickness of the cell layers in the periphery of normal eyes lead to difficulties in comparing and grading any changes in the periphery of the glaucomatous eyes. The peripheral retina was therefore excluded from the correlation analysis. There was a significant correlation at the 0.1 significance level between the total degree of central retinal degeneration, and total aqueous humor and vitreal ET-1 levels of glaucomatous dogs [Spearman correlation coefficient 0.6, $p = 0.0901$) (Figure 3-14)].

Nitric Oxide Levels in Aqueous Humor and Vitreous

The ranges for all normal aqueous humor and vitreal NO levels were 1.41 - 11.46 and 0.24 - 16.47 μM respectively. The NO aqueous humor and vitreal ranges for all glaucomatous dogs were 2.25 - 37.94 and 1.07 - 46.98 μM respectively. The NO levels for normal and glaucoma dogs are shown in Tables 3-5 and 3-6 and the least-squares means from the ANOVA 2*2 factorial analysis are plotted in Figures 3-15 and 3-16.

Analysis of Aqueous Humor

The mean normal and glaucomatous canine NO aqueous levels for all breeds were 3.9 (± 1.93) and 12.48 (± 13.46) μM respectively. The increase in the glaucomatous eyes of the non-Cocker group was considered statistically significant ($p = 0.0476$). There was insufficient evidence to indicate that the two factors, disease and breed, interacted (Figure 3-15).

Analysis of Vitreous

The mean normal and glaucomatous canine NO vitreal levels for all breeds were 4.47 (± 2.92) and 15.33 (± 16.22) μM respectively. The increase in the glaucomatous eyes was considered statistically significant ($p = 0.0085$) but due to the presence of interaction, the differences between least-squares means were analyzed for each level of the two factors. In the non-Cocker group, there was a significant increase in NO for the glaucomatous eyes ($p = 0.0148$), while for the Cockers the difference between the normal and glaucomatous eyes was not significant (Figure 3-16). There was no significant difference between the Cocker group and the non-Cocker group neither for the normal eyes nor for the glaucomatous eyes.

Endothelin Receptor Protein Expression in the Retina and Choroid

The ratios of the expression levels of ET_A versus control, and ET_B versus control in the retina and choroid for normal and glaucoma dogs are shown in Tables 3-7 and 3-8 and the least-squares means from the ANOVA 2*2 factorial analysis model are plotted in Figures 3-17 and 3-18.

ET_A Receptors in the Retina

There was a statistically insignificant reduction of the ET_A receptors in the retina of the glaucomatous eyes. There was no evidence to indicate that the two factors interacted (Figure 3-17).

ET_B Receptors in the Retina

There was a significant difference in the ET_B receptors between the glaucomatous and normal dogs ($p = 0.0386$); since the interaction between the breed and disease was significant, the simple effects of the two factors were investigated separately. For the non-Cocker group, there was a significant decrease in the ET_B receptors between the

glaucomatous and normal dogs ($p = 0.0072$). Also for the normal eyes, the level of ET_B receptors was significantly lower for the Cocker group versus the non-Cocker group. ($p = 0.0025$) (Figure 3-18).

ET_A and ET_B Receptors in the Choroid

Choroidal tissues from normal and glaucomatous dogs in the non-Cocker group were compared. There was a decrease of both receptors in the glaucomatous eyes that was not statistically significant. The Cocker group had a higher expression of the ET_A receptor and a lower expression of the ET_B receptor than the non-Cocker group, in a comparison of glaucomatous choroidal tissue. Neither difference between the two groups was significant.

Endothelin Receptor mRNA Levels in the Retina

Parameters for normal and glaucomatous dogs are shown in Tables 3-9 and 3-10 and the least-squares means from the ANOVA 2*2 factorial analysis model are plotted in Figures 3-19 and 3-20.

Evaluation of the Real Time PCR Reaction

Endothelin A receptor plasmid DNA was amplified with a mix of the ET_A receptor primer and ET_A receptor fluorogenic probe (A/A), showing an early amplification of the DNA sequence above background in the 13th cycle of the Real Time PCR (Figure 3-21). The mixtures of the ET_A receptor primer with ET_B receptor fluorogenic probe (A/B), and the ET_B receptor primer with ET_A receptor fluorogenic probe (B/A), gave only background noise below detectable level. DNA amplification was detected above background when the ET_B receptor primer with ET_B receptor fluorogenic probe (B/B) was used on ET_A DNA. Amplification above background was also seen of 18S rRNA using the 20X Eukaryotic 18S rRNA Endogenous Control on ET_A DNA.

Endothelin B receptor plasmid DNA was amplified with the mix of ET_B receptor primer with ET_B receptor probe (B/B) showing an early amplification of the DNA sequence above background in the 12th cycle of the Real Time PCR (Figure 3-22). The mixtures A/B and B/A give only background noise below detectable level. Amplification was detected above background when the ET_A receptor primer with ET_A receptor probe (A/A) was used on ET_B cDNA. Amplification above background was also seen of 18S rRNA using the 20X Eukaryotic 18S rRNA Endogenous Control on ET_B cDNA.

Since the amplifications by the mismatched primer/fluorogenic probes were detected after the 29th cycle for both ET receptors, these signals are probably due to PCR artefacts. The difference with the true match of primer and fluorogenic probe is more than 15 cycles, showing that there was no cross-reactivity between different primers and probes.

No amplification curves of the ET receptors were seen when the Real Time PCR, with the primers and probes for the ET receptors and 18S, was run with no template. This showed that there was no nonspecific amplification due to contamination of solutions. When using total RNA as template, with the primers and probes for the ET receptors and 18S, no amplification curves were seen for the receptors (Figure 3-23). This proved that there was no genomic DNA in the RNA samples. Traces of 18S rRNA were amplified in both reactions.

Tissue

The tissue had been stored in two different ways, i.e. frozen dry or frozen in RNase Later preservative. It was therefore necessary to check whether this affected the RNA in the samples. This was done by extracting RNA from two normal dog retinas, one that had been stored frozen in the preservative RNAlater (Retina 1) and the other (Retina 2) stored

frozen dry without any preservative. The yields of total RNA from the samples were 2.1 and 1.9 mg/mL respectively. Both samples were split in half. One half of each sample was treated with DNase to eliminate any residual genomic DNA. RT-PCR was then run on total RNA and DNAse treated RNA for each sample (Figure 3-24). The primers used for the reaction are listed in Table 2-5. The detected bands of the ET receptors and β-actin were identical for all samples indicating that the two methods of storage did not alter the size or configuration of the mRNA.

The same samples (Retina 1 and 2) were run with the Real Time PCR as for the RT-PCR. Both samples were run in triplicate. The primers used for the reaction are listed in Table 2-5. The mean C_T values for the ET_A receptor from the two samples were 28.5 (Retina 1) and 28.64 (Retina 2) respectively (Figure 3-25) and for the ET_B receptor 26.8 (Retina 1) and 26.6 (Retina 2) respectively. This showed that the two methods of storage had minimal effect on the initial amount of mRNA and amplification of the cDNA of the samples.

ET_A Receptor mRNA in the Retina

There was a significant increase in the mRNA levels ($p = 0.0347$) in the glaucomatous retinas but it was confounded by interaction. For the Cocker group there was a highly significant increase in mRNA levels ($p = 0.0064$) between the glaucomatous and normal eyes. There was a small, but statistically insignificant, increase in the non-Cocker group. There was also a significant difference in the glaucomatous eyes with the Cockers having significantly higher levels, at a significance level of 0.1, than the non-Cocker group ($p = 0.0917$) (Figure 3-19).

ET_B Receptor mRNA in the Retina

There was a significant increase in the mRNA levels at a significance level of 0.1 ($p = 0.0854$) in the glaucomatous retinas, but it was confounded by interaction. For the Cocker group the mRNA level was significantly higher for the glaucomatous eyes than for the normal eyes ($p = 0.0075$). The mRNA level in glaucomatous eyes of the non-Cocker group was slightly lower than for the normal eyes, yet not significant. There was no significant difference in mRNA levels in normal or glaucomatous eyes between the Cocker group and the non-Cocker group (Figure 3-20).

Summary of Results

Results for all breeds are summarized below.

- All iridocorneal angles in the glaucomatous eyes were distorted with varying degree of collapse.
- Retinal changes in the glaucomatous eyes varied from minor thinning of the ganglion cell layer and disorganization of the inner nuclear layer, to complete atrophy of all retinal layers. The peripheral retina was most affected in all eyes. The degree of degeneration of the central retina was positively correlated to the ET-1 levels in aqueous humor and vitreous.
- The location of ET receptor labeling was similar in the normal and glaucomatous retinal and choroidal sections for both ET receptors.
- The results for the glaucomatous eyes separating the Cocker and the non-Cocker group are shown in Table 3-11.

Table 3-1: Ranking of degree of degeneration in the glaucomatous retinas.

Dog	Dorsal Central	Ventral Central	Total mean
14	2	2	2
16	1	2	1.5
17	1	2	1.5
19	1	1	1
M6	1	2	1.5
22	2	2	2
23	3	3	3
24	2	2	2
25	1	2	1.5

Table 3-2: Endothelin-1 levels in pg/mL for normal dogs. BQL, Below limit of quantification; ., Missing data point; OS, Left eye; OD, Right eye; ET-1, Endothelin-1.

Dog	Breed	ET-1 aqueous	ET-1 vitreous
1OS	German Shepherd Mix	2.01	1.53
1OD		3.56	0.7
2OS	Hound Dog	1.95	0.7
2OD		3.5	1.65
3OS	Beagle	2.43	0.64
3OD		2.31	2.49
4OS	Beagle	1.42	BQL
4OD		2.07	6.83
5OS	Beagle	2.84	1.24
5OD		1.77	3.92
6OS	Beagle	2.37	1.53
6OD		1.24	5.64
7OS	Beagle	2.49	1.47
7OD		1.65	3.38
8OS	Beagle	2.73	2.19
8OD		3.38	0.4
10OS	Walker Hound	4.81	4.63
10OD		6.3	3.02
11OS	Greyhound	5.29	4.75
12OS	Greyhound	5.88	1.06
12OD		5.82	2.84
15OS	Walker Hound	2.11	.
15OD		1.67	.
M1 OS	Cocker	1.7	BQL
M2 OD	Cocker	0.87	0.32
M3 OD	Cocker	0.99	0.23
M4 OS	Cocker	2.31	0.48
M5 OS	Cocker	3.04	0.29
Non-cocker mean (±STD)		3.03 (±1.54)	2.53 (±1.82)
Cocker mean (±STD		1.78 (±0.91)	0.33(±0.11)
Total mean (±STD)		2.80 (±1.52)	1.56 (±1.86)

Table 3-3: Endothelin-1 levels in pg/mL for glaucomatous dogs. OD, Right eye; OS, Left eye; ET-1, Endothelin-1.

Dog	Breed	ET-1 aqueous	ET-1 vitreous
14 OD	Cocker	6.7	5.2
19 OS	Cocker	2.52	2.68
22 OD	Cocker	4.95	2.09
23 OS	Cocker	9.67	4.06
24 OD	Cocker	6.8	2.88
25 OS	Cocker	8.58	3.16
27 OS	Cocker	14.56	5.96
M6 OD	Poodle	8.48	1.7
16 OD	Bouvier de Flandres	1.91	1.13
17 OD	Beagle	5.55	4.05
28 OS	Basset	5.6	5.28
Non-cocker mean (±STD)		5.38 (±2.69)	3.04 (±1.96)
Cocker mean (±STD)		7.7 (±2.52)	3.72 (±1.42)
Total mean (±STD)		6.86 (±3.49)	3.47 (±1.57)

Table 3-4: Mean ratios of ET-1/ 18S mRNA in arbitrary units for normal and glaucomatous retinal samples. ET-1, Endothelin-1; 18S, 20X Eukaryotic 18S rRNA Endogenous Control.

	Normal			Glaucoma	
Dog	Breed	ET-1/18S	Dog	Breed	ET-1/18S
7	Beagle	2.05	14	Cocker	2.15
8	Beagle	2.14	19	Cocker	2.12
10	Walker Hound	2.16	22	Cocker	1.94
11	Greyhound	2.19	23	Cocker	2.18
18	Hound Dog	1.95	24	Cocker	2.23
M1	Cocker	2.06	25	Cocker	1.82
M2	Cocker	2.07	26	Mix Terrier	2.09
M3	Cocker	2.12	27	Cocker	2.07
M4	Cocker	2.09	28	Basset	2.18
M5	Cocker	2.0	M6	Poodle	2.21
Non-cocker mean(±STD)		2.1 (±0.1)	Non-cocker mean (±STD)		2.14 (±0.07)
Cocker mean (±STD)		2.07 (±0.04)	Cocker mean (±STD)		2.07 (±0.16)
Total mean (±STD)		2.08 (±0.07)	Total mean (±STD)		2.1 (±0.13)

Table 3-5: Nitrate (NO) levels in μM of normal dogs. BQL, Below limit of quantification; NO, Nitric oxide; ., Missing data point; OS, Left eye; OD, Right eye.

Dog	Breed	NO aqueous	NO vitreous
1OS	German Shepherd Mix	3.67	2.7
1OD		2.51	3.92
2OS	Hound Dog	1.41	10.91
2OD		3.75	4.11
3OS	Beagle	1.41	1.19
3OD		7.02	2.32
4OS	Beagle	.	3.26
4 OD		.	4.3
5 OS	Beagle	.	BQL
5 OD		.	2.23
6OS	Beagle	11.46	4.4
6OD		3.84	1
7OD	Beagle	2.75	3.73
8OS	Beagle	2.58	BQL
8OD		2.58	9.02
10OS	Walker Hound	3.73	3.26
10OD		7.6	4.4
11OS	Greyhound	8.03	0.24
12OS	Greyhound	7.61	2.79
12OD		3.25	16.47
13 OS	Greyhound	.	1.66
15OS	Walker Hound	BQL	.
15OD		3.08	.
M1 OS	Cocker	1.58	5.18
M2 OD	Cocker	2.75	8.36
M3 OD	Cocker	3.42	7.94
M4 OS	Cocker	2.5	3.08
M5 OS	Cocker	3.17	2.08
Non-cocker mean (±STD)		4.51 (±2.09)	4.12 (±3.0)
Cocker mean (±STD)		2.68 (±0.71)	5.33 (±2.81)
Total mean (±STD)		3.9 (±1.93)	4.47 (±2.92)

Table 3-6: Nitrate (NO) levels in μM. of glaucomatous dogs. BQL, Below limit of quantification; NO, Nitric Oxide; ., Missing data point; OS, Left eye; OD, Right eye.

Dog	Breed	NO aqueous	NO vitreous
14 OD	Cocker	6.52	9.28
16 OD	Bouvier de Flandres	6.10	12.8
17 OD	Beagle	8.7	.
M6 OD	Poodle	34.17	33.16
19 OS	Cocker	4.34	7.02
22 OD	Cocker	8.53	10.46
23 OS	Cocker	2.25	1.83
24 OD	Cocker	3.75	1.07
25 OS	Cocker	37.94	46.98
Non-cocker mean (±STD)		16.33 (±15.51)	22.98 (±14.4)
Cocker mean (±STD)		10.56 (±13.6)	12.77 (±17.19)
Total mean (±STD)		12.48 (±13.46)	15.33 (±16.22)

Table 3-7: Ratios of ET_A receptor/ control protein in arbitrary units for normal and glaucomatous retinas and choroids. ET_A, Endothelin A; **.**, Missing data point.

	Normal				Glaucoma		
Dog	Breed	ET_A /control Retina	ET_A /control Choroid	Dog	Breed	ET_A/control Retina	ET_A/control Choroid
5	Beagle	2.26	1.16	14	Cocker	0.87	5.66
6	Beagle	2.83	2.44	16	Bouvier de Flandres	.	0.29
7	Beagle	3.69	7.26	17	Beagle	4.04	0.43
8	Beagle	.	6.55	19	Cocker	0.04	5.10
10	Walker Hound	0.78	7.61	21	Samoyed	1.25	1.95
11	Greyhound	.	6.08	22	Cocker	0.49	0.36
M1	Cocker	3.69	.	23	Cocker	1.90	6.06
M2	Cocker	3.29	.	24	Cocker	0.22	4.25
M3	Cocker	2.36	.	25	Cocker	2.49	5.27
M4	Cocker	2.49	.	26	Mix Terrier	1.08	6.7
M5	Cocker	1.11	.	27	Cocker	6.97	8.69
				28	Basset	1.38	8.18
				M6	Poodle	0.48	.
Non-cocker mean (±STD)		2.39 (±1.22)	5.18 (±2.71)	Non-cocker mean (±STD)		1.64 (±1.38)	3.51 (±3.68)
Cocker mean (±STD)		2.59 (±0.99)	N/A	Cocker mean (±STD)		1.86 (±2.43)	5.06 (±2.49)
Total mean (±STD)		2.04 (±1.87)	N/A	Total mean (±STD)		1.77 (±1.98)	4.41 (±2.99)

Table 3-8: Ratios of ET_B receptor/ control protein in arbitrary units for normal and glaucomatous retinas and choroids. ET_B, Endothelin B; **.**, Missing data point.

	Normal				Glaucoma		
Dog	Breed	ET_B /control Retina	ET_B /control Choroid	Dog	Breed	ET_B/control Retina	ET_B/control Choroid
5	Beagle	5.17	2.18	14	Cocker	0.35	0.06
6	Beagle	0.98	0.95	16	Bouvier de Flandres	.	0.17
7	Beagle	2.04	1.44	17	Beagle	0.86	0.22
8	Beagle	1.35	0.23	19	Cocker	0.12	0.03
10	Walker Hound	0.84	0.35	21	Samoyed	0.81	1.24
11	Greyhound	.	0.10	22	Cocker	0.26	0.09
M1	Cocker	0.14	.	23	Cocker	0.12	0.08
M2	Cocker	0.12	.	24	Cocker	0.09	0.29
M3	Cocker	0.16	.	25	Cocker	0.08	0.04
M4	Cocker	0.14	.	26	Mix Terrier	0.28	0.11
M5	Cocker	0.21	.	27	Cocker	0.02	0.08
				28	Basset	0.07	0.22
				M6	Poodle	0.05	.
Non-cocker mean (±STD)		2.08 (±1.79)	0.88 (±0.82)	Non-cocker mean (±STD)		0.41 (±0.39)	0.39 (±0.48)
Cocker mean (±STD)		0.16 (±0.03)	N/A	Cocker mean (±STD)		0.15 (±0.11)	0.09 (±0.09)
Total mean (±STD)		1.12 (±1.57)	N/A	Total mean (±STD)		0.26 (±0.29)	0.22 (±0.33)

Table 3-9: Mean ratios of ET_A receptor/ 18S mRNA in arbitrary units for normal and glaucomatous retinal samples. ET_A, Endothelin A; 18S, 20X Eukaryotic 18S rRNA Endogenous Control.

	Normal			Glaucoma	
Dog	Breed	ET_A /18S	Dog	Breed	ET_A /18S
7	Beagle	2.18	14	Cocker	1.80
8	Beagle	2.32	19	Cocker	1.85
10	Walker Hound	2.00	22	Cocker	2.03
11	Greyhound	2.08	23	Cocker	1.87
M1	Cocker	2.19	24	Cocker	1.92
M2	Cocker	2.09	25	Cocker	2.07
M3	Cocker	2.12	26	Mix Terrier	2.15
M4	Cocker	2.21	27	Cocker	2.17
M5	Cocker	2.31	28	Basset	2.01
			M6	Poodle	2.14
Non-cocker mean (±STD)		2.15 (±0.14)	Non-cocker mean (±STD)		2.1(±0.08)
Cocker mean (±STD)		2.18 (±0.09)	Cocker mean (±STD)		1.96 (±0.13)
Total mean (±STD)		2.17 (±0.11)	Total mean (±STD)		2.00(±0.13)

Table 3-10: Mean ratios of ET_B receptor/ 18S mRNA in arbitrary units for normal and glaucomatous retinal samples. ET_B, Endothelin B; 18S, 20X Eukaryotic 18S rRNA Endogenous Control.

	Normal			Glaucoma	
Dog	Breed	ET_B /18S	Dog	Breed	ET_B /18S
7	Beagle	2.13	14	Cocker	1.9
8	Beagle	2.17	19	Cocker	1.76
10	Walker Hound	2.01	22	Cocker	2.05
11	Greyhound	1.99	23	Cocker	1.98
M1	Cocker	2.21	24	Cocker	1.99
M2	Cocker	2.09	25	Cocker	2.02
M3	Cocker	2.09	26	Mix Terrier	2.13
M4	Cocker	2.17	27	Cocker	2.04
M5	Cocker	2.20	28	Basset	1.89
			M6	Poodle	2.22
Non-cocker mean (±STD)		2.08 (±0.09)	Non-cocker mean (±STD)		2.08 (±0.17)
Cocker mean (±STD)		2.15 (±0.06)	Cocker mean (±STD)		1.96 (±0.1)
Total mean (±STD)		2.12 (±0.08)	Total mean (±STD)		2.00 (±0.13)

Table 3-11: Summary of results for the glaucomatous eyes separating the Cocker Spaniel group and the non-Cocker group.

Parameter	Glaucoma, Cocker Spaniels	Glaucoma, Non-Cockers
ET-1 peptide		
Aqueous humor	Increase, p = 0.0003	Increase, p = 0.1144
Vitreous	Increase, p = 0.0005	Increase, p = 0.5062
ET-1 mRNA Retina	Increase, p = 0.9569	Decrease, p = 0.4273
Nitric Oxide		
Aqueous humor	Increase, p = 0.1421	Increase, p = 0.0476
Vitreous	Increase, p = 0.2003	Increase, p = 0.0148
ET receptor protein expression		
ET_A Retina	Decrease, p = 0.4826	Decrease, p = 0.5319
ET_B Retina	Decrease, p = 0.9916	Decrease, p = 0.0072
ET_A Choroid [a, b]	Higher expression, p = 0.4024 [a]	Decrease, p = 0.4066 [b]
ET_B Choroid [a, b]	Lower expression, p = 0.1291 [a]	Decrease, p = 0.2759 [b]
ET receptor mRNA		
ET_A Retina	Increase, p = 0.0064	Increase, p = 0.6248
ET_B Retina	Increase, p = 0.0075	Decrease, p = 0.9617

[a] No normal choroidal cocker tissue. Choroid from glaucomatous Cockers compared with choroid from glaucomatous non-Cockers. [b] Normal versus glaucomatous. The level of significance was set at 0.05.

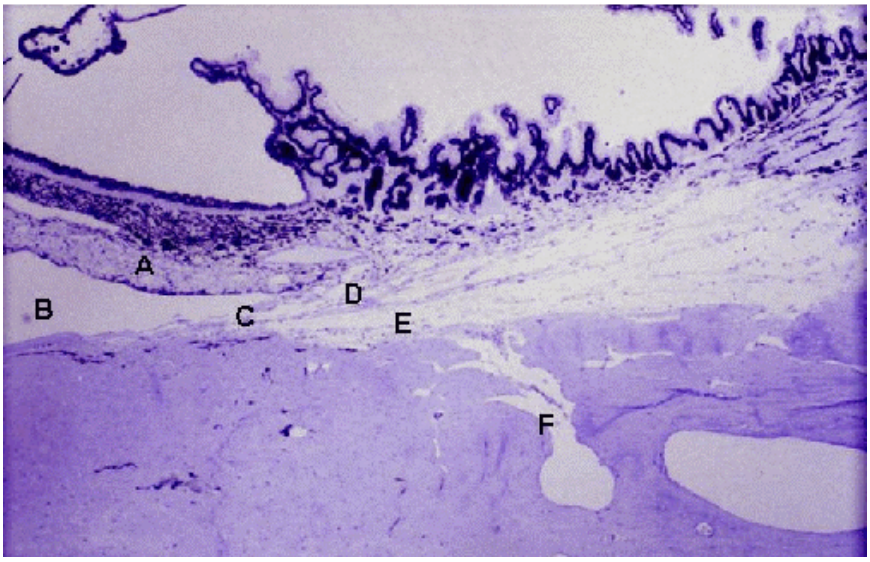

Figure 3-1: Normal iridocorneal angle stained with toluidine blue (Dog M3, original magnification 100X). A) Iris. B) Anterior chamber. C) Pectinate ligament. D) Uveal trabecular meshwork. E) Corneoscleral trabecular meshwork. F) Angular aqueous plexus/sinus.

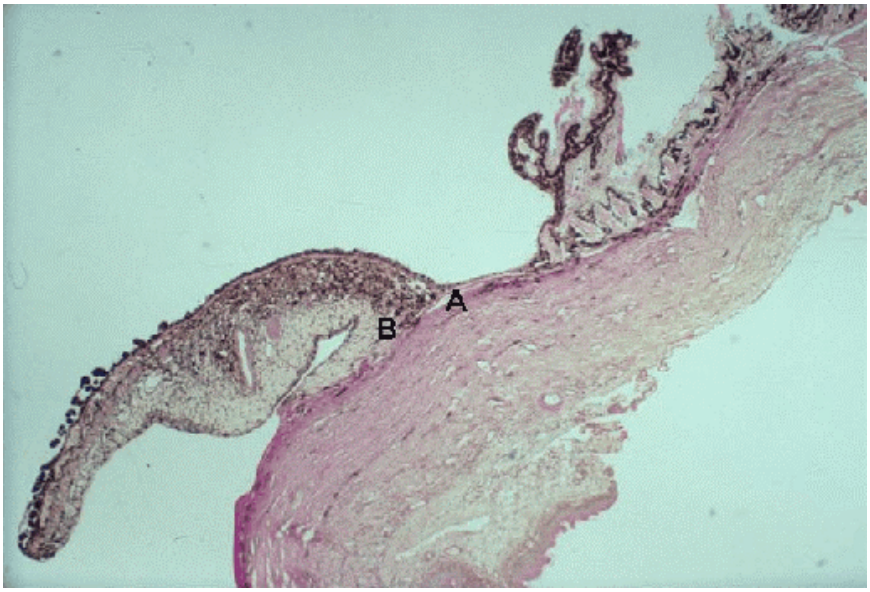

Figure 3-2: Iridocorneal angle of a glaucomatous dog (Dog 20, original magnification 40X, PAS stained). A) Compressed trabecular meshwork. B) Connective tissue at the entrance of the angle.

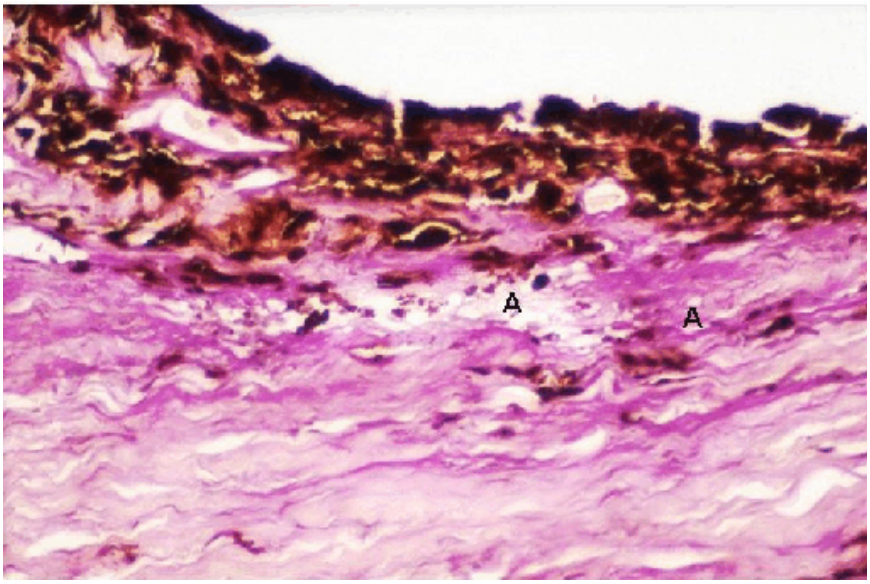

Figure 3-3: Trabecular meshwork of a glaucomatous dog (Dog 25, original magnification 200X, PAS stained). A) The uveoscleral meshwork has openings of varying sizes.

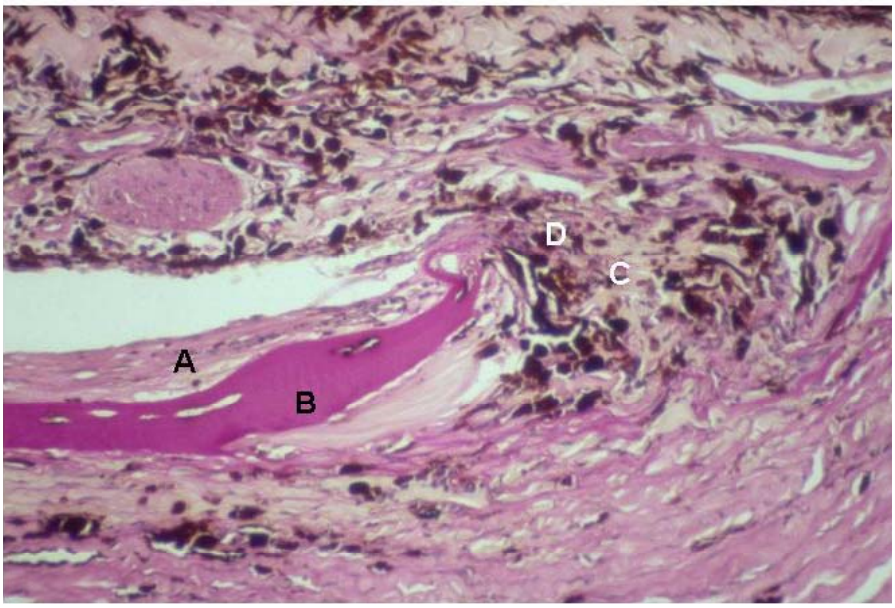

Figure 3-4: Iridocorneal angle of a glaucomatous dog (Dog 19, original magnification 200X, PAS stained). Evidence of previous synechia is present: A) Fibrosis lining the inner surface of Descemet's membrane. B) Termination of Descemet's membrane is enlarged. The entrance of the angle is covered: C) By connective tissue. D) By melanin-containing cells.

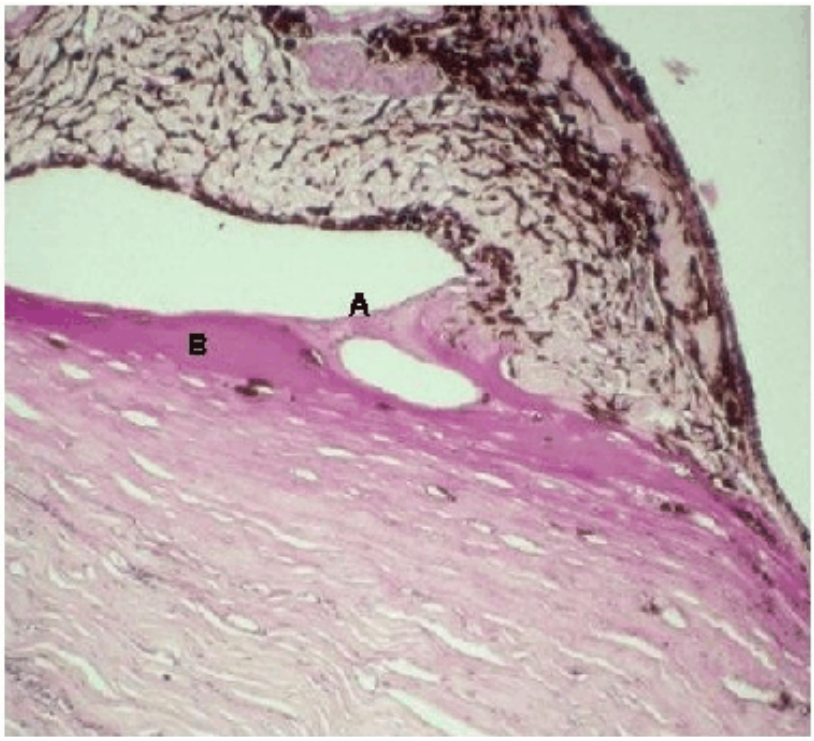

Figure 3-5: Iridocorneal angle of a glaucomatous dog (Dog 22, original magnification 100X, PAS stained). A) Synechia between the cornea and the iris. B) Enlarged termination of Descemet's membrane.

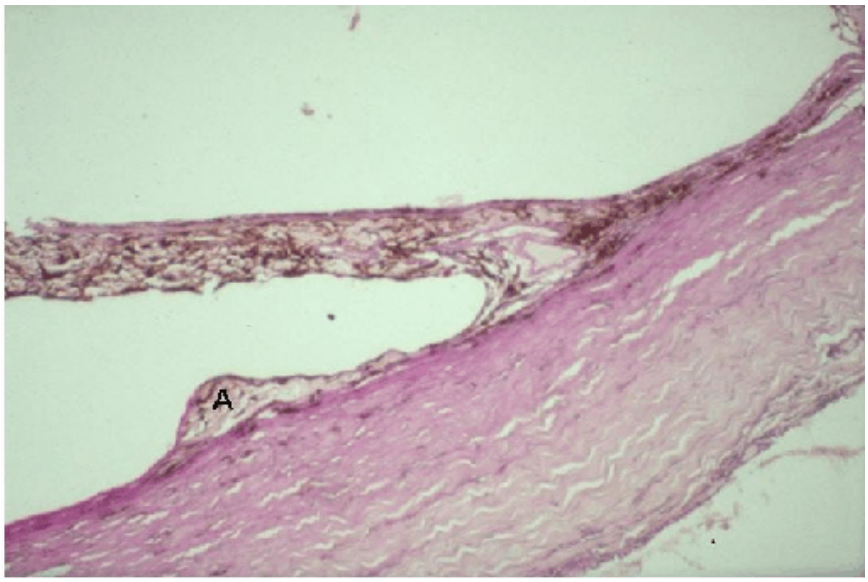

Figure 3-6: Iridocorneal angle of a glaucomatous dog (Dog 26, original magnification 100X, PAS stained). A) Fibrous tissue covering the endothelium of the cornea.

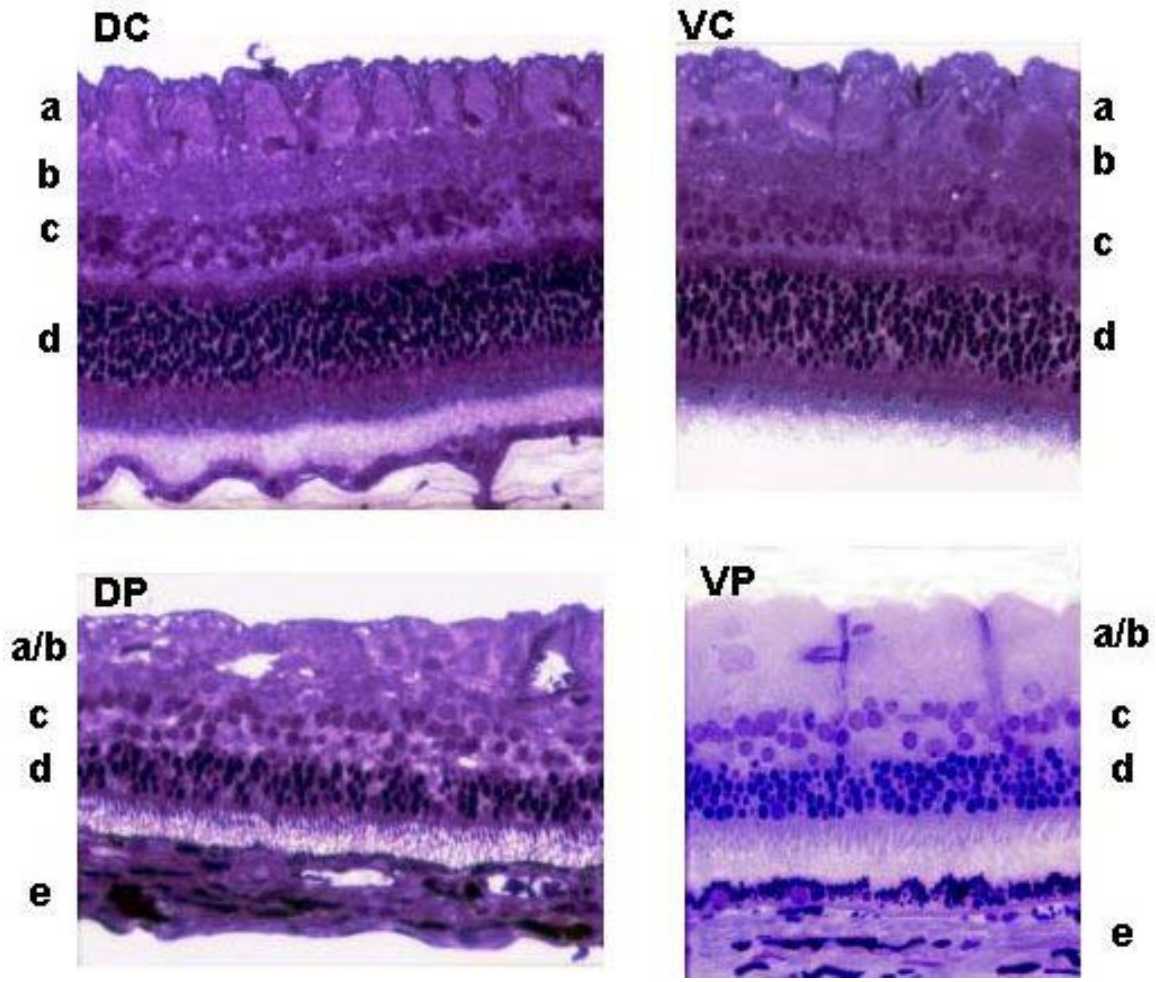

Figure 3-7: Semi-thin (1µm) sections of the retina from a normal dog (Dog M4, original magnification 400X) stained with toluidine blue. The sections are from four different locations: DC) Central retina dorsal of the optic nerve head. VC) Central retina ventral of the optic nerve head. DP) Peripheral retina dorsal of the optic nerve head. VP) Peripheral retina ventral of the optic nerve head. a, nerve fiber layer; b, ganglion cell layer; c, inner nuclear layer; d, outer nuclear layer; e, choroid.

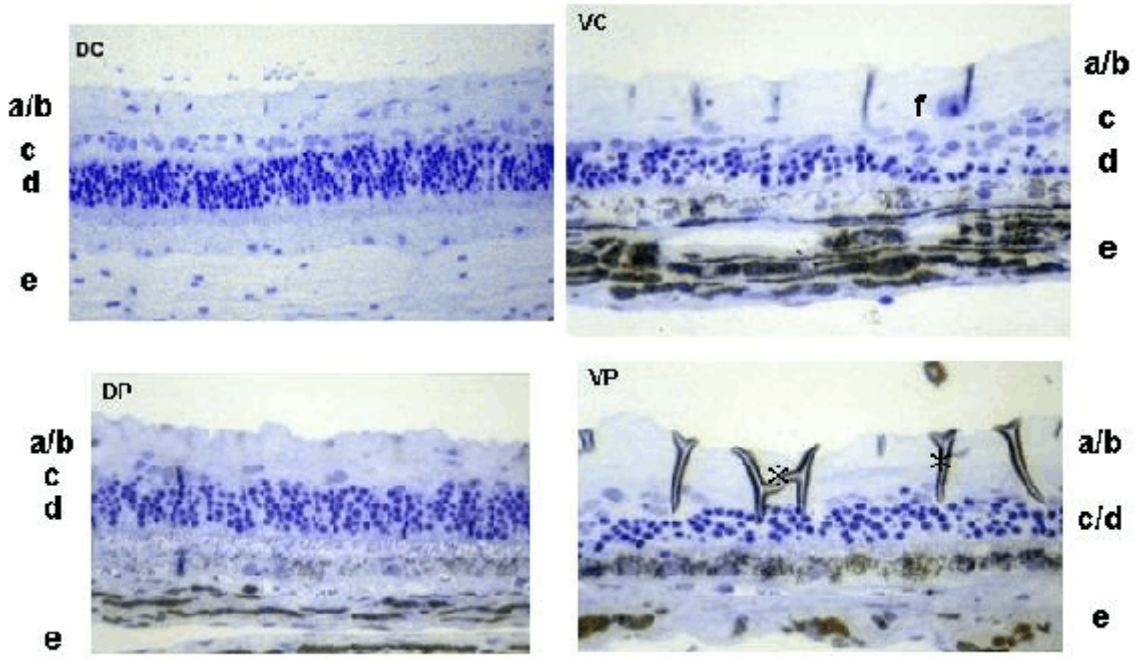

Figure 3-8: Semi-thin (1 µm) sections of the retina from a glaucomatous dog (Dog 24, original magnification 400X) stained with toluidine blue. The sections are from four different locations: DC) Central retina dorsal of the optic nerve head. VC) Central retina ventral of the optic nerve head. DP) Peripheral retina dorsal of the optic nerve head. VP) Peripheral retina ventral of the optic nerve head. a, nerve fiber layer; b, ganglion cell layer; c, inner nuclear layer; d, outer nuclear layer; e, choroid; f, ganglion cell; ❿, artifact.

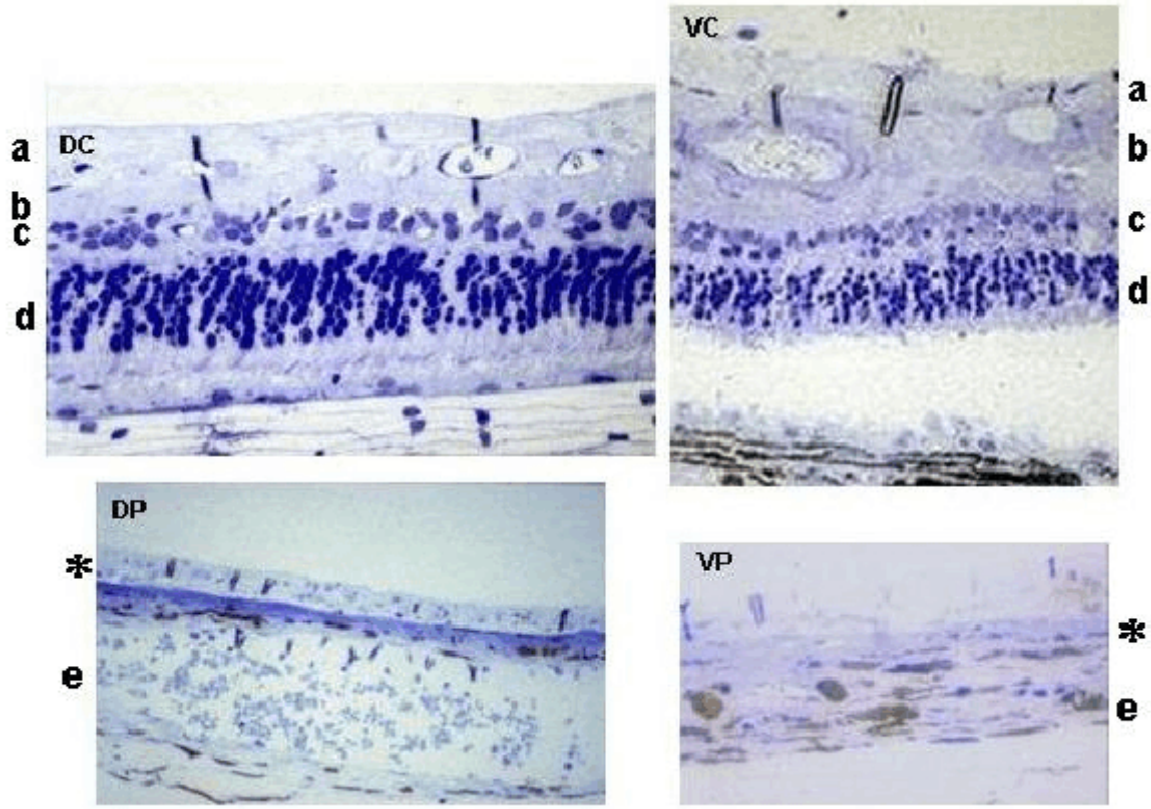

Figure 3-9: Semi-thin (1 µm) sections of the retina from a glaucomatous dog (Dog 25, original magnification 400X) stained with toluidine blue. The sections are from four different locations: DC) Central retina dorsal of the optic nerve head. VC) Central retina ventral of the optic nerve head. DP) Peripheral retina dorsal of the optic nerve head. VP) Peripheral retina ventral of the optic nerve head. a, nerve fiber layer; b, ganglion cell layer; c, inner nuclear layer; d, outer nuclear layer; e, choroid; ❿, complete atrophy.

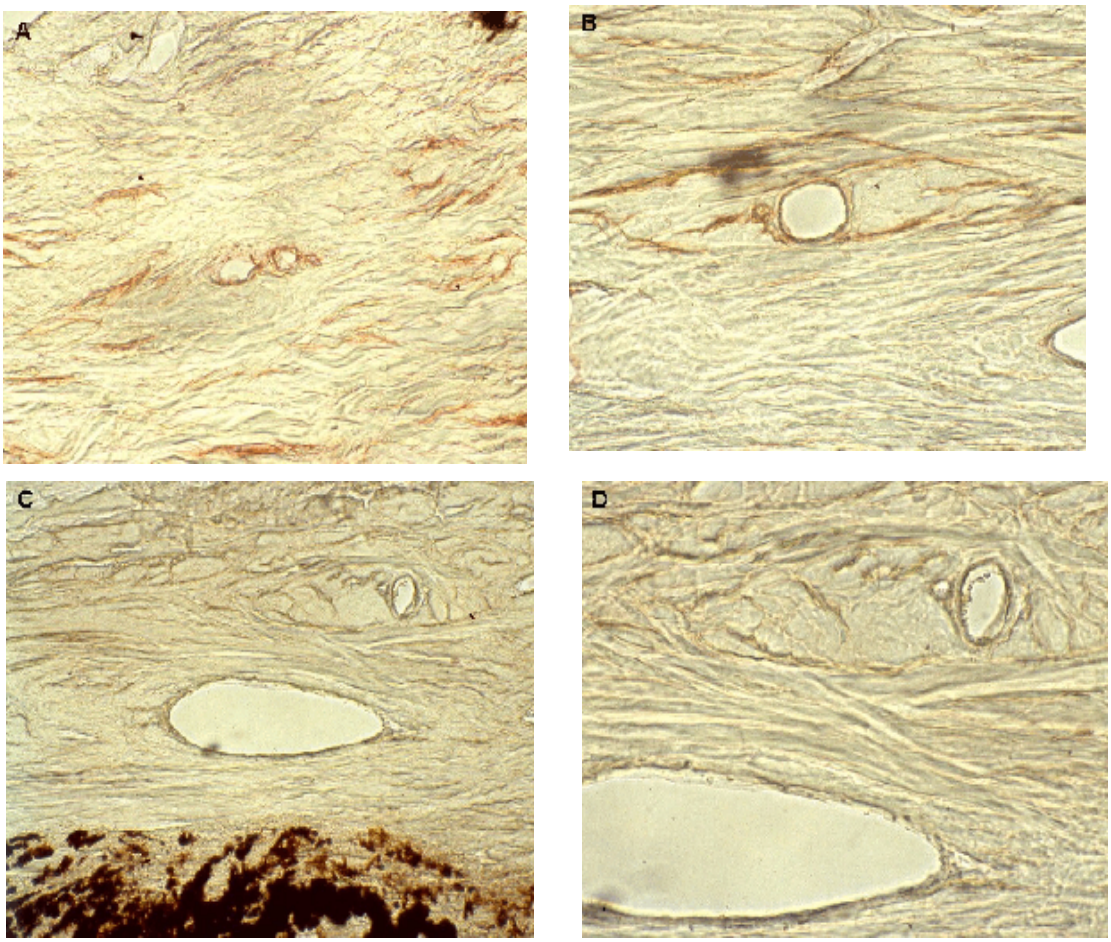

Figure 3-10: Label of normal canine scleral vessels and elastic fibers with the ET_B antibody. A) 1:50 dilution at original magnification of 100X. B) 1:50 dilution at original magnification of 200X. C) Control where the primary antibody is replaced with PBS, original magnification 100X. D) Control where the primary antibody is replaced with PBS, original magnification 200X.

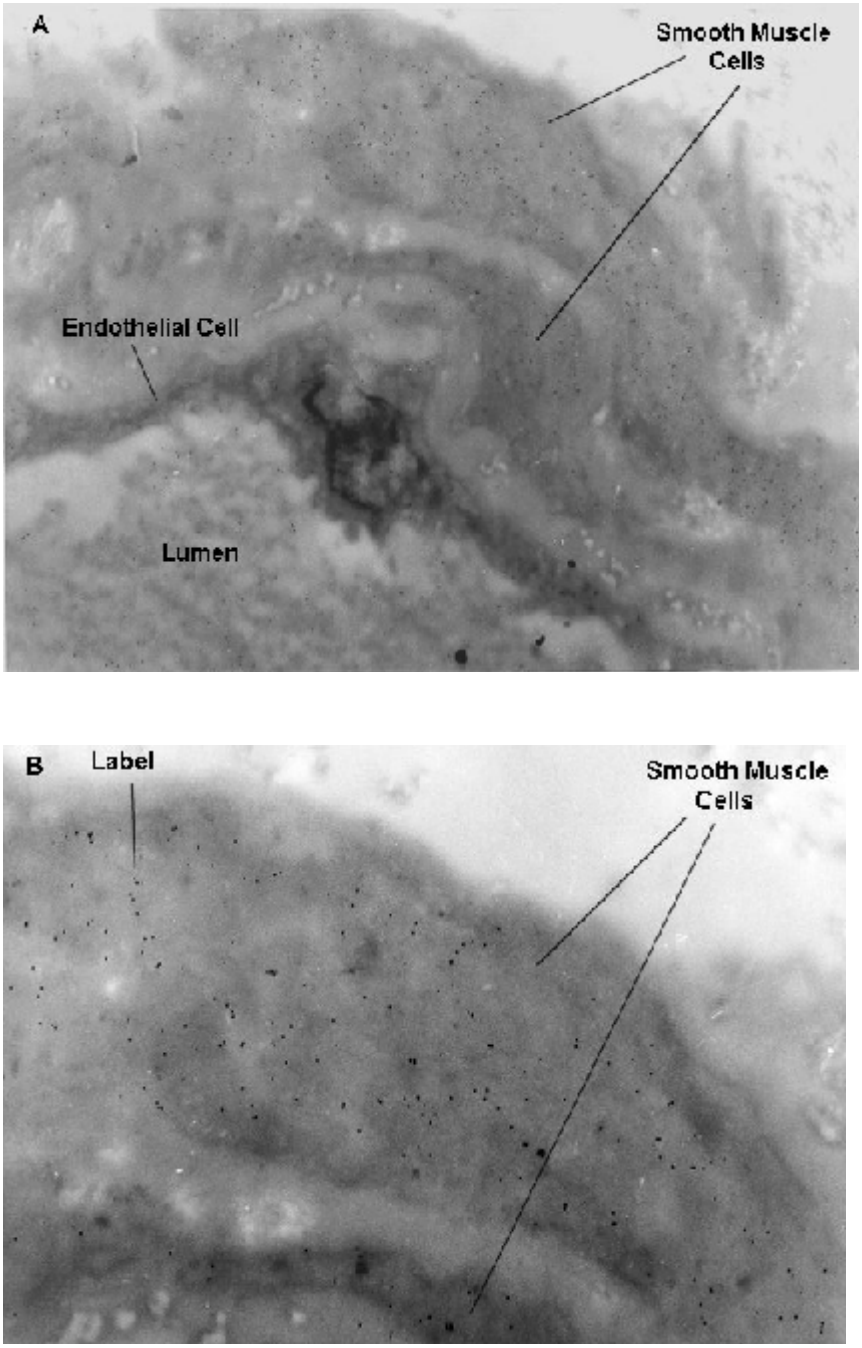

Figure 3-11: Arteriole of the choroid of a normal dog. A) Smooth muscle and endothelial cells labeled with ET_B antibody (1:100) at original magnification of 10,000X. B) Smooth muscle and endothelial cells labeled with ET_B antibody (1:100) at original magnification of 20,000X.

A

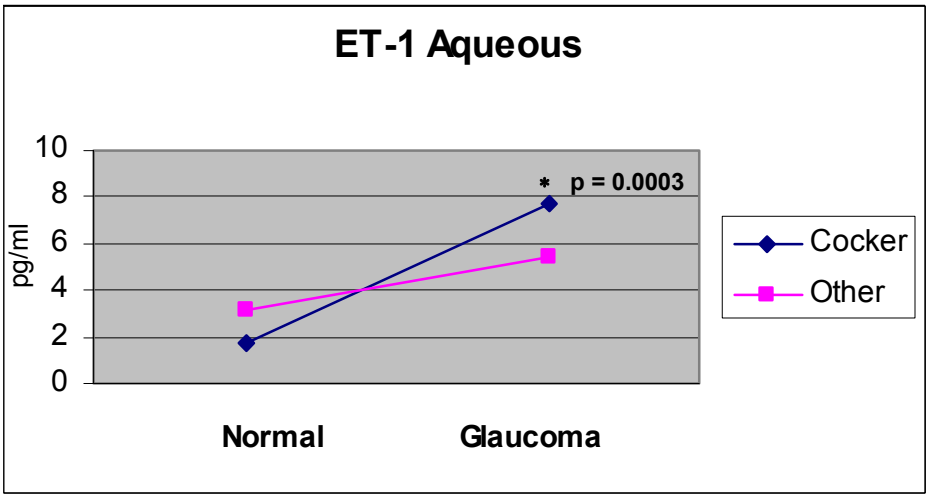

B

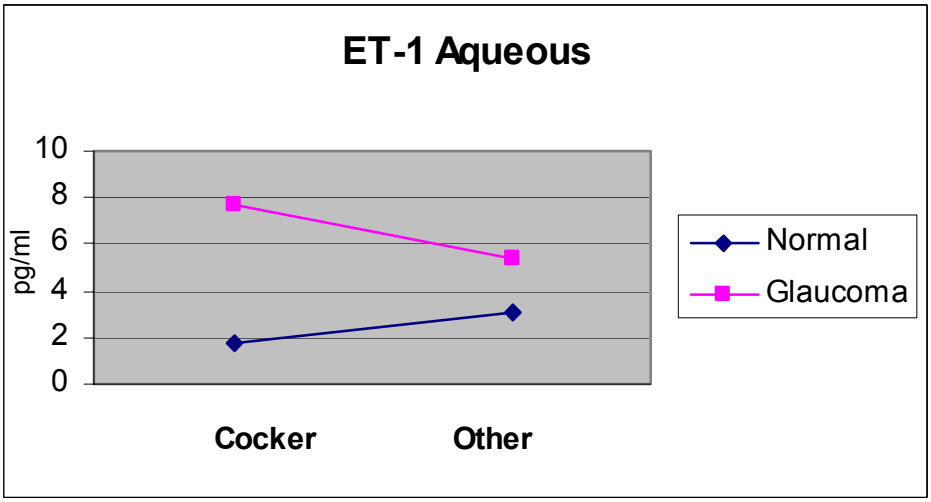

Figure 3-12: Endothelin-1 in aqueous humor of normal and glaucomatous eyes (see Tables 3-2 and 3-3). A) In the Cocker group, there is a significant increase in ET-1 for the glaucomatous eyes ($p = 0.0003$), while for the non-Cocker group the difference between the normal and glaucomatous eyes is not significant. B) There is no significant difference between Cockers and non-Cockers neither for the normal nor for the glaucomatous eyes. ET-1, Endothelin-1

A

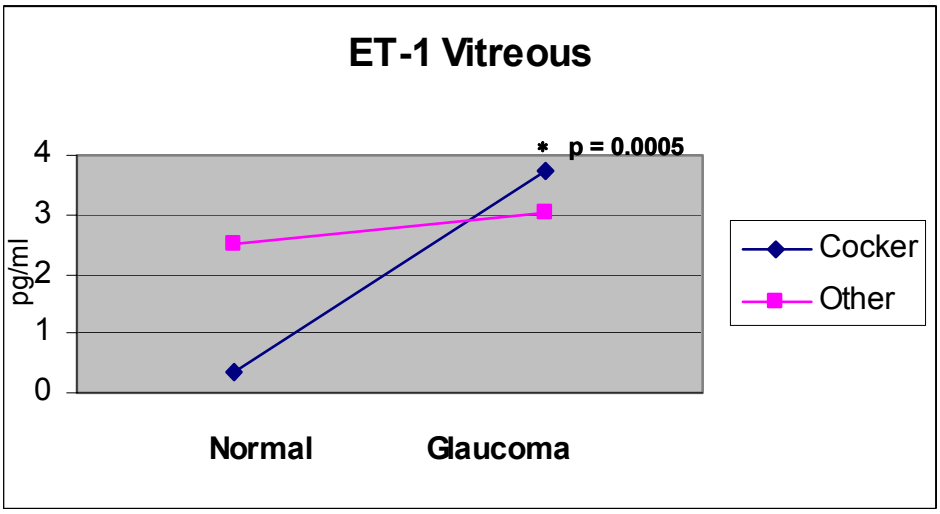

B

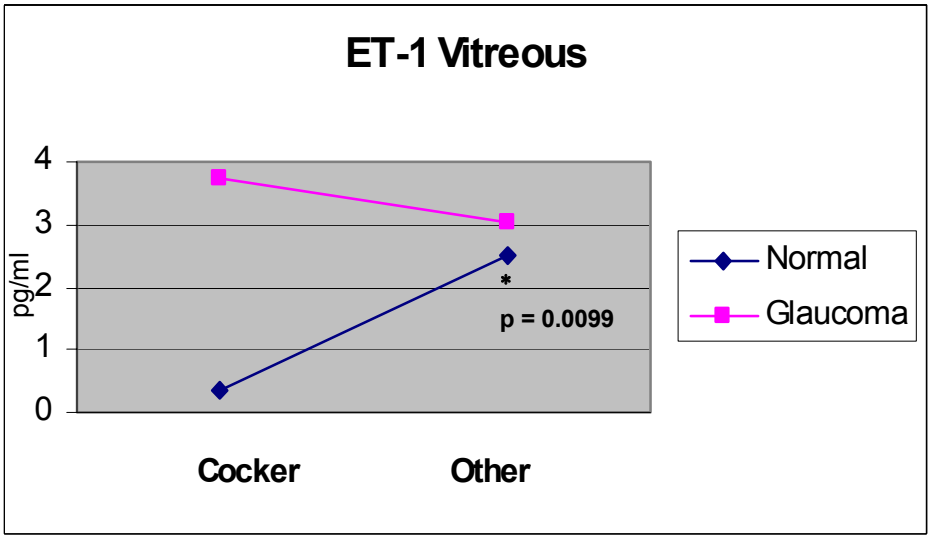

Figure 3-13: Endothelin-1 in vitreous of normal and glaucomatous eyes (see Tables 3-2 and 3-3). A) In the Cocker group, there is a significant increase in ET-1 for the glaucomatous eyes ($p = 0.0005$), while for the non-Cocker group the difference between the normal and glaucomatous eyes is not significant. B) There is a significant difference between the Cocker group and the non-Cocker group ($p = 0.0099$) for the normal eyes but not for the glaucomatous eyes. ET-1, Endothelin-1.

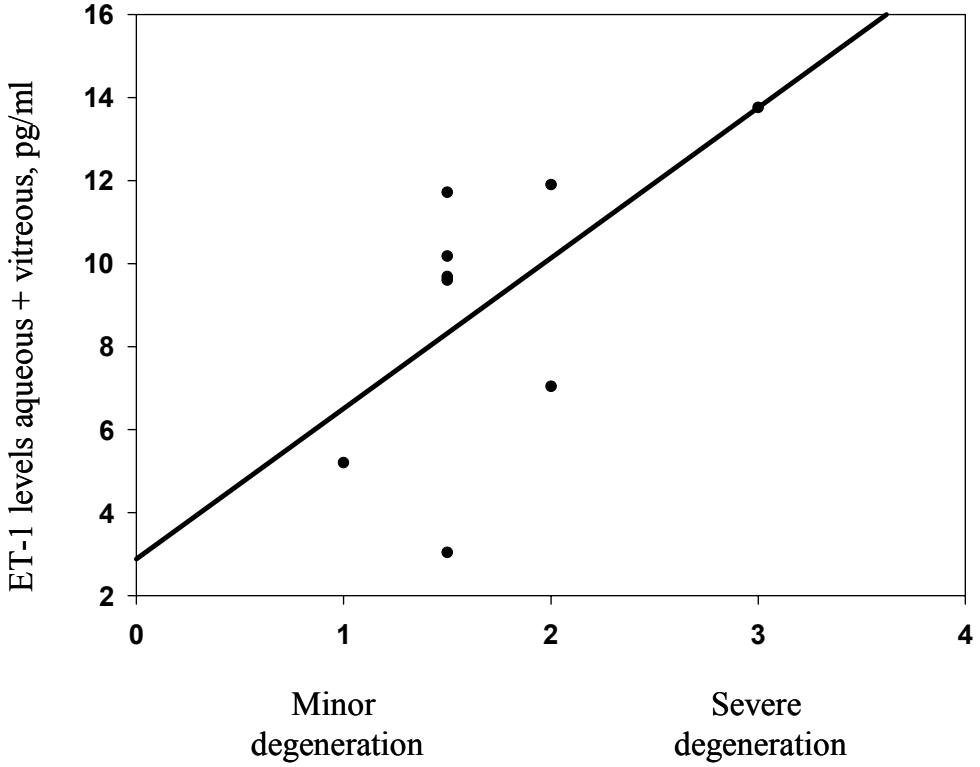

Figure 3-14: Scatter plot showing the correlation between the degree of degeneration in central retina and total aqueous humor and vitreal ET-1 levels of glaucomatous dogs (Spearman correlation coefficient 0.6, p = 0.0901). ET-1, Endothelin-1

A

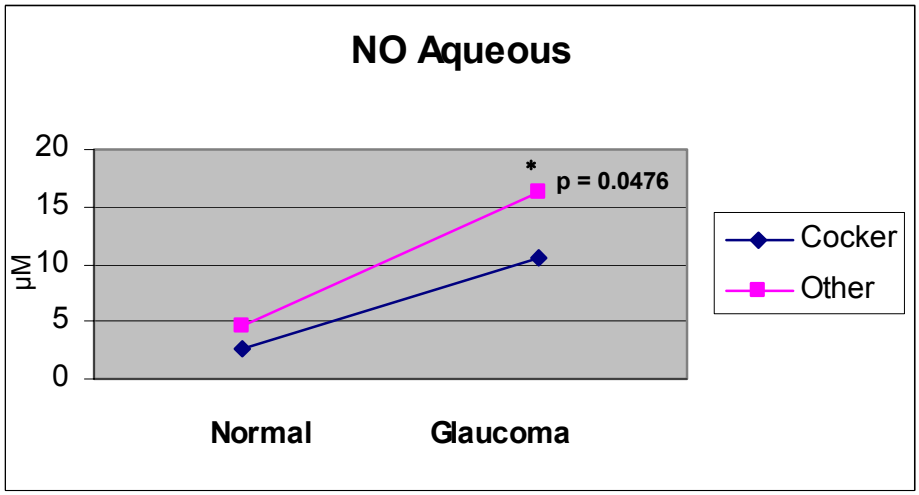

B

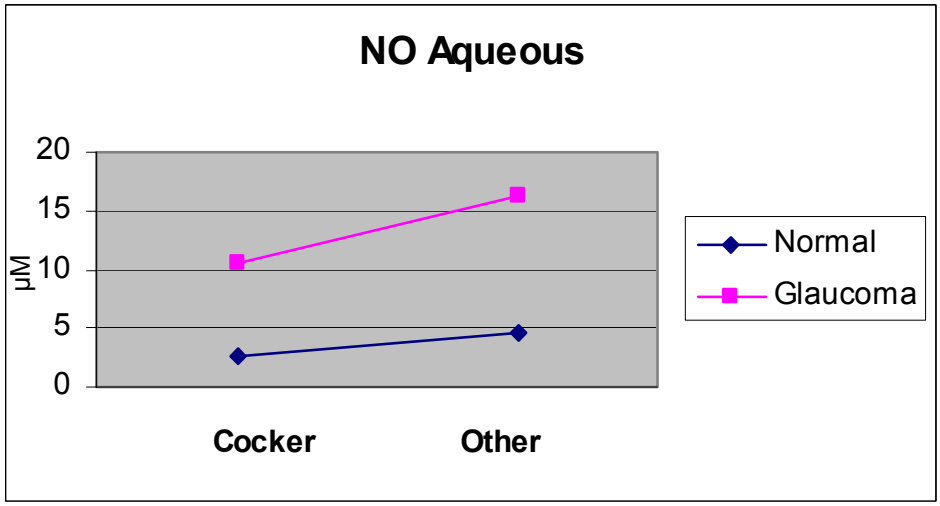

Figure 3-15: Nitric oxide in aqueous humor of normal and glaucomatous eyes (see Tables 3-5 and 3-6). A) There is a significant difference between NO levels in normal and glaucomatous eyes for the non-Cocker group ($p = 0.0476$); but not for the Cocker group. B) There is no significant difference between Cockers and non-Cockers neither for the normal nor for the glaucomatous eyes. NO, Nitric Oxide.

A

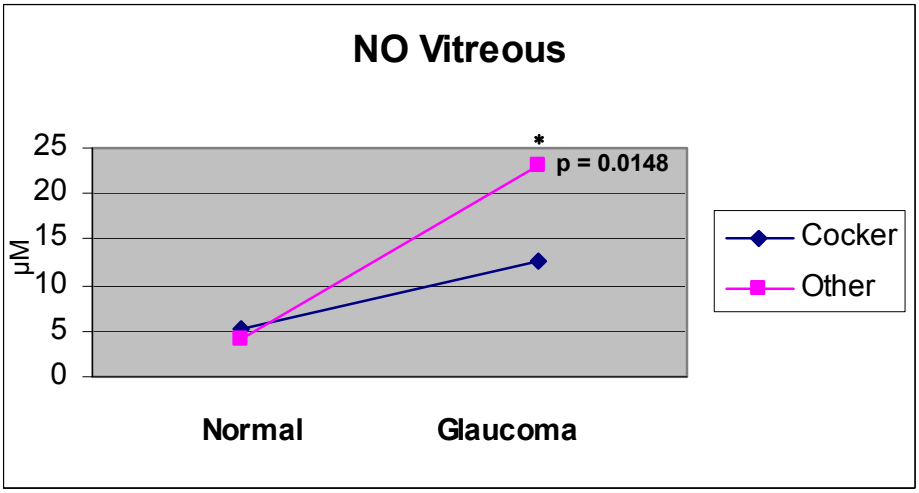

B

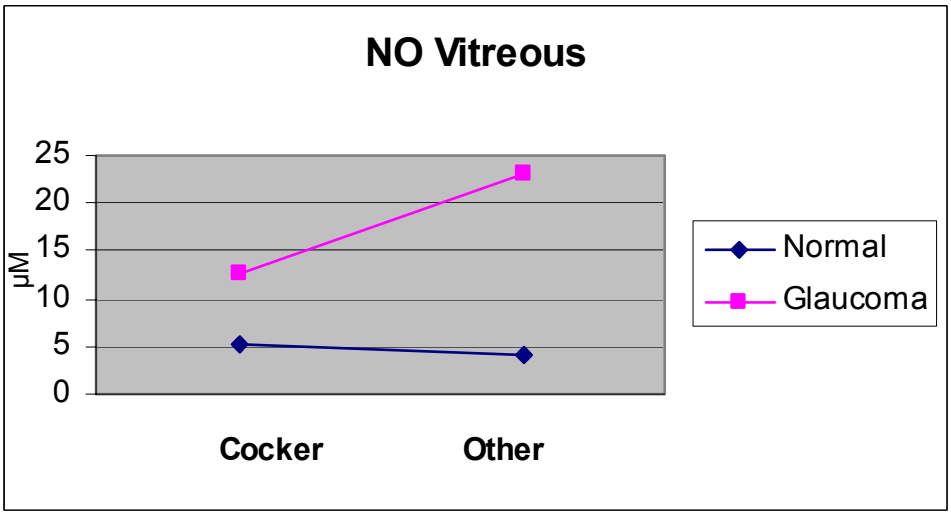

Figure 3-16: Nitric oxide in vitreous of normal and glaucomatous eyes (see Tables 3-5 and 3-6). A) In the non-Cocker group, there is a significant increase in NO for the glaucomatous eyes ($p = 0.0148$), while for the Cockers the difference between the normal and glaucomatous eyes is not significant. B) There is no significant difference between the Cocker group and the non-Cocker group neither for the normal eyes nor for the glaucomatous eyes. NO, Nitric Oxide.

A

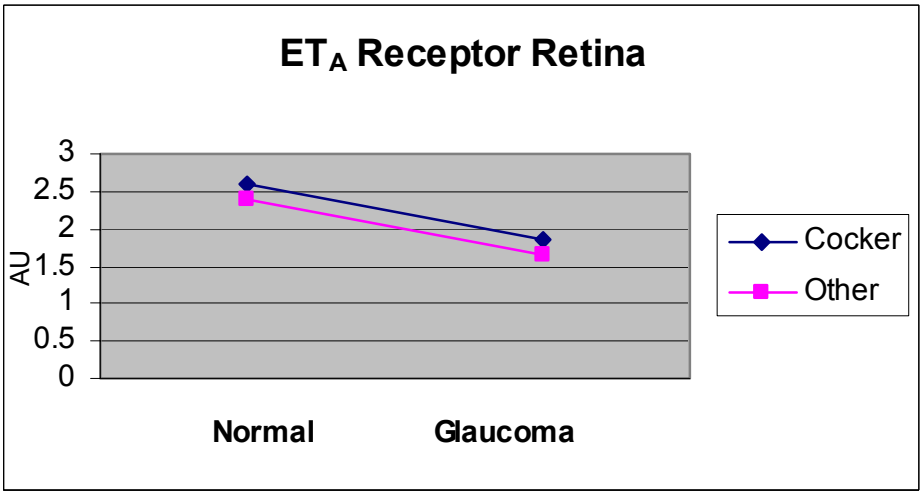

B

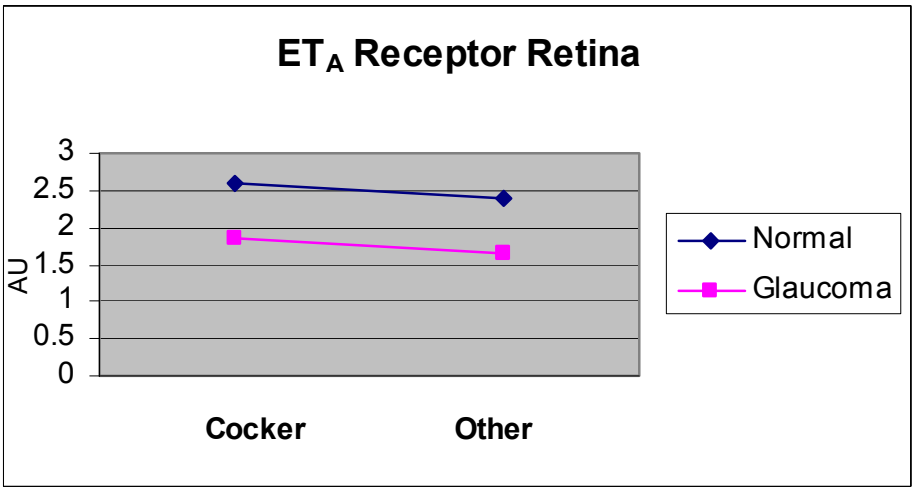

Figure 3-17: Endothelin receptor A protein in the retina of normal and glaucomatous eyes (see Table 3-7). A) There is no significant difference between the normal and glaucomatous eyes. B) There is no interaction with breed. ET_A, Endothelin A.

A

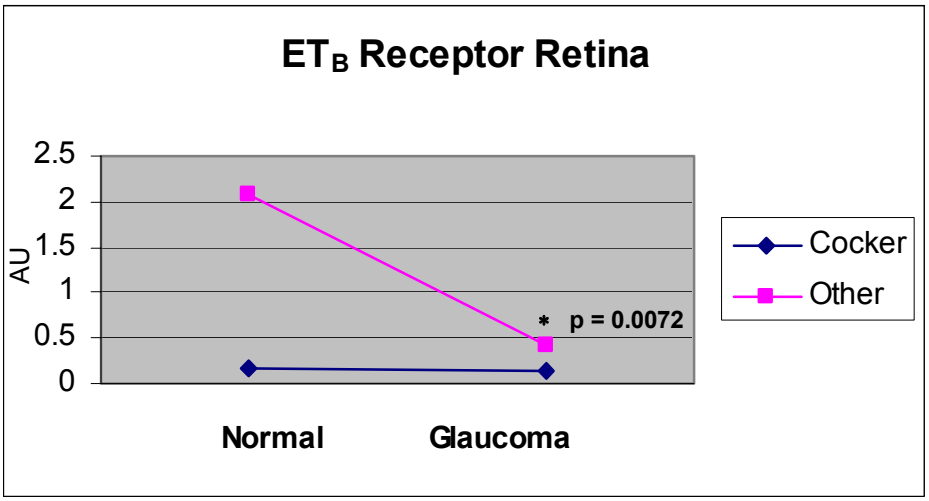

B

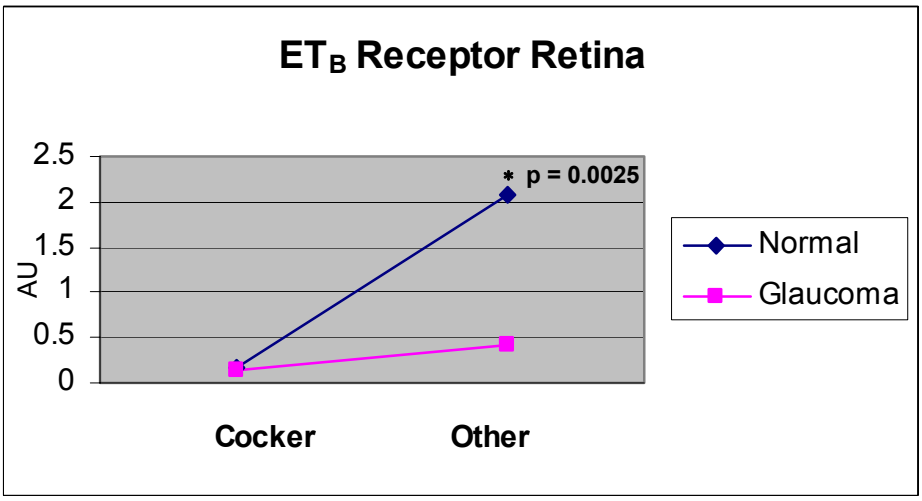

Figure 3-18: Endothelin receptor B protein in the retina of normal and glaucomatous eyes (see Table 3-8). A) The difference between normal and glaucomatous eyes of the non-Cocker group ($p = 0.0072$) is highly significant while the small decrease of the Cocker group is not significant. B) There is a difference between normal eyes with the non-Cocker group being significantly higher than the Cocker group ($p = 0.0025$) (B). ET_B, Endothelin B.

A

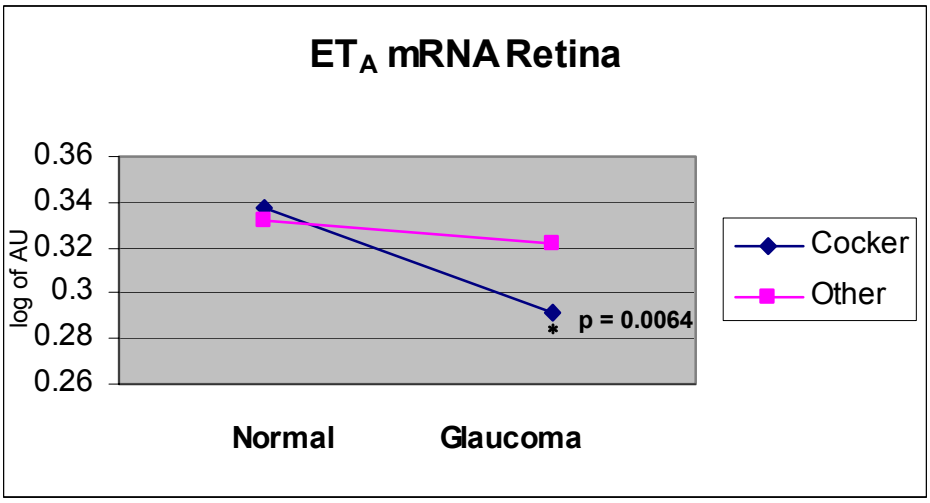

B

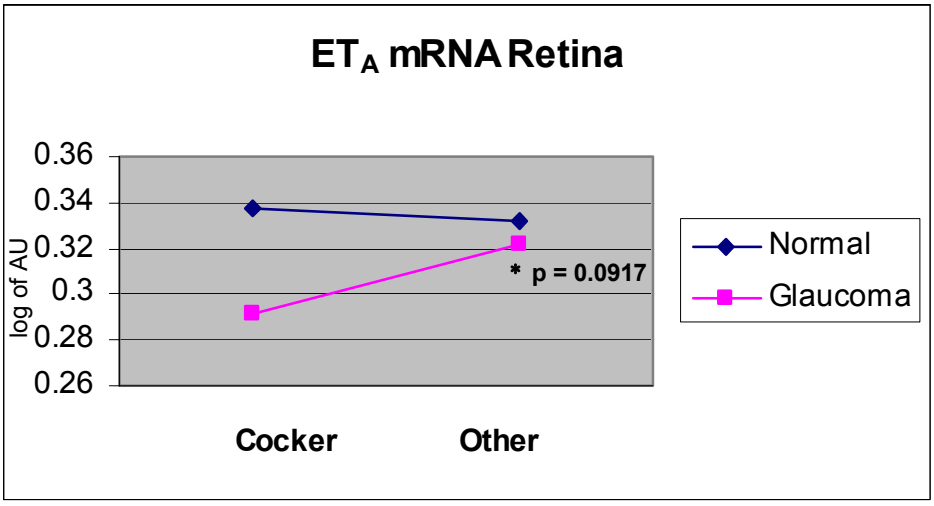

Figure 3-19: Endothelin receptor A mRNA in the retina of normal and glaucomatous eyes (see Table 3-9). A) The increase in the Cocker group is highly significant ($p = 0.0064$). The small increase in the non-Cocker group is not significant. B) The difference between groups of the glaucomatous eyes is significant at a 0.1 significance level ($p = 0.0917$). ET_A, Endothelin A.

A

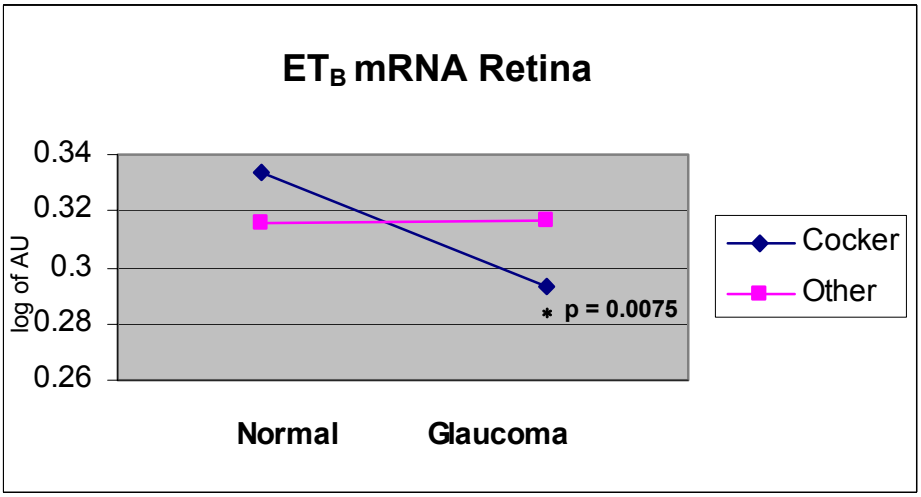

B

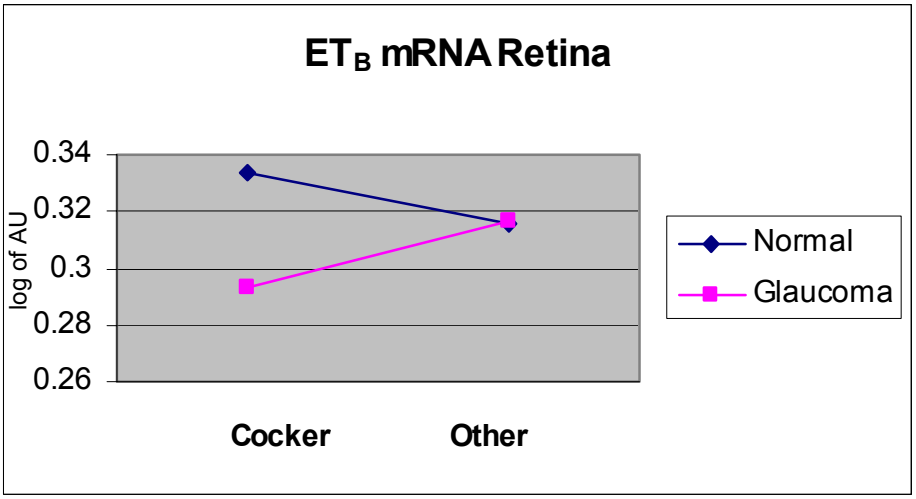

Figure 3-20: Endothelin receptor B mRNA in the retina of normal and glaucomatous eyes (see Table 3-10). A) The increase in the glaucomatous eyes in the Cocker group is highly significant ($p = 0.0075$). B) There is no significant difference in normal or glaucomatous eyes between the Cocker group and the non-Cocker group (B). ET_B, Endothelin B.

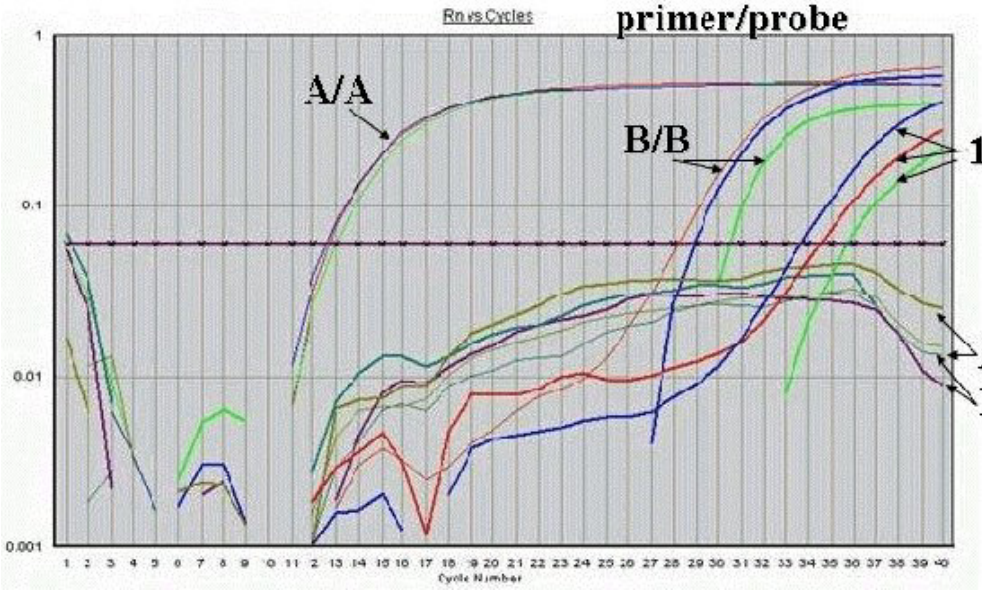

Figure 3-21: Real Time PCR amplification curves of the cloned ET_A receptor DNA sequence run with different mixes of primers and probes (see Table 2-6). All samples are run in triplicate. The (A/A) mix shows an early amplification of the DNA sequence. The mixes A/B and B/A give only background noise below detectable level. Amplification curves are seen late in the reaction with the mix (B/B) and 18S respectively. ET_A, Endothelin receptor A; ET_B, Endothelin receptor B; A/A, ET_A primer/ET_A probe; A/B, ET_A primer/ET_B probe; B/B, ET_B primer/ET_B probe; 18S, 20X Eukaryotic 18S rRNA Endogenous Control.

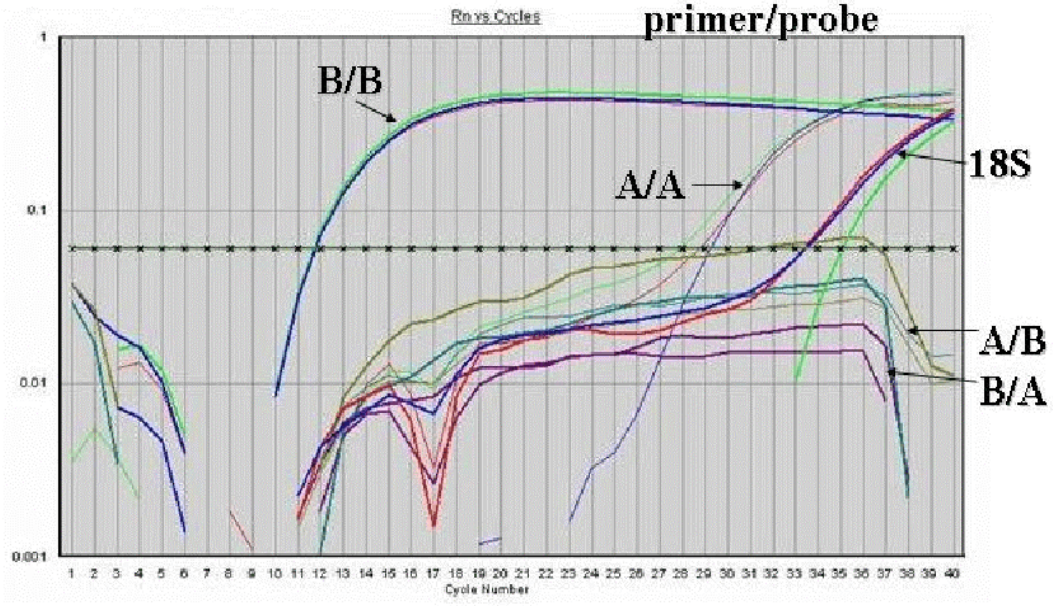

Figure 3-22: Real Time PCR amplification curves of the cloned ET_B receptor DNA sequence run with different mixes of primers and probes (see Table 2-6). All samples are run in triplicate. The (B/B) mix shows an early amplification of the DNA sequence. The mixes A/B and B/A give only background noise below detectable level. Amplification curves are seen late in the reaction with the (A/A) mix and 18S respectively. ET_A, Endothelin receptor A; ET_B, Endothelin receptor B; A/A, ET_A primer/ET_A probe; A/B, ET_A primer/ET_B probe; B/B, ET_B primer/ET_B probe; 18S, 20X Eukaryotic 18S rRNA Endogenous Control

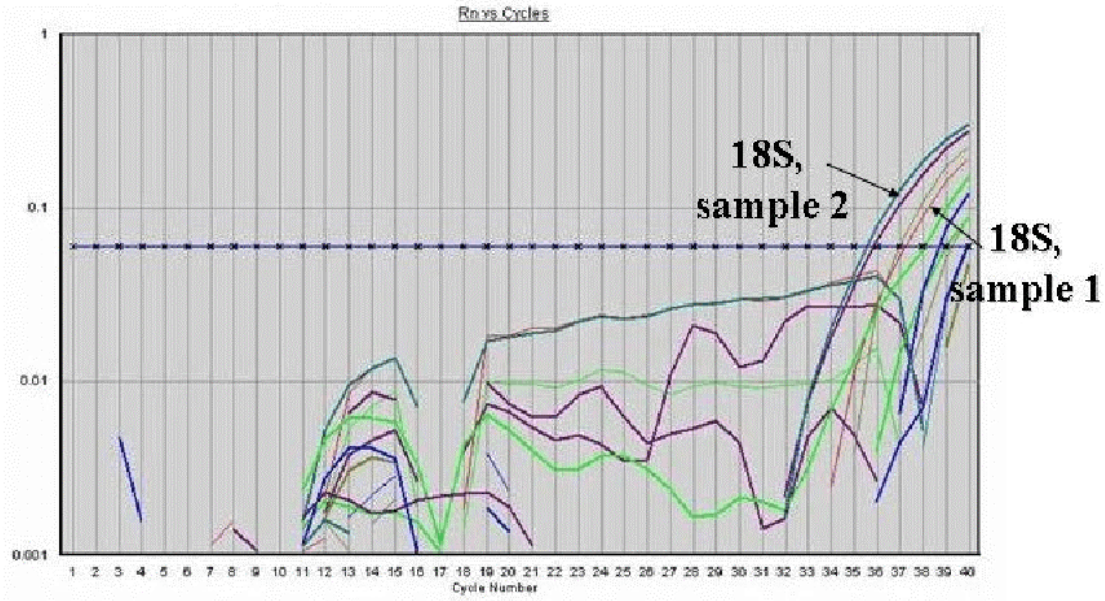

Figure 3-23: Real Time PCR run with no template (1) and total RNA (2) run with the primers and probes for the ET receptors and 18S (see Table 2-6). The ET receptors are not amplified in the reaction. Traces of 18S rRNA are amplified in both samples.ET, Endothelin; 18S, 20X Eukaryotic 18S rRNA Endogenous Control

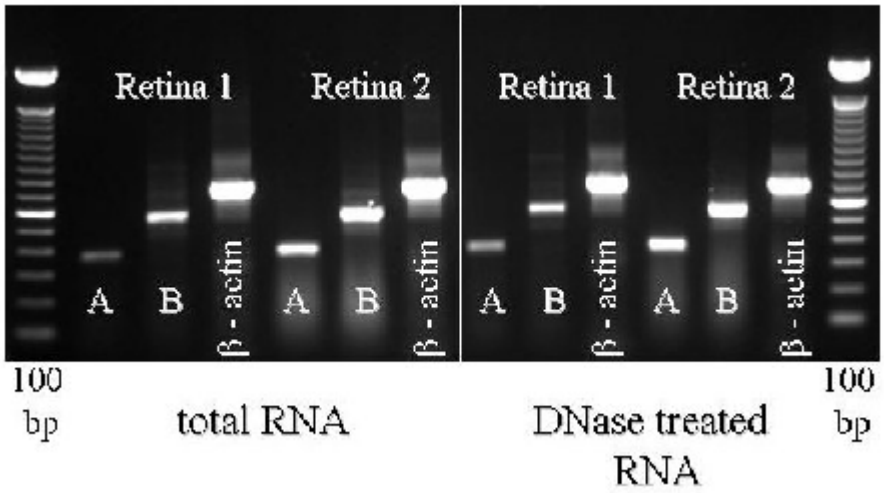

Figure 3-24: RT-PCR of two samples from normal dog retinas. The sample labeled Retina 1 was stored frozen in the preservative RNAlater and the sample labeled Retina 2 stored frozen dry without any preservative. The RT-PCR was run on total RNA and DNAse treated RNA from each sample to visualize any genomic DNA in the samples with total RNA. The primers used for the reaction are listed in Table 2-5.

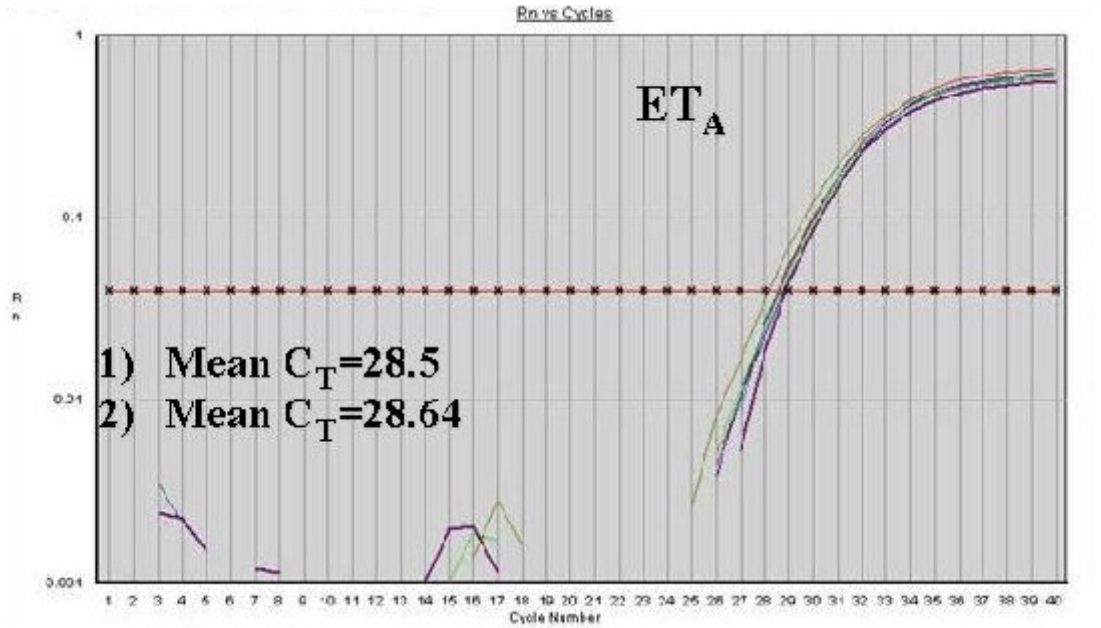

Figure 3-25: Real Time PCR amplification curves of the ET_A receptor for two normal retinal samples stored frozen in RNAlater (sample 1) and frozen dry without preservative (sample 2). Both samples were run in triplicate. The primers used for the reaction are listed in Table 2-5. ET_A, Endothelin receptor A; C_T, Cycle Threshold

CHAPTER 4
DISCUSSION

Morphology

The iridocorneal angle (ICA) is designed specifically for the removal of aqueous humor. Aqueous humor passes between the pectinate ligaments to large extratrabecular spaces of the deep ciliary cleft [uveal trabecular meshwork (Figure 3-1)] [98,99]. It then passes through the more dense meshwork of the corneoscleral trabecular meshwork in the shallow scleral sulcus [98]. The trabecular cells lining the beams of the corneoscleral and uveal meshworks are fibroblast-like cells with slender cell processes [39]. Aqueous humor in the corneoscleral trabecular meshwork drains to a plexus of aqueous humor collector vessels (angular aqueous plexus) where it exits the eye and enters the circulation. A small percentage of aqueous humor (15% in the dog) drains from the eye via unconventional routes (uveoscleral outflow) through the iris stroma and/or between the fibers of the ciliary muscle to the supraciliary and suprachoroidal spaces.

The mechanism of development of narrow and closed ICA in the American Cocker Spaniel is not completely clear, but a hypothesis is that tight apposition of the iris slightly increases the pressure within the posterior chamber, which in turn causes forward displacement of the basal iris [27]. Eventually, the basal iris narrows the ICA and opening of the ciliary cleft. Apposition of basal iris across the filtration angle causes a potentially reversible angle closure. With continued apposition, peripheral anterior synechiae (PAS) develop, thereby permanently closing the pathways of aqueous outflow.

The ICA progressively narrows, eventually closes, and the ciliary cleft collapses. The intrascleral plexus collapses as a consequence of the enlarged globe [27].

The ICAs of the glaucomatous eyes in our study were partially or completely collapsed, irregardless of the breed and age of the dog, reflecting the fact that the eyes were approaching or at the end-stage of glaucoma (Figure 3-2).

The degree of retinal degeneration in our study also did not correlate with the length of disease. This is in accordance with a study by Smedes and Dubielzig [100] where extensive retinal degeneration was found in glaucomatous eyes with a brief clinical history of increased intraocular pressure (IOP) ranging from 1-11 days. There was no difference in degree of retinal degeneration between the Cocker group and the non-Cocker group in our study.

Endothelin-1 in Aqueous Humor and Vitreous

The mean endothelin (ET)-1 levels in aqueous humor and vitreous in our study were significantly increased in the glaucomatous dog eyes, although the range of ET-1 levels was large (Tables 3-2 and 3-3, and Figures 3-12 and 3-13). Despite this variability, the data indicated a definite increase in ET-1 level in the canine glaucomatous eyes.

Elevations of aqueous humor ET-1 are found in human primary open angle glaucoma (POAG) and normal tension glaucoma (NTG) [15-17,101]. The 2.5-fold increase of ET-1 in aqueous humor of the glaucomatous dogs in our study (from 2.8 ± 1.52 to 6.86 ± 3.49 pg/mL) is much higher than the 0.05-fold increase seen in human POAG patients (from 42.17 ± 1.6 to 44.26 ± 2.6 pg/mL) [15]. One explanation for this finding is the much higher IOPs in the canine eyes causing more severe ischemic/reperfusion injury as compared with that of human eyes. The aqueous humor samples in our study were all from advanced cases with uncontrolled IOP and severe

retinal damage. Although no significant correlation was seen between the IOP immediately prior to collection of aqueous humor and the ET-1 levels in the canine glaucoma group, the high IOPs could cause severe ischemic/reperfusion injury, and hence induce ET-1 release at levels far surpassing the ones normally seen in human patients with POAG.

Sources of Endothelin-1

The ET-1 in the canine aqueous humor could come from several sources. Cytokines associated with ischemia from elevated IOP might induce increased ET-1 production and release from non-pigmented ciliary epithelial cells or ischemic endothelial cells [102]. Functional endothelin converting enzyme-1 (ECE-1) has been found in human non-pigmented ciliary epithelial cells, which makes these cells a likely source for aqueous humor levels of ET-1 [103]. Transformed human non-pigmented ciliary epithelial cells in culture have also been shown to produce and release ET-1 in response to tumor necrosis factor-α (TNF-α) [102]. According to a study by Smith et al. [104], dogs with glaucoma have a vacuolization, degeneration and atrophy of the ciliary epithelium in late stages of the disease. This could have a negative effect on the production and release of ET-1 from the ciliary epithelium in the chronic stages of the canine disease, making the ciliary epithelium less likely as a source of the elevated ET-1 levels found in dogs with glaucoma.

Plasma ET-1 levels in our glaucoma dogs were not determined in this study for technical reasons. Levels of ET-1 have been measured in human aqueous humor and found to be two to three times higher than in plasma both in normals and in patients with POAG [15]. This argues against the influx of ET-1 from plasma unless they were actively secreted into the aqueous. Since systematically administered ET does not cross the blood-

brain barrier, it is highly unlikely that it would cross the blood-aqueous barrier under normal conditions [72]. The concentration of ET-1 in plasma in normal dogs varies between 14 and 52 pg/mL and is considerably higher than the levels found in human plasma (12.48 ± 1.3 pg/mL), which may represent a species difference [15,105]. In the event of a disruption of the blood-aqueous barrier, plasma ET-1 might contribute to the increased levels of ET-1 in aqueous humor of glaucomatous dog eyes. This possibility should be investigated in future studies.

Vitreal ET-1 levels have to our knowledge not been measured previously in glaucomatous eyes. The levels, mean (± STD) in the normal and glaucomatous eyes were 1.56 (± 1.86) and 3.47 (± 1.57) pg/mL respectively in our study. The vitreal ET-1 levels were lower than the aqueous humor ET-1 levels for both the normal and glaucomatous group. The mRNA levels of ET-1 in the glaucomatous retinas were not significantly changed indicating that the production of ET-1 remains essentially the same in the glaucomatous retinas as in the normal retinas. The increased vitreal ET-1 might emanate from ET-1 in the aqueous humor by reverse diffusion from the anterior chamber or from a decrease in the vitreal clearance of the peptide.

Another potential source for ET-1 in the vitreous are the retinal pigment epithelial cells. Narayan et al. [85] showed that human retinal pigment epithelial cells stimulated with carbachol synthesize and release ET-1.

The increased levels of ET-1 in aqueous humor and vitreous in our study may be due to reduced removal of the hormone. The ET-1 is normally flushed out with the aqueous humor through the outflow pathways. The function of this mechanism may be decreased in a glaucomatous eye with a collapsed iridocorneal angle. Endothelin-1

inactivating peptidases have been found in human and rat kidney [106,107]. It is not known whether these peptidases exist in the aqueous humor or vitreous. Another mechanism that helps in the clearance of ET-1 is internalization and degradation of the ET_B receptor and its associated peptide [44,66,73].

Although the Western Blot technique does not render itself to exact quantification, there were clear trends in our analyses of the receptors. There was a decrease of the protein expression of the ET_B receptor in the glaucomatous retinas. (Table 3-8, and Figure 3-18). There was also a decrease of the ET_B receptor in the choroid of the non-Cocker group that was not significant. This leads to a decreased clearance of ET-1 by these tissues. Future studies will tell if this trend is true also for the anterior segment, which would in part explain the increase of ET-1 in the aqueous humor.

An alternative mechanism explaining the elevated ET-1 levels is the ability of the peptide to upregulate its own gene expression. Saito et al. [108] have demonstrated a dose-dependent increase in prepro-ET-1 levels in cultured rat aortic endothelial cells through activation of the ET_B receptor by exogenous ET-1. Primary rat astrocytes were shown to express high-affinity receptors for endothelins [109]. In a study by Ehrenreich et al. [110], rat astrocytes responded to stimulation by ET-1 agonists with an increase in the release of ET-1 through induction of the transcriptional factor AP-1. This group suggested that the astrocytes are capable of a selective, autoregulatory mechanism that maintains high levels of ET-1. The increase of ET-1 mRNA in the glaucomatous retinas of the Cocker group was nonsignificant, while the non-Cocker group showed a nonsignificant decrease, making this mechanism less likely as being responsible for the large increase in ET-1 levels in our study (Table 3-4). We did not determine the content

of ET-1 mRNA in the optic nerve heads. However, an increased release of ET-1 from the astrocytes of the optic nerve head would most likely make only a minor contribution to the ET-1 levels in the vitreous and aqueous humor.

The Effect of Steroid Treatment

The expression of the ET_A receptor was also decreased in the glaucomatous retinal samples compared to normals. One reason for this decrease may have been the fact that a majority of the glaucomatous dogs (7 out of 10 dogs) were treated with corticosteroids due to a concurrent uveitis which could have affected the transcription of the ET receptors and the levels of ET-1. Yorio et al. [111] showed that dexamethasone increased ET-1 levels, down-regulated ET_A receptor mRNA and protein levels, while having up-regulated ET_B receptor mRNA and protein levels in human non-pigmented ciliary epithelial cells. Decreased amount of high affinity (ET_A) binding sites by treatment with dexamethasone has also been shown in cultured rat aortic smooth muscle cells and human cerebromicovascular endothelial cells in culture [112,113]. Endothelin receptor mRNA levels were not measured in these studies. Dexamethasone has also been shown to increase the levels of prepro-ET-1 mRNA and ET-1, and decrease the levels of ET_A receptor mRNA in vascular smooth muscle cells [113,114]. Although these results differed somewhat from the results in our study, they clearly showed an impact on ET-1 levels and receptor expression by steroid treatment that might have influenced our data.

Cellular Response to Endothelin-1 Treatment

The cellular responses to ET-1 treatment vary between various studies and may be an indication of different responses between cell types. Krishnamoorthy et al. [115] showed that ET-1 treatment of human non-pigmented ciliary epithelial cells increased both DNA binding activity of AP-1, a known transcription factor for regulating ET

receptor expression, and the protein expression of ET_B receptors. In contrast, studies on human and rat endothelial and smooth muscle cells incubated with ET-1, have shown a decrease in both ET_A and ET_B receptor binding sites [113,116]. Clozel et al. [117] showed on rat mesangial cells (ET_A receptors), and human and rat endothelial cells (ET_B receptors), that autocrine production of ET-1 decreases, either by binding or downregulation, the number of binding sites for both receptors.

The trend in our study was that the protein expression of the ET receptors was decreased while the mRNA levels were increased in the retina, with exception of the non-Cocker group showing a non-significant decrease of the ET_B receptor mRNA levels (Tables 3-7 to 3-10, and Figures 3-17 to 3-20). That would imply that the transcription of the ET receptors is stimulated by the increased ET-1 levels, and therefore the decreased receptor protein expression must be due to either decreased translation or increased destruction.

Unfortunately, we were not able to determine the mRNA levels in the choroid with the Real Time PCR, as the choroidal samples gave a very weak and variable fluorescent signal. The weak signal was probably due to the pigment in the choroid. An attempt was made to extract the pigment using the RNAqueous-4 PCR kit (Ambion, Austin, TX). Since most of the pigment remained in the samples we decided not to use the choroidal samples for the Real Time PCR due to unreliable data.

The complexity of the response of the eye to glaucomatous damage may be better appreciated by comparing with studies done on neurotrauma models of the brain. Siren et al. [118] characterized the time-course, intensity of expression and cellular origin of components of the ET system in the rat brain after standardized neurotrauma. Their study

showed that cortical injury induced a strong expression of ET-1 in astrocytes while the expression in the basilar artery was not altered. The expression of ET_B receptors increased in the astrocytes but decreased significantly in the basilar artery indicating distinct differences in the regulation of the ET_B receptor regulation by these cell types. Immunoreactivity of the ET_A receptor was only associated to blood vesssels and was not altered by the injury. Neurotrauma failed to induce any alterations in mRNA expression of the ET peptides or the ET receptors in the basilar artery.

Extravascular Endothelin Receptor Binding Sites

Extravascular ET receptor binding sites might have influenced our results. Mac Cumber et al. [86] described ET receptor binding sites in human and rabbit eyes using radioligand binding that was inferred from pharmacological antagonism. This study showed extravascular ET_B -like binding sites of the photoreceptor inner segment layer, the outer nuclear layer, the inner nuclear layer, the ganglion cell layer, and the nerve fiber layer. On the other hand, Stitt et al. [119] using the same technique, found extravascular ET_B -like binding sites mainly in the ganglion cell layer in human and rat retinas. In our study we focused on the vascular localization of the ET receptors in the retina and choroid. It is likely though that the canine retina has a similar localization of the ET receptors as that of the species used in previous studies. The Western Blot and Real Time PCR used in our study were done on whole retinas. Consequently, any change in ET receptor levels cannot be attributable to a specific cell type. Thus, the decrease in ET_B receptor expression in the glaucomatous eyes seen in our study may, at least in part, be due to atrophy of the nerve fiber layer and the ganglion cell layer.

Previous studies have localized the ET_A receptor in the retinal and choroidal smooth muscle cells but could not detect any ET_A like binding sites in the neural retinal

tissue [86,119]. If this is true also for the canine eye, the decrease in ET_A receptor expression in the glaucomatous eyes seen in our study is most probably attributable to ET_A receptors located on vascular smooth muscle cells. Future work on cell cultures from normal and glaucomatous eyes is necessary to unravel which cell types are responsible for the changes in ET receptor expression seen in our study.

Pericytes and Endothelin Receptor Expression

The need for an identification of which cell types change their ET receptor expression in glaucoma is further underlined by the fact that the ET receptors of retinal pericytes function differently from the receptors of smooth muscle cells. The pericyte ET_A receptor mediates contraction through the same pathway as the ET_A receptor on smooth muscle cells, i.e. through the phospholipase C/inositol phosphate signaling pathway [43]. The exact nature of the second messenger signaling downstream to ET_B receptor activation in the retinal pericyte remains uncharacterized. However, a study has linked endothelin-3 stimulation of renal mesangial cells (also classified as pericytes) to the production of NO [43]. This mechanism was postulated to buffer the contractile effects of ET-1, especially when local levels are inappropriately high. This is in opposition to the constrictor response evoked by activation of the ET_B receptor on smooth muscle cells. Receptor binding studies have revealed the presence of several hundred thousand high-affinity ET_A receptors but only twenty to thirty thousand ET_B receptors on a single cell. It is also noteworthy that retinal pericytes have been shown to express many more ET_A receptors than vascular smooth muscle [75]. The decreased ET receptor expression in the glaucomatous retinas in our study may reflect changes in the density of ET receptors of the pericytes. Since the ET_A receptors far out number the ET_B receptors, a decrease in both receptors may have a larger functional effect on the ET_B

receptors impairing their buffering effect. This leads to a reduction of blood flow in the retinal microcirculation.

Yield of Protein and RNA

The changes of ET receptor expression in our study cannot be explained by differences in amount of tissue from the normal and glaucomatous eyes. Although there was a degeneration of the retina in the glaucomatous eyes, the protein yields in both groups were similar. The total protein median levels in the normal and glaucomatous retinas were 250 and 280 μg respectively, and in the normal and glaucomatous choroid were 277.5 and 250 μg respectively.

The yield of total RNA differed between the normal and glaucomatous group. The total RNA median levels for the normal and glaucomatous retinas were 22.5 and 30.14 μg respectively. This had no affect on the results of the real time PCR since the quantities of cDNA from each sample were normalized by using the ratio of the sample and the endogenous control rRNA 18S.

Nitric Oxide in Aqueous Humor and Vitreous

The increase of NO levels in aqueous humor and vitreous in our study is in accordance with a study by Chiou et al. [120] on human patients with acute angle-closure glaucoma (Tables 3-5 and 3-6, and Figures 3-15 and 3-16). In contrast, Galassi et al. [121] found a reduction in cGMP, the intracellular mediator of NO action in the peripheral plasma, in aqueous humor of patients with normal pressure glaucoma. This may imply a difference in NO synthesis in various kinds of glaucoma. All three isoforms of nitric oxide synthase (NOS) are elevated in the optic nerve head of human patients with POAG as shown by Neufeld et al. [122]. This finding is in contrast with a study by Samuelson et al. [25] which showed that the endothelial form (NOS-3) is decreased in the

inner retina of Beagles with POAG. On the other hand, in the same study the inducible form (NOS-2) was localized in the trabecular meshwork of the glaucomatous dogs. Our results are also in contrast with a study by Gunia et al. (personal communication) where NO concentrations were measured in aqueous humor of glaucomatous dogs having transcleral cyclophotocoagulation surgery due to acute onset glaucoma. In their study the mean concentration of NO in the glaucomatous dogs was 9.628 μM as compared to 15.17 μM in the control group (normal greyhounds). The main difference between the studies is the concentration of NO in the aqueous humor of the control groups. In our study the mean concentration of NO in glaucomatous dogs was 12.48 μM as compared to 3.9 μM in the control group (Tables 3-5 and 3-6). The lack of agreement between the studies may represent a species difference.

Prasanna et al. [123] demonstrated that ET-1 increases NO production, in part via the activation of NOS-2, in cultured human non-pigmented ciliary epithelial cells. In addition, intravitreal injections of ET-1 in rabbits have been shown to increase NO levels [124]. When the synthesis of NOS-2 is induced the enzyme produces massive amounts of NO that is destructive to neighboring cells [122]. Franco-Burland et al. [125] showed an increase in neuronal NOS (NOS-1) in surviving retinal ganglion cells of dogs with glaucoma. The influence of ET-1 on NOS-1 levels have, to our knowledge, not been determined.

We did not examine the various isoforms of NOS in our study. However, the increased levels of NO in both aqueous humor and vitreous are likely to influence the mechanisms of both aqueous humor inflow and outflow, and the development of optic nerve degeneration. In addition, if there is a decrease in NOS-3, as shown by Samuelson

et al. [25], the neuroprotective effect caused by circulatory vasodilation is diminished in glaucomatous canine retinas.

The Cocker Spaniel versus Other Breeds

American Cocker Spaniels with glaucoma can have fan-shaped zones of retinal and choroidal degeneration radiating from the ONH. These areas of retinal ischemia correspond to the areas supplied by individual short posterior ciliary arteries and may be caused by vasospasm of the arteries [27]. The ischemia may be a result of the inability of the vessels to alter their diameter in response to a demand for an increase in blood flow by the tissue due to elevated levels of ET-1. This finding suggests a role for ET-1 in contributing to the glaucomatous damage in American Cocker Spaniels, either by increased release of ET-1 or a nonfunctional circulatory response due to modulation of its receptors.

Although several parameters in our study were not significantly different, the Cocker glaucoma group seemed to differ from the non-Cocker glaucoma group. The increase of ET-1 in aqueous humor and vitreous was greater in the Cocker group compared to the non-Cocker group, while the increase in NO was greater in the non-Cocker breed group compared to that of the Cockers (Tables 3-2 to 3-6, and Figures 3-12, 3-13, 3-15, and 3-16).

There was a decrease of the ET_B receptor protein expression in the glaucomatous retinas which was significant in the non-Cocker group, but not significant in the Cocker group (Table 3-8, and Figure 3-18). For technical reasons we did not have any normal choroid in the Cocker group to compare with the glaucomatous Cockers. A comparison of glaucomatous choroid samples showed that the expression of the ET_B receptor in the

choroids of the glaucomatous Cockers was lower, although not significantly, than the non-Cocker breed group (Table 3-8).

The expression of the ET_A receptor was decreased in both groups in the glaucomatous retinal samples compared to normals (Table 3-7 and Figure 3-17). In contrast, the glaucomatous choroidal samples of the Cocker group had higher expression of the ET_A receptor than the non-Cocker group (Table 3-7). None of the differences was significant but did show an interesting trend. The choroid of the glaucomatous Cockers showed a higher expression of the ET_A receptor and a lower expression of the ET_B receptor compared to the non-Cocker group. This creates an imbalance between the receptors increasing the risk for vasoconstriction by the ET_A receptors, which cannot be counter-balanced by the vasodilating effect by the ET_B receptors, thus increasing the risk for ischemic ocular damage.

The mRNA levels in the retina were significantly increased in the Cocker group for both receptors, while the non-Cocker group showed a non-significant increased level of the ET_A receptor and a non-significant decrease of the ET_B receptor levels (Tables 3-9 and 3-10, and Figures 3-19 and 3-20).

These differences between the groups might imply that the narrow-angle glaucoma in Cocker Spaniels represent a separate type of glaucoma with an unique response to increased IOP. The role of ET-1 in glaucoma in Cocker Spaniels should be further evaluated by characterizing the components of the ET system in the anterior and posterior part of the eye at various stages of the disease.

Implications for the Canine Eye

Ultrastructural differences in capillaries of the lamina cribrosa, circulatory abnormalities of the mid-peripheral retina, failure of the orbital circulation to respond to

calcium channel blocking drugs, and irregularities in the blood flow of the orbital arteries are present in dogs with hereditary glaucoma prior to elevations in IOP [37,36,126,127]. An ET-1 related ocular micro-circulatory problem may thus be present early in the glaucomatous disease process in dogs.

In our study we showed that the aqueous humor and vitreous of dogs with hypertensive glaucoma contains significantly higher levels of ET-1 than normal dogs. There is no indication from our data whether the increase in ET-1 in the aqueous humor of canine glaucomatous eyes is the cause of elevated IOP or just a secondary event.

The effects of elevated ET-1 in the anterior chamber must take anatomical differences between species into consideration. The effect on contractility of the trabecular meshwork is functionally antagonistic to the direct effect on ciliary muscle [96]. Since the canine ciliary muscle is poorly developed as compared to primates, the effect of ET-1 might be dominated by the effect on the trabecular meshwork. That could give an increased resistance to aqueous outflow and lead to an increased IOP.

The decrease in ET receptors seen in our study is a mass response of the whole retina, including the vessels. As for the vascular component of the ET system, a decrease of the receptors may be a reflection of endothelial cell damage consistent with ischemic events. This would decrease the amount of ET_B receptors located on the endothelial cells leading to vasoconstriction. In the case of a concurrent damage to the smooth muscle cells both ET receptors would decrease. Even with a decrease of ET_A receptors on the smooth muscle cells, the net effect would probably be an increased vasoconstriction caused by the remaining ET_A receptors and ET_B receptors located on the smooth muscle

cells. As discussed in the section “Pericytes and Receptor Expression”, a decrease of both ET receptor types might lead to vasoconstriction.

The balance between ET-1 and NO is absent in the canine glaucomatous eyes in our study. The source of the excessive NO production has to be determined. If the increased concentration of NO is produced by glial cells (NOS-1 and NOS-2) it most likely participates in neurodestruction of the retina and ONH. Conversely, NO produced by the vascular endothelial cells (NOS-3) may be neuroprotective by causing vasodilation and increased blood flow in the tissue.

The increase of ET-1 in the aqueous humor and vitreous of dogs with glaucoma may contribute not only to the uncontrolled IOP, but also explain the rapid progression to ONH atrophy in canine glaucoma that occurs more slowly in human POAG [128]. Acute increases of IOP induce ischemia of the optic nerve and retina [2]. The ischemia leads to an increase in endothelin-mediated vasoconstriction concomitant with a loss of tonic NO-dependent vasodilation. This effect may persist several hours after the ischemic insult. Ischemia and reperfusion are known to increase both ET-1 and glutamate levels in tissue and plasma [3,129,130]. Elevated intravitreal glutamate levels indicating ischemia are increased during glaucoma in the dog [28]. Defective or inadequate autoregulation and microcirculatory dysfunction of the vessels of the dog eye may result in ischemic injury to the canine retina and optic nerve under normotensive and hypertensive conditions resulting in further release of ET-1. The increased levels of ET may also exacerbate neurodegeneration by stimulating efflux of glutamate from the astrocytes.

The rapid degeneration of the optic nerve head found in canine glaucoma despite aggressive IOP reduction therapy may thus be due to the combined, chronic effect of

ET-1 inducing vascular ischemia and associated glutamate release, and a neurotoxic effect of NO [27]. The increased ET-1 levels could also cause astrogliosis disrupting axonal transport and inhibiting axon regrowth in the glaucomatous canine ONH.

LIST OF REFERENCES

1. Brooks D E, Komaromy A M, Kallberg M E. Comparative optic nerve physiology: implications for glaucoma, neuroprotection, and neuroregeneration. *Vet Ophthalmol* 1999; 2: 13-25.

2. Chung H S, Harris A, Evans D W, Kagemann L, Garzozi H J, Martin B. Vascular aspects in the pathophysiology of glaucomatous optic neuropathy. *Surv Ophthalmol* 1999; 43 Suppl 1: S43-S50.

3. Adachi K, Kashii S, Masai H, Ueda M, Morizane C, Kaneda K, Kume T, Akaike A, Honda Y. Mechanism of the pathogenesis of glutamate neurotoxicity in retinal ischemia. *Graefes Arch Clin Exp Ophthalmol* 1998; 236: 766-774.

4. Osborne N N, Ugarte M, Chao M, Chidlow G, Bae J H, Wood J P, Nash M S. Neuroprotection in relation to retinal ischemia and relevance to glaucoma. *Surv Ophthalmol* 1999; 43 Suppl 1: S102-S128.

5. Pillunat L E, Stodtmeister R, Wilmanns I, Christ T. Autoregulation of ocular blood flow during changes in intraocular pressure. Preliminary results. *Graefes Arch Clin Exp Ophthalmol* 1985; 223: 219-223.

6. Pillunat L E, Stodtmeister R, Wilmanns I, Metzner D. Effect of timolol on optic nerve head autoregulation. *Ophthalmologica* 1986; 193: 146-153.

7. Pillunat L E, Stodtmeister R, Wilmanns I. Pressure compliance of the optic nerve head in low tension glaucoma. *Br J Ophthalmol* 1987; 71: 181-187.

8. Robert Y, Steiner D, Hendrickson P. Papillary circulation dynamics in glaucoma. *Graefes Arch Clin Exp Ophthalmol* 1989; 227: 436-439.

9. Grunwald J E, Riva C E, Stone R A, Keates E U, Petrig B L. Retinal autoregulation in open-angle glaucoma. *Ophthalmology* 1984; 91: 1690-1694.

10. Gherghel D, Orgul S, Gugleta K, Gekkieva M, Flammer J. Relationship between ocular perfusion pressure and retrobulbar blood flow in patients with glaucoma with progressive damage. *Am J Ophthalmol* 2000; 130: 597-605.

11. Cheng C Y, Liu C J, Chiou H J, Chou J C, Hsu W M, Liu J H. Color Doppler imaging study of retrobulbar hemodynamics in chronic angle-closure glaucoma. *Ophthalmology* 2001; 108: 1445-1451.

12. Cioffi G A, Sullivan P. The effect of chronic ischemia on the primate optic nerve. *Eur J Ophthalmol* 1999; 9 Suppl 1:S34-6: S34-S36.

13. Oku H, Sugiyama T, Kojima S, Watanabe T, Azuma I. Experimental optic cup enlargement caused by endothelin-1-induced chronic optic nerve head ischemia. *Surv Ophthalmol* 1999; 44 Suppl 1: S74-S84.

14. Henry E, Newby D E, Webb D J, O'Brien C. Peripheral endothelial dysfunction in normal pressure glaucoma. *Invest Ophthalmol Vis Sci* 1999; 40: 1710-1714.

15. Tezel G, Kass M A, Kolker A E, Becker B, Wax M B. Plasma and aqueous humor endothelin levels in primary open-angle glaucoma. *J Glaucoma* 1997; 6: 83-89.

16. Noske W, Hensen J, Wiederholt M. Endothelin-like immunoreactivity in aqueous humor of patients with primary open-angle glaucoma and cataract. *Graefes Arch Clin Exp Ophthalmol* 1997; 235: 551-552.

17. Sugiyama T, Moriya S, Oku H, Azuma I. Association of endothelin-1 with normal tension glaucoma: clinical and fundamental studies. *Surv Ophthalmol* 1995; 39 Suppl 1: S49-S56.

18. Sasaki Y, Takimoto M, Oda K, Fruh T, Takai M, Okada T, Hori S. Endothelin evokes efflux of glutamate in cultures of rat astrocytes. *J Neurochem* 1997; 68: 2194-2200.

19. Gidday J M, Zhu Y. Endothelium-dependent changes in retinal blood flow following ischemia. *Curr Eye Res* 1998; 17: 798-807.

20. Morgan J E. Optic nerve head structure in glaucoma: astrocytes as mediators of axonal damage. *Eye* 2000; 14 (Pt 3B): 437-444.

21. Goss J R, O'Malley M E, Zou L, Styren S D, Kochanek P M, DeKosky S T. Astrocytes are the major source of nerve growth factor upregulation following traumatic brain injury in the rat. *Exp Neurol* 1998; 149: 301-309.

22. Hernandez M R. The optic nerve head in glaucoma: role of astrocytes in tissue remodeling. *Prog Retin Eye Res* 2000; 19: 297-321.

23. Prasanna G, Krishnamoorthy R, Clark A F, Wordinger R J, Yorio T. Human optic nerve head astrocytes as a target for endothelin-1. *Investigative Ophthalmology and Visual Science* 2002; 43: 2704-2713.

24. Stokely M E, Brady S T, Yorio T. Effects of endothelin-1 on components of anterograde axonal transport in optic nerve. *Invest Ophthalmol Vis Sci* 2002; 43: 3223-3230.

25. Samuelson D A, Ellis E A, Kallberg M, Lewis P A, Brooks D E, Gelatt K N. Immunocytochemical localization of nitric oxide synthase in the normal and glaucomatous canine eye. *Invest Ophthalmol Vis Sci* 42[4], S139. 3-15-2001.

26. Gelatt K N, Brooks D E, Samuelson D A. Comparative glaucomatology. I: The spontaneous glaucomas. *J Glaucoma* 1998; 7: 187-201.

27. Gelatt K N, Brooks D E. The Canine Glaucomas. In: *Veterinary Ophthalmology* 3rd edition (ed. Gelatt K. N.). Lippincott Williams & Wilkins: Baltimore, 1999; 701-754.

28. Brooks D E, Garcia G A, Dreyer E B, Zurakowski D, Franco-Bourland R E. Vitreous body glutamate concentration in dogs with glaucoma. *Am J Vet Res* 1997; 58: 864-867.

29. Kallberg M E, Brooks D E, Garcia-Sanchez G A, Komaromy A M, Szabo N J, PhD L T. Endothelin 1 levels in the aqueous humor of dogs with glaucoma. *J Glaucoma* 2002; 11: 105-109.

30. Ritch R, Lowe R F. Angle-closure glaucoma: Mechanisms and epidemiology. In: *The Glaucomas. Clinical science.* 2nd edition (eds. Ritch R., Shields M.B., Krupin T.). Mosby: 1996; 801-819.

31. Ritch R, Lowe R F. Angle-closure glaucoma: Clinical types. In: *The glaucomas. Clinical science.* 2nd edition (eds. Ritch R., Shields M.B., Krupin T.). Mosby: 1996; 821-840.

32. Magrane W G. Canine glaucoma: II. Primary classification. *J Am Vet Med Assoc* 1957; 131: 372-378.

33. Lovekin L G, Ben Refael Z. Clinicopathologic changes in primary glaucoma in the cocker spaniel. *Am J Vet Res* 1968; 29: 379-385.

34. Peiffer R L, Jr., Gelatt K N. Aqueous humor outflow in Beagles with inherited glaucoma: gross and light microscopic observations of the iridocorneal angle. *Am J Vet Res* 1980; 41: 861-867.

35. Samuelson D A, Gum G G, Gelatt K N. Ultrastructural changes in the aqueous outflow apparatus of beagles with inherited glaucoma. *Invest Ophthalmol Vis Sci* 1989; 30: 550-561.

36. Brooks D E, Samuelson D A, Gelatt K N. Ultrastructural changes in laminar optic nerve capillaries of beagles with primary open-angle glaucoma. *Am J Vet Res* 1989; 50: 929-935.

37. Gelatt-Nicholson K J, Gelatt K N, MacKay E O, Brooks D E, Newell S M. Comparative Doppler imaging of the ophthalmic vasculature in normal Beagles and Beagles with inherited primary open-angle glaucoma. *Vet Ophthalmol* 1999; 2: 97-105.

38. Orgul S, Gugleta K, Flammer J. Physiology of perfusion as it relates to the optic nerve head. *Surv Ophthalmol* 1999; 43 Suppl 1:S17-26.: S17-S26.

39. Samuelson D A. Ophthalmic anatomy. In: *Veterinary Ophthalmology* 3rd edition (ed. Gelatt K. N.). Lippincott Wiliams and Wilkins: Maryland, 1999; 31-150.

40. Brooks D E, Komaromy A M, Kallberg M E. Comparative retinal ganglion cell and optic nerve morphology. *Vet Ophthalmol* 1999; 2: 3-11.

41. Snodderly D M, Weinhaus R S, Choi J C. Neural-vascular relationships in central retina of macaque monkeys (Macaca fascicularis). *J Neurosci* 1992; 12: 1169-1193.

42. Orgul S, Cioffi G A. Embryology, anatomy, and histology of the optic nerve vasculature. *J Glaucoma* 1996; 5: 285-294.

43. Chakravarthy U, Gardiner T A. Endothelium-derived agents in pericyte function/dysfunction. *ProgRetin Eye Res* 1999; 18: 511-527.

44. Gray G A, Webb D J. The endothelin system and its potential as a therapeutic target in cardiovascular disease. *Pharmacology & Therapeutics* 1996; 72: 109-148.

45. Haefliger I O, Flammer J, Beny J L, Luscher T F. Endothelium-dependent vasoactive modulation in the ophthalmic circulation. *Progress in Retinal and Eye Research* 2001; 20: 209-225.

46. Hayreh S S. Factors influencing blood flow in the optic nerve head. *J Glaucoma* 1997; 6: 412-425.

47. Flammer J, Orgul S. Optic nerve blood-flow abnormalities in glaucoma. *Prog Retin Eye Res* 1998; 17: 267-289.

48. Bevan J A. Shear stress, the endothelium and the balance between flow-induced contraction and dilation in animals and man. *International Journal of Microcirculation: Clinical and Experimental* 1997; 17: 248-256.

49. Haefliger I O, Dettmann E S. Nitric oxide and endothelin in the pathogenesis of glaucoma: An overview. In: *Nitric oxide and endothelin in the pathogenesis of glaucoma* 1 edition (eds. Haefliger I. O., Flammer J.). Lippincott-Raven: Philadelphia, 1998; 22-33.

50. Funk R H. Blood supply of the retina. *Ophthalmic Res* 1997; 29: 320-325.

51. Kiryu J, Asrani S, Shahidi M, Mori M, Zeimer R. Local response of the primate retinal microcirculation to increased metabolic demand induced by flicker. *Invest Ophthalmol Vis Sci* 1995; 36: 1240-1246.

52. Kulkarni P, Joshua I G, Roberts A M, Barnes G. A novel method to assess reactivities of retinal microcirculation. *Microvasc Res* 1994; 48: 39-49.

53. Harris A, Ciulla T A, Chung H S, Martin B. Regulation of retinal and optic nerve blood flow. *Arch Ophthalmol* 1998; 116: 1491-1495.

54. Arend O, Harris A, Martin B J, Holin M, Wolf S. Retinal blood velocities during carbogen breathing using scanning laser ophthalmoscopy. *Acta Ophthalmol (Copenh)* 1994; 72: 332-336.

55. Bill A, Sperber G O. Control of retinal and choroidal blood flow. *Eye* 1990; 4 (Pt 2): 319-325.

56. Orgul S, Meyer P, Cioffi G A. Physiology of blood flow regulation and mechanisms involved in optic nerve perfusion. *J Glaucoma* 1995; 4: 427-443.

57. Kiel J W, van Heuven W A. Ocular perfusion pressure and choroidal blood flow in the rabbit. *Invest Ophthalmol Vis Sci* 1995; 36: 579-585.

58. Yanagisawa M, Kurihara H, Kimura S, Tomobe Y, Kobayashi M, Mitsui Y, Yazaki Y, Goto K, Masaki T. A novel potent vasoconstrictor peptide produced by vascular endothelial cells. *Nature* 1988; 332: 411-415.

59. Yanagisawa M, Kurihara H, Kimura S, Goto K, Masaki T. A novel peptide vasoconstrictor, endothelin, is produced by vascular endothelium and modulates smooth muscle Ca2+ channels. *J Hypertens Suppl* 1988; 6: S188-S191.

60. Ortega M A, de Artinano A A. Highlights on endothelins: a review. *Pharmacol Res* 1997; 36: 339-351.

61. Chakravarthy U, Gardiner T A, Anderson P, Archer D B, Trimble E R. The effect of endothelin 1 on the retinal microvascular pericyte. *Microvasc Res* 1992; 43: 241-254.

62. Hisaki K, Matsumura Y, Nishiguchi S, Fujita K, Takaoka M, Morimoto S. Endothelium-independent pressor effect of big endothelin-1 and its inhibition by phosphoramidon in rat mesenteric artery. *Eur J Pharmacol* 1993; 241: 75-81.

63. Warner T D. Relationships between the endothelin and nitric oxide pathways. *Clin Exp Pharmacol Physiol* 1999; 26: 247-252.

64. Love M P, Haynes W G, Gray G A, Webb D J, McMurray J J. Vasodilator effects of endothelin-converting enzyme inhibition and endothelin ETA receptor blockade in chronic heart failure patients treated with ACE inhibitors. *Circulation* 1996; 94: 2131-2137.

65. Wang J, Chiou W J, Gagne G D, Wu-Wong J R. Internalization of type-A endothelin receptor. *J Cardiovasc Pharmacol* 2000; 36: S61-S65.

66. Oksche A, Boese G, Horstmeyer A, Papsdorf G, Furkert J, Beyermann M, Bienert M, Rosenthal W. Evidence for downregulation of the endothelin-B-receptor by the use of fluorescent endothelin-1 and a fusion protein consisting of the endothelin-B-receptor and the green fluorescent protein. *J Cardiovasc Pharmacol* 2000; 36: S44-S47.

67. Haefliger I O, Meyer P, Flammer J, Luscher T F. The vascular endothelium as a regulator of the ocular circulation: a new concept in ophthalmology? *Surv Ophthalmol* 1994; 39: 123-132.

68. Chakravarthy U, Stitt A W, McNally J, Bailie J R, Hoey E M, Duprex P. Nitric oxide synthase activity and expression in retinal capillary endothelial cells and pericytes. *Curr Eye Res* 1995; 14: 285-294.

69. Haefliger I O, Zschauer A, Anderson D R. Relaxation of retinal pericyte contractile tone through the nitric oxide-cyclic guanosine monophosphate pathway. *Invest Ophthalmol Vis Sci* 1994; 35: 991-997.

70. Masaki T. The endothelin family: an overview. *J Cardiovasc Pharmacol* 2000; 35: S3-S5.

71. Zhang X F, Iwamuro Y, Okamoto Y, Kawanabe Y, Masaki T, Miwa S. Endothelin-1-induced contraction of rat thoracic aorta depends on calcium entry through three types of calcium channel. *J Cardiovasc Pharmacol* 2000; 36: S105-S106.

72. Pang I H, Yorio T. Ocular actions of endothelins. *Proceedings of the Society for Experimental Biology and Medicine* 1997; 215: 21-34.

73. Bremnes T, Paasche J D, Mehlum A, Sandberg C, Bremnes B, Attramadal H. Regulation and intracellular trafficking pathways of the endothelin receptors. *Journal of Biological Chemistry* 2000; 275: 17596-17604.

74. Chun M, Lin H Y, Henis Y I, Lodish H F. Endothelin-induced endocytosis of cell surface ETA receptors. Endothelin remains intact and bound to the ETA receptor. *J Biol Chem* 1995; 270: 10855-10860.

75. McDonald D M, Bailie J R, Archer D B, Chakravarthy U. Characterization of endothelin A (ETA) and endothelin B (ETB) receptors in cultured bovine retinal pericytes. *Invest Ophthalmol Vis Sci* 1995; 36: 1088-1094.

76. McDonald D M, Bailie J R, Archer D B, Chakravarthy U. Receptor binding and biologic activity of synthetic ET-1 peptides in the retinal pericyte. *Invest Ophthalmol Vis Sci* 1996; 37: 1067-1073.

77. Martin E R, Brenner B M, Ballermann B J. Heterogeneity of cell surface endothelin receptors. *J Biol Chem* 1990; 265: 14044-14049.

78. Haefliger I O, Flammer J, Luscher T F. Heterogeneity of endothelium-dependent regulation in ophthalmic and ciliary arteries. *Invest Ophthalmol Vis Sci* 1993; 34: 1722-1730.

79. Dallinger S, Dorner G T, Wenzel R, Graselli U, Findl O, Eichler H G, Wolzt M, Schmetterer L. Endothelin-1 contributes to hyperoxia-induced vasoconstriction in the human retina. *Invest Ophthalmol Vis Sci* 2000; 41: 864-869.

80. Schmetterer L, Findl O, Strenn K, Jilma B, Graselli U, Eichler H G, Wolzt M. Effects of endothelin-1 (ET-1) on ocular hemodynamics. *Curr Eye Res* 1997; 16: 687-692.

81. Granstam E, Wang L, Bill A. Ocular effects of endothelin-1 in the cat. *Curr Eye Res* 1992; 11: 325-332.

82. Kiel J W, Reitsamer H A, Walker J S, Kiel F W. Effects of nitric oxide synthase inhibition on ciliary blood flow, aqueous production and intraocular pressure. *Exp Eye Res* 2001; 73: 355-364.

83. Stitt A W, Chakravarthy U, Archer D B, Gardiner T A. Increased endocytosis in retinal vascular endothelial cells grown in high glucose medium is modulated by inhibitors of nonenzymatic glycosylation. *Diabetologia* 1995; 38: 1271-1275.

84. Zhao Y D, Xu L X, Chandler J W. Localization of endothelin-like immunoreactivity and endothelin binding sites in rabbit eyes. *J Cardiovasc Pharmacol* 1995; 26 Suppl 3: S332-S335.

85. Narayan S, Prasanna, G., Krishnamoorthy, R., Hulet, C., and Yorio, T. Cholinergic regulation of endothelin-1 (ET-1) synthesis and expression in human retinal pigment epithelial cells (ARPE-19). *Invest Ophthalmol Vis Sci* 42[4], S762. 2001.

86. MacCumber M W, D'Anna S A. Endothelin receptor-binding subtypes in the human retina and choroid. *Arch Ophthalmol* 1994; 112: 1231-1235.

87. Tao W, Prasanna G, Dimitrijevich S, Yorio T. Endothelin receptor A is expressed and mediates the [$Ca2^{+}$]i mobilization of cells in human ciliary smooth muscle, ciliary nonpigmented epithelium, and trabecular meshwork. *Curr Eye Res* 1998; 17: 31-38.

88. Yorio T, Narayan S, Lambert W, Wordinger R J, Agarwal R, Krishnamoorthy R, Hulet C, Prasanna G. Regulation of endothelin receptor expression in ocular tissues. *Invest Ophthalmol Vis Sci* 41[4], S251. 2000.

89. Prasanna G, Dibas A I, Yorio T. Cholinergic and adrenergic modulation of the $Ca2^{+}$ response to endothelin-1 in human ciliary muscle cells. *Invest Ophthalmol Vis Sci* 2000; 41: 1142-1148.

90. Sugiyama K, Haque M S, Okada K, Taniguchi T, Kitazawa Y. Intraocular pressure response to intravitreal injection of endothelin-1 and the mediatory role of ETA receptor, ETB receptor, and cyclooxygenase products in rabbits. *Curr Eye Res* 1995; 14: 479-486.

91. Lepple-Wienhues A, Becker M, Stahl F, Berweck S, Hensen J, Noske W, Eichhorn M, Wiederholt M. Endothelin-like immunoreactivity in the aqueous humour and in conditioned medium from cultured ciliary epithelial cells. *Curr Eye Res* 1992; 11: 1041-1046.

92. Okada K, Sugiyama K, Haque M S, Taniguchi T, Kitazawa Y. The effects of endothelin-1 on intraocular pressure and pupillary diameter in rabbits. *Japanese Journal of Ophthalmology* 1995; 39: 233-241.

93. Taniguchi T, Okada K, Haque M S, Sugiyama K, Kitazawa Y. Effects of endothelin-1 on intraocular pressure and aqueous humor dynamics in the rabbit eye. *Curr Eye Res* 1994; 13: 461-464.

94. Erickson-Lamy K, Korbmacher C, Schuman J S, Nathanson J A. Effect of endothelin on outflow facility and accommodation in the monkey eye in vivo. *Invest Ophthalmol Vis Sci* 1991; 32: 492-495.

95. Krishnamoorthy R, Prasanna G, Hulet C, Yorio T. Regulation of Na, K-ATPase mRNA levels by endothelin-1 in transformed human non-pigmented ciliary epithelial (t-HNPE) cells. *Invest Ophthalmol Vis Sci* 41[4], S253. 2000.

96. Wiederholt M, Bielka S, Schweig F, Lutjen-Drecoll E, Lepple-Wienhues A. Regulation of outflow rate and resistance in the perfused anterior segment of the bovine eye. *Exp Eye Res* 1995; 61: 223-234.

97. Louden C S, Nambi P, Pullen M A, Thomas R A, Tierney L A, Solleveld H A, Schwartz L W. Endothelin receptor subtype distribution predisposes coronary arteries to damage. *Am J Pathol* 2000; 157: 123-134.

98. Samuelson D A. A reevaluation of the comparative anatomy of the eutherian iridocorneal angle and associated ciliary body musculature. *Veterinary and Comparative Ophthalmology* 1996; 6: 153-172.

99. Brooks D E. Glaucoma in the dog and cat. *Vet Clin North Am Small Anim Pract* 1990; 20: 775-797.

100. Smedes S L, Dubielzig R R. Early degenerative changes associated with spontaneous glaucoma in dogs. *Journal of Veterinary Diagnostics* 1994; 6: 259-263.

101. Kaiser H J, Flammer J, Wenk M, Luscher T. Endothelin-1 plasma levels in normal-tension glaucoma: abnormal response to postural changes. *Graefes Arch Clin Exp Ophthalmol* 1995; 233: 484-488.

102. Prasanna G, Dibas A, Tao W, White K, Yorio T. Regulation of endothelin-1 in human non-pigmented ciliary epithelial cells by tumor necrosis factor-alpha. *Exp Eye Res* 1998; 66: 9-18.

103. Prasanna G, Dibas A, Finkley A, Yorio T. Identification of endothelin converting enzyme-1 in human non-pigmented ciliary epithelial cells. *Exp Eye Res* 1999; 69: 175-183.

104. Smith R I E, Peiffer R L, Wilcock BP. Some aspects of the pathology of canine glaucoma. *Progress in Veterinary and Comparative Ophthalmology* 1993; 3: 16-28.

105. Vollmar A M, Preusser U, Gerbes A L, Kraft W, Schulz R. Endothelin concentration in plasma of healthy dogs and dogs with congestive heart failure, renal failure, diabetes mellitus, and hyperadrenocorticism. *J Vet Intern Med* 1995; 9: 105-111.

106. Nambi P, Pullen M, Wu H L, Prabhakar U, Hersh L, Gellai M. Down regulation of kidney neutral endopeptidase mRNA, protein and activity during acute renal failure: possible mechanism for ischemia-induced acute renal failure in rats? *Mol Cell Biochem* 1999; 197: 53-59.

107. Janas J, Sitkiewicz D, Januszewicz A, Szczesniak C, Grenda R, Janas R M. Endothelin-1 inactivating peptidase in the human kidney and urine. *J Hypertension* 2000; 18: 475-483.

108. Saito S, Hirata Y, Imai T, Marumo F. Autocrine regulation of the endothelin-1 gene in rat endothelial cells. *J Cardiovasc Pharmacol* 1995; 26 Suppl 3: S84-S87.

109. MacCumber M W, Ross C A, Snyder S H. Endothelin in brain: receptors, mitogenesis, and biosynthesis in glial cells. *Proc Natl Acad Sci U S A* 1990; 87: 2359-2363.

110. Ehrenreich H, Anderson R W, Ogino Y, Rieckmann P, Costa T, Wood G P, Coligan J E, Kehrl J H, Fauci A S. Selective autoregulation of endothelins in primary astrocyte cultures: endothelin receptor-mediated potentiation of endothelin-1 secretion. *New Biologist* 1991; 3: 135-141.

111. Yorio T, Zhang X, Krishnamoorthy R, Prasanna G, Narayan S. Dexamethasone endothelin-1 interactions in human non-pigmented ciliary epithelial cells. ARVO Presentation number 4076. 5-7-2002.

112. Stanimirovic D B, Bacic F, Uematsu S, Spatz M. Profile of prostaglandins induced by endothelin-1 in human brain capillary endothelium. *Neurochem Int* 1993; 23: 385-393.

113. Roubert P, Viossat I, Lonchampt M O, Chapelat M, Schulz J, Plas P, Gillard-Roubert V, Chabrier P E, Braquet P. Endothelin receptor regulation by endothelin synthesis in vascular smooth muscle cells: effects of dexamethasone and phosphoramidon. *J Vasc Res* 1993; 30: 139-144.

114. Koshino Y, Hayashi T, Matsukawa S, Asazuma K, Eguchi K, Kato H, Nakai T, Miyamori I. Dexamethasone modulates the expression of endothelin-1 and -A receptors in A7r5 vascular smooth muscle cells. *J Cardiovasc Pharmacol* 1998; 32: 665-672.

115. Krishnamoorthy R, Prasanna G, Dauphin R, Hulet C, Kelly C, Yorio T. Transcriptional regulation of the ETB gene in human non-pigmented ciliary epithelial (HNPE) cells. Meeting Program Summary Book, ARVO # 3244, 131. 5-8-2002.

116. Masaki T. Overview: Reduced sensitivity of vascular response to endothelin. *Circulation* 1993; 87: V-33-V-35.

117. Clozel M, Loffler B M, Breu V, Hilfiger L, Maire J P, Butscha B. Downregulation of endothelin receptors by autocrine production of endothelin-1. *Am J Physiol* 1993; 265: C188-C192.

118. Siren A L, Knerlich F, Schilling L, Kamrowski-Kruck H, Hahn A, Ehrenreich H. Differential glial and vascular expression of endothelins and their receptors in rat brain after neurotrauma. *Neurochem Res* 2000; 25: 957-969.

119. Stitt A W, Chakravarthy U, Gardiner T A, Archer D B. Endothelin-like immunoreactivity and receptor binding in the choroid and retina. *Curr Eye Res* 1996; 15: 111-117.

120. Chiou S H, Chang C J, Hsu W M, Kao C L, Liu J H, Chen W L, Tsai D C, Wu C C, Chou C K. Elevated nitric oxide level in aqueous humor of patients with acute angle-closure glaucoma. *Ophthalmologica* 2001; 215: 113-116.

121. Galassi F, Sodi A, Ucci F, Renieri G, Pieri B, Masini E. Ocular haemodynamics and nitric oxide in normal pressure glaucoma. *Acta Ophthalmol Scand Suppl* 2000; 78: 37-38.

122. Neufeld A H, Hernandez M R, Gonzalez M. Nitric oxide synthase in the human glaucomatous optic nerve head. *Arch Ophthalmol* 1997; 115: 497-503.

123. Prasanna G, Krishnamoorthy R, Hulet C, Zhang H, Zhang X, Yorio T. Endothelin-1 induces nitric oxide synthase-2 expression in human non-pigmented ciliary epithelial cells. *Exp Eye Res* 2000; 71: 535-539.

124. Oku H, Okuno T, Sugiyama T, Goto W, Ikeda T. Evaluation for alteration of nitric oxide synthesis in the optic nerve head in vivo induced by endothelin-1. ARVO Presentation number 4048. 5-7-2002.

125. Franco-Bourland R E, Guizar-Sahagun G, Garcia G A, Odor-Morales A, Alvarez A, Esquivel F, Rodriguez S. Retinal vulnerability to glutamate excitotoxicity in canine glaucoma: Induction of neuronal nitric oxide synthase in retinal ganglion cells. *Proc West Pharmacol Soc* 1998; 41: 201-204.

126. Gelatt K N, van der W A, Ketring K L, Andrew S E, Brooks D E, Biros D J, Denis H M, Cutler T J. Enrofloxacin-associated retinal degeneration in cats. *Veterinary Ophthalmology* 2001; 4: 99-106.

127. Ofri R, Dawson W W, Foli K, Gelatt K N. Chronic ocular hypertension alters local retinal responsiveness. *Br J Ophthalmol* 1993; 77: 502-508.

128. Anderson D R, Cynader M S. Glaucomatous optic nerve cupping as an optic neuropathy. *Clin Neurosci* 1997; 4: 274-278.

129. Okada M, Yamashita C, Okada M, Okada K. Contribution of endothelin-1 to warm ischemia/reperfusion injury of the rat lung. *Am J Resp Crit Care Med* 1995; 152: 2105-2110.

130. Kawamura E, Yamanaka N, Okamoto E, Tomoda F, Furukawa K. Response of plasma and tissue endothelin-1 to liver ischemia and its implication in ischemia-reperfusion injury. *Hepatology* 1995; 21: 1138-1143.

BIOGRAPHICAL SKETCH

Maria Elisabeth Källberg was born on September 26, 1957, in Stockholm, Sweden. She attended elementary and secondary schools in Sweden. Maria attended the College of Veterinary Medicine at the Swedish University of Agricultural Sciences in Uppsala, Sweden, from 1976-1981. After attending veterinary school, Maria worked as a small animal general practitioner for 3 years. In 1985, Maria became co-owner of an animal hospital where she served as chief of staff for the Small Animal Clinic until 1998. During this time Maria took continuous, practical training in eye examination for hereditary diseases in dogs and cats. After passing the exam set by the Swedish Society for Veterinary Ophthalmology, Maria became a member of the Swedish Eye Panel in 1995. In 1998 Maria became a graduate student at the College of Veterinary Medicine, University of Florida in Gainesville, Florida with duties as a teaching and research assistant. In 2002 she started her residency in comparative ophthalmology at the University of Florida, which she will finish in 2005. Her special interests include regulation of blood flow in the healthy and diseased eye.